.

Determining the bond characteristics of 7.5-mm and 7.8-mm prestressing wires.

by

Evan Ryan McMillan

B.S., Kansas State University, 2017

A THESIS

submitted in partial fulfillment of the requirements for the degree

MASTER OF SCIENCE

Department of Civil Engineering
Carl. R. Ice College of Engineering

KANSAS STATE UNIVERSITY
Manhattan, Kansas

2023

Approved by:

Major Professor
Dr. Robert Peterman

Copyright

Abstract

A study was conducted to investigate the bond properties of three different types of large-diameter chevron-indented prestressing wires. Nine 6”x10” beams were cast for each type of wire at lengths of 5.5-ft, 6.5-ft, and 7.5-ft. The Type III concrete mixture used was kept constant throughout the study to investigate the effects of the wire profile and concrete release strength on bond behavior. During beam fabrication, prestressing reinforcement was gradually detensioned when concrete compressive strengths reached 3,500 psi, 4,500 psi, and 6,000 psi. To better understand the bond properties of each wire and to evaluate the effect of differing concrete release strengths on bond, prestressing wire end-slip measurements and concrete surface displacement measurements were made on all beams immediately after detensioning, 1-week after detensioning, and prior to flexural testing. Transfer lengths for each specimen were then determined from the plotted values of surface strain.

All 27 beams were tested under three-point bending to determine the development lengths for each specimen. Results from the data obtained in this study were then used to compare bonding properties, assess accuracy of current equations for transfer and development length, and develop equations to predict transfer length and development length in members manufactured with the large-diameter indented prestressing wire used in this research.

Table of Contents

List of Figures

List of Tables

Chapter 1 - Introduction

1.1 Background of Prestressing

The application of pretensioned concrete has become increasingly popular over the years due to its economic advantages, efficiency in construction, and impressive strength capabilities. Heavy integration of this technology in the structural industry has brought about the need to be able to evaluate and predict types of failure in prestressed members. While several studies have been performed in efforts to predict flexural and shear failures due to bond in these members, research regarding the bond performance of single prestressing wire is still in its early stages.

One particular industry that depends heavily on prestressing bond performance is the concrete railroad tie industry. Concrete crossties offer several advantages in comparison to wood crossties including much longer life expectancy, higher and more dependable strength capacities, and reduced fuel consumption of trains. Records to date show that pretensioned concrete crossties have produced a more economical design and better structural behavior, which improves overall stability and performance of the railroad track (Lu Z., Boothby, Bakis, & Nanni). While concrete ties present a promising replacement for wooden ties, they are still susceptible to cracking and bond failure. To improve the lifespan and consistency of ties used in the field, research is needed to better understand the bond behavior of prestressing wire.

Several recent studies have been performed in efforts to investigate and improve the bond between the prestressing wire and concrete ties. Research has shown that concrete material properties, prestressing wire surface properties, and concrete release strengths all have an impact on the bond between the steel and concrete. Experimental data regarding the bond of pretensioned concrete ties indicated that the indentation pattern used on small diameter (5.32-

mm) wire used in ties has a large impact on the development length and flexural capacity of crossties in end regions (Momeni, 2016).

1.2 Problem Statement

The ability to predict bond behavior between prestressing reinforcement and concrete is imperative when determining the potential of certain reinforcement in structural applications. Development length is one of the most important parameters in predicting premature bond failure. A pretensioned member's development length is comprised of two lengths, the transfer length and the flexural bond length. Transfer length is the length required to transfer the initial prestressed forces from the prestressing steel to the concrete. In order to load a pretensioned member to its ultimate capacity and develop the ultimate stress of the prestressing wire, an additional bond length is required, known as the flexural bond length. If sufficient development length is not provided for the prestressing steel, the pretensioned member will fail in bond prior to reaching its ultimate capacity.

While several studies have been performed regarding the use of small diameter prestressing strand and 5.32-mm prestressing indented wire (most commonly used in concrete crossties), little research has been done on the performance of larger diameter indented wire. Large diameter indented prestressing wire could possibly hold promise in concrete railroad ties or other structural applications such as prestressed sandwich wall paneling. This study looks to further investigate the bond performance of large diameter prestressing wire.

1.3 Research Objectives

The primary objectives of this study are as follows:

1. Determine the resulting transfer length from 3 types of indented prestressing wire in pretensioned beams
2. Load the pretensioned beams in flexure to determine the resulting development length for each type of wire
3. Use the information obtained to analyze and compare bond properties of the three wires

1.4 Research Scope

This study was divided into two separate parts. In the first phase of the research, surface displacement and end-slip measurements were taken on 27 pretensioned concrete beams with a rectangular cross section of 6"x10". Three different types of indented prestressing wire were used in this study, which consisted of 7.8-mm-diameter HSM-1 and HSM-3 wire, and a 7.5-mm-diameter Voestylpine wire. Two of the same wires were used in each beam, spaced 2 inches on center and embedded 2 inches from the bottom of the member. The prestressing reinforcement was initially tensioned to 75% of its ultimate stress, and gradually detensioned at concrete strengths of 3500 psi, 4500 psi, and 6000 psi in efforts to better understand the influence of concrete release strength on bond. Beam lengths of 5.5', 6.5', and 7.5' were cast to also study the effects of specimen length on force transfer. The concrete mixture in this study was kept constant with type III cement, granite aggregate, and an 8" slump. The measurements taken in this phase of the research were used to estimate the transfer length and give insight on the bond characteristics of the different wires.

In the second phase of the research, the beams were tested in three-point bending at variable span lengths to acquire estimations of the development length for each of the three wires. For each test, a concentrated load with a loading rate of 1000 lb/min (4448.2 N/min) was applied until the specimen failed by strand rupture or from bond failure. Load, deflection of the beam at the point of loading, and end-slip of the prestressing wires were monitored and recorded during testing. This information was then plotted to compare the bond properties of the different wires.

1.5 Organization of Dissertation

This dissertation is organized into 5 chapters. Chapter 2 consists of a literature review covering information regarding past research on prestressing reinforcement in pretensioned concrete members. Chapter 3 provides explanations of the materials and methods used in this study. Chapter 4 summarizes and analyzes the results found in this study and Chapter 5 includes the conclusions and recommendations for future research.

Chapter 2 - Literature Review

2.1 Background of Prestressing

The use of prestressing steel in concrete members has become increasingly popular over the years due to its impressive strength capacities, ease of construction, and economic advantage. Manufacturing of prestressed members can be performed off-site, leading to more rapid and cost-effective construction. The heavy integration of prestressed members in buildings, transportation, and other structural applications has made predicting failures in these members even more imperative. Failure due to flexure and shear has long been researched, however premature failure of prestressed members due to loss of bond is in its earlier stages.

Typical prestressing steel consists of helically wound multiple wire strand ranging from 3/8” to 5/8” diameter. These multiple wire strands are commonly used in prestressed girders and beams. The railroad industry has been applying this prestressing science to concrete ties since the 1970’s, trying to create a stronger and more efficient crosstie than the typical wooden crosstie previously used. “Experience to date indicates that use of concrete ties is desirable for reasons of economy as well as for the superior structural properties that add considerably to the overall stability and performance of the track structure.” (Hanna, 1979, p 31). In early concrete tie designs, failure was most commonly due to prestressing bond and allowable stresses of the concrete in tension. These bond and stress issues have since been resolved through the use of smaller diameter wire set in uniform patterns to avoid concrete cracking upon prestressing transfer. Indenting the prestressing wire has further improved the bond between the steel/concrete interface, resulting in more efficient transfer of prestress forces and shorter development lengths. Transfer length and development length are essential parameters in determining proper transfer of forces and provide valuable insight on how the member will perform under maximum loading.

2.2 Transfer Length vs. Development Length

The transfer of prestress forces in pretensioned members is heavily dependent on the bond between the concrete and reinforcement being used. The length of bond from the end of the member to the point where the member reaches its ultimate flexural capacity is known as the development length. The development length is made up of two lengths:

1) Transfer length, L_t, is the length from the end of the member required to transfer the total effective prestress force, f_{pe}, from the reinforcement to the concrete through bond.
2) Flexural bond length, L_{fb}, is the additional length of bond required to ensure the prestressing steel reaches its ultimate tensile stress, f_{ps}.

Loading or cracking of a member within the development length will result in inadequate bond, causing premature failure of the beam. Members are said to fail in bond when the prestressing reinforcement in a member loses bond with the surrounding concrete and slips, thus reducing the ultimate capacity of the member. Bond development is heavily dependent on the size and surface profile of the reinforcement, the concrete strength, and the physical mechanisms present between the materials in the member.

2.2.1 Physical Bonding Mechanisms

Prestressing reinforcement primarily acquires bond through mechanical interlock due to friction with the surrounding concrete. During the initial pretensioning of steel, the elongation of the reinforcement causes it to shrink radially due to the Poisson effect. Once the concrete is cast and has reached the desired compressive strength, the prestress forces are released causing the reinforcement to expand radially back toward its original diameter. The amount of radial contraction and expansion during the prestressing process is dependent on the Poisson's ratio of the reinforcement. As the reinforcement attempts to return to its original shape, forces normal to the wire surface are generated and a wedging effect takes place. This wedging effect between the wire and concrete creates additional shear and radial stresses in the concrete, improving the bond between the steel and the concrete in a phenomenon known as the Hoyer Effect.

The opposite effect happens when the member is loaded in flexure. As the member is loaded the prestressing reinforcement approaches its ultimate tensile capacity, shrinking radially along flexural bond length. The decreased diameter of the wire results in reduced contact between the concrete and reinforcement, thus reducing bond. Bonding capacities within the transfer length are larger than those within the flexural bond length due to the Hoyer Effect. This causes the slope of the accrued pretensioning forces within the transfer length to be steeper than that within the flexural bond length. For this reason, structural concrete requirements recommend a bilinear model to represent the prestressing forces present in reinforcement over the development length. The bilinear model for prestress forces within the development length is shown in Figure 2.1.

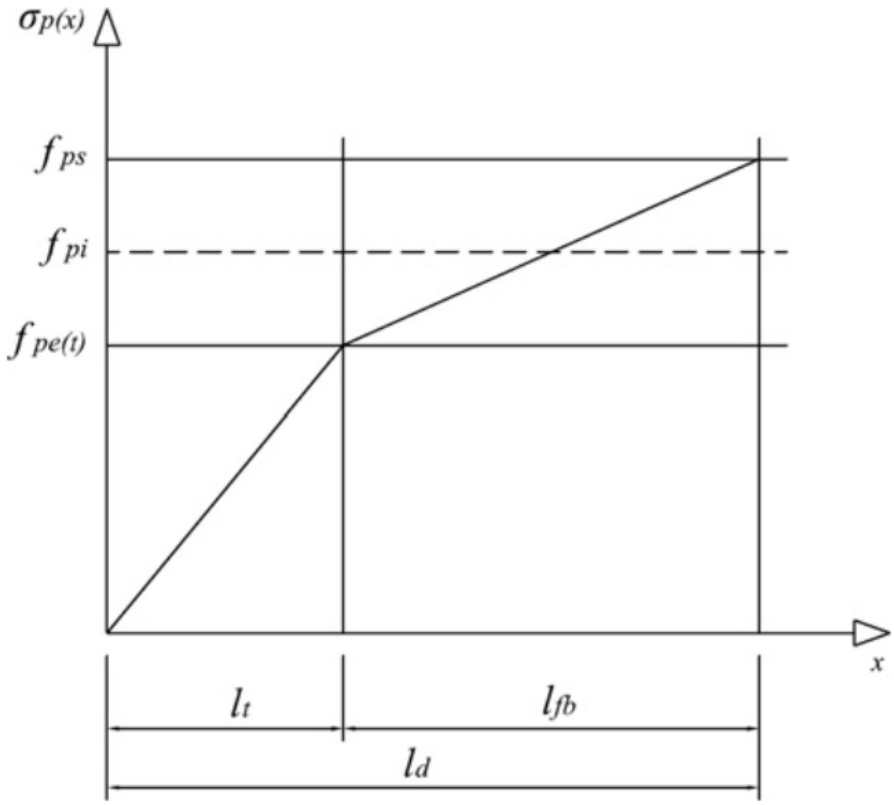

Figure 2.1: Bilinear Model for Transfer and Flexural Bond Length (Vazquez-Herrero, Martinez-Lage, Aquilar, & Martinez-Abella, 2013).

Multiple wire strands, which are wound in a helical pattern, rotate, or "screw in" to the concrete upon detensioning. This action produces additional shear stresses in the concrete resulting in additional radial stresses, thus increasing the bond due to friction and mechanical interlocking. Indented wire, commonly used in concrete railroad ties, also produces additional shear stresses along the steel and concrete interface. These auxiliary stresses further improve the mechanical interlock between the reinforcement and concrete, resulting in better bond between the materials and lower transfer and development lengths.

2.2.2 Experimental Methods for Characterizing Prestressed Steel Bond Behavior

Several experimental methods exist that can closely exemplify the bond behavior of prestressed steel in concrete:

I. Methods that use the change in a prestressed concrete member's surface profile to determine transfer lengths.

II. Methods that use flexural load testing to determine development lengths in eccentrically prestressed members.

III. Methods using small-scale test samples to define bond behavior or prestressing reinforcement, which can be categorized as either:

   a. Pull-out tests, in which a concrete sample is cast around reinforcement with or without initial tensioning. Once the concrete reaches the desired compressive strength, reinforcement at one side of the specimen is increased in tension.

   b. Push-in tests, where a concrete sample is cast around initially pretensioned reinforcement. Once the concrete reaches desired strength, the tensile force is slowly released on a certain end of the sample, creating a gradient of stresses along the bond length of the sample.

   c. Combined testing, using both the pull-out and push-in methods (Vasquez-Herrero, Martinez-Lage, Aquilar, 2013)

The most accurate representation of bond performance is found through analyzing a prestressed member's transfer length. However, this is typically a costly and time-consuming process. Over the years, numerous experiments have been performed in attempts to characterize the bond behavior of prestressing wire. These tests are known as: Large Block Pull-Out tests, Post-Tensioning Institute (PTI) bond tests, and North American Strand Producers (NASPs) bond tests.

Large block pull-out tests, later named the Moustafa test after Dr. Saad Moustafa, were performed in 1974 at the Concrete Technology Corporation (CTC) to test 0.5 in. diameter strand's potential for lifting loops in precast concrete memebers. The test consisted of embedding 18 inches of wire into a concrete block, and pulling the wire with a hydraulic jack until failure. Additional testing was performed in 1992 via the Moustafa test to investigate a lifting loop failure that took place at CTC, along with other anchorage failures observed in the rock anchor industry at the time (Rose & Russell, 1997).

Figure 2.2: Example of Moustafa's Large Block Pull-out Test (Logan, 1997, p. 62).

The PTI bond test, also known as the Prestressing Strand Bond Capacity Test, was developed by the Post-Tensioning Institute to determine the bonding capability of 0.6-inch diameter prestressing strand in cement grout, mainly for use in tensioned ground anchors. In this test, individual strand samples were cast into a 5-inch diameter grout cylinder. The strand was then pulled at a rate of 0.1 inch/minute until the non-tensioned end of the wire reached a slip of 0.01 inches, indicating the strand's bond strength. This procedure has since been adopted by the standards code as ASTM A981, the Standard Test Method for Evaluating Bond in 0.6-inch Diameter Steel Prestressing Strand, Grade 270, Un-coated, used in Prestressed Ground Anchors (Russell and Paulsgrove, NASP Strand Bond Testing Round 1, 1999).

Since the ASTM A981 bond test was primarily for determining bond behavior of prestressed anchors, the North American Strand Producers (NASPs) modified the test to be more representative of prestressed strand. The NASP bond test specimens consisted of strand embedded 18 inches into a 5-inch outer diameter cylinder filled with sand cement mortar, with a 2" bond breaker as shown in Figure 2.3 below. The strand was pulled in tension, documenting the tensile load when the non-tensioned side of the strand slipped 0.01 inches and 0.1 inches, along with recording the ultimate load (Ramirez and Russell, 2008).

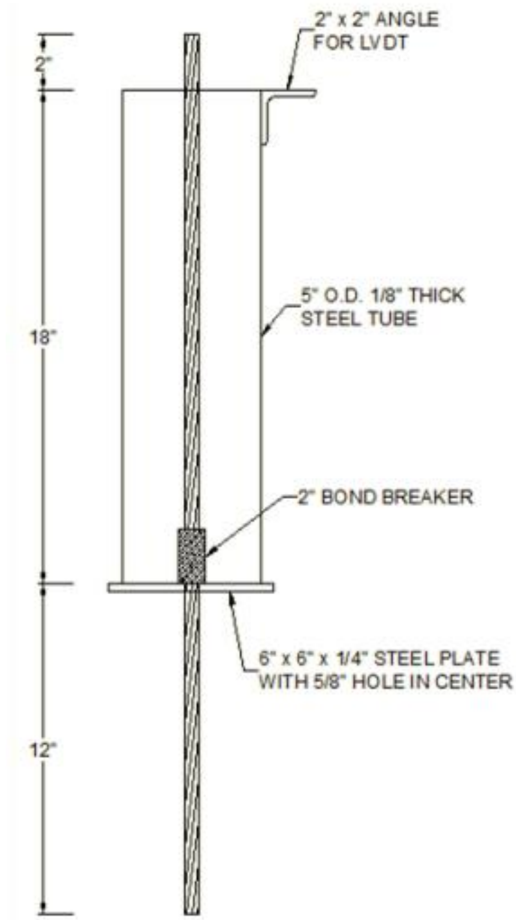

Figure 2.3: Example of Test Specimen for the NASP Bond Test, or ASTM A1081 (Porterfield, Volz, Myers, Sneed, 2012, p 43).

In the second round of the NASP testing, nine different strands were tested at different laboratories to evaluate the accuracy of each method listed above. Results of the testing showed that all three of the test methods were successful in differentiating strands with good quality to those with poor bond quality. It was also found that the NASP pullout test method had the most consistent results when compared to the Moustafa and PTI pullout test methods (Russell & Paulsgrove, NASP Strand Bond Testing Round II, 1999). A third round of the NASP testing study was performed to investigate the level of consistency and reproducibility of the three tests. In addition, the results from each testing laboratory were compared to the transfer and development lengths found from testing rectangular and AASHTO sections to determine accuracy. The results of this study indicated that the NASP bond test was the most reproducible and the most descriptive of prestressing strand bond behavior (Russell B.W., NASP Strand Bond Testing Round III). Following these results, it was recommended that further research be performed to develop the NASP pullout test by investigating the effects of mortar flow and compressive strength, loading rate of displacement-controlled tests, testing with load control versus displacement control, and the effects of temperature during the curing process. As expected, it was found that the mortar mixture's compressive strength had a large role in pullout strengths. By using a higher compressive strength, strands could be differentiated and ranked in bond performance much more easily. The results also recommended that the testing procedure remain utilizing displacement control loading since no direct correlation was found through applying different loading rates. Further testing confirmed that the NASP testing method is a reproducible test method when testing at different laboratories with differing materials. (Russell B., NASP Strand Bond Testing Round IV, 2006). The NASP pullout testing method was accepted by ASTM in 2012 as the Standard Test for Strand Bond as ASTM A1081, the "Standard Test Method for Evaluating Bond of Seven-Wire Prestressing Strand" (ASTM A1081, 2012). Further testing of the NASP testing procedure showed that the test method was able to successfully differentiate different strands' ability to meet ACI development length requirements, concluding that the test method was a proven method for evaluating bond in prestressing strand.

In the due diligence report for the NASP pullout test, it was stated that concrete manufacturers should not solely rely on the test for bonding properties, but should also run additional quality assurance tests to confirm bonding properties. Two quality assurance methods that were recommended were the Moustafa or Peterman Beam Test specimens (Hawkins & Ramirez, 2010). Additional investigation of the NASP method resulted in the recommendation that protocols be added to the NASP test procedure to ensure reliability and accuracy of results.

While bond pullout tests had become a more common indication of bond characteristics for 0.5-inch and larger prestressing strand, no pullout tests had been conducted on smaller diameter strands or prestressing wire. To address this deficiency, Matthew Arnold conducted a testing program at Kansas State University to develop and test the validity for wire and smaller diameter (less than 0.5 in.) prestressing strand pullout tests. For this study, a total of thirteen 5.32-mm wires and six strands were tested. Similar to the Standard Test for Strand Bond (ASTM A1081) for 0.5-in. diameter seven-wire strand, prestressing wires were cast into a 4-in. outer-diameter tube with a 1/8-in. wall thickness. The cylinder was then filled with a sand-cement mortar mixture with a water-to-cement ratio of 0.427 and a sand-to-cement ratio of 2.0. The cement used was a Type III cement from Monarch Cement Company which conformed to ASTM C150. The sand was pre-sieved, conforming to ASTM A778, and was sourced from Humboldt Manufacturing Co., Ottawa, Illinois (Arnold, 2013). Lengths of 20” wires were inserted 10 inches into the cylinder, with only 6 inches in contact with the Ottawa sand-cement mortar and another 2 inches extending past the top of the cylinder, as shown below.

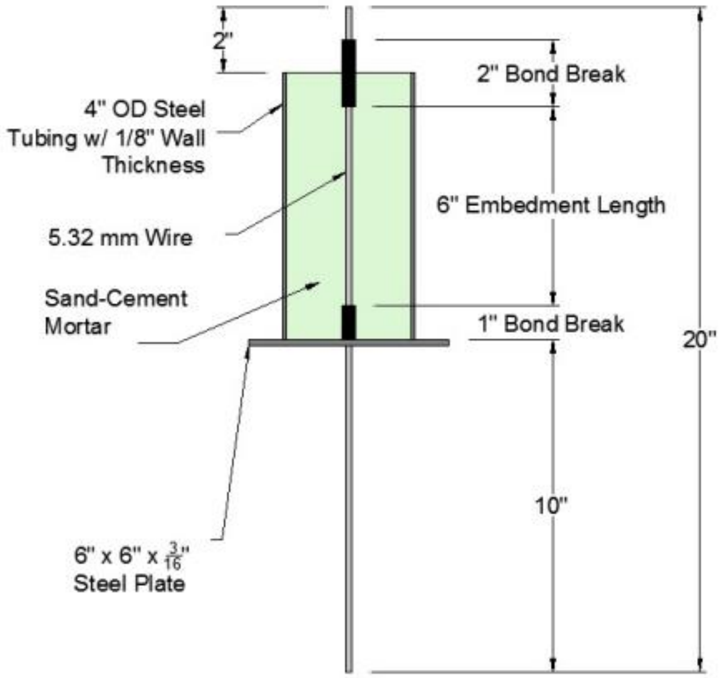

Figure 2.4: Dimensions of Wire Pullout Test Specimen (Arnold, 2013).

Pullout tests were then performed shortly after the mortar reached a cube compressive strength of 4,500 psi, and before the strength reached 5,000 psi (Arnold, 2013). Wires were pulled at a rate of 2,000 lbs/minute at the bottom of the cylinder, while the applied load and free-end slip at the top of the cylinder were monitored. Two testing specimen sizes were used for the strand testing phase of the study. The first size was the same as the NASP Standard Bond Test, which was 16 inches. The second specimen size used only 9 inches of embedment length. Schematics of both the standard bond test and the reduced, 9-inch test, are shown below in Figure 2.5.

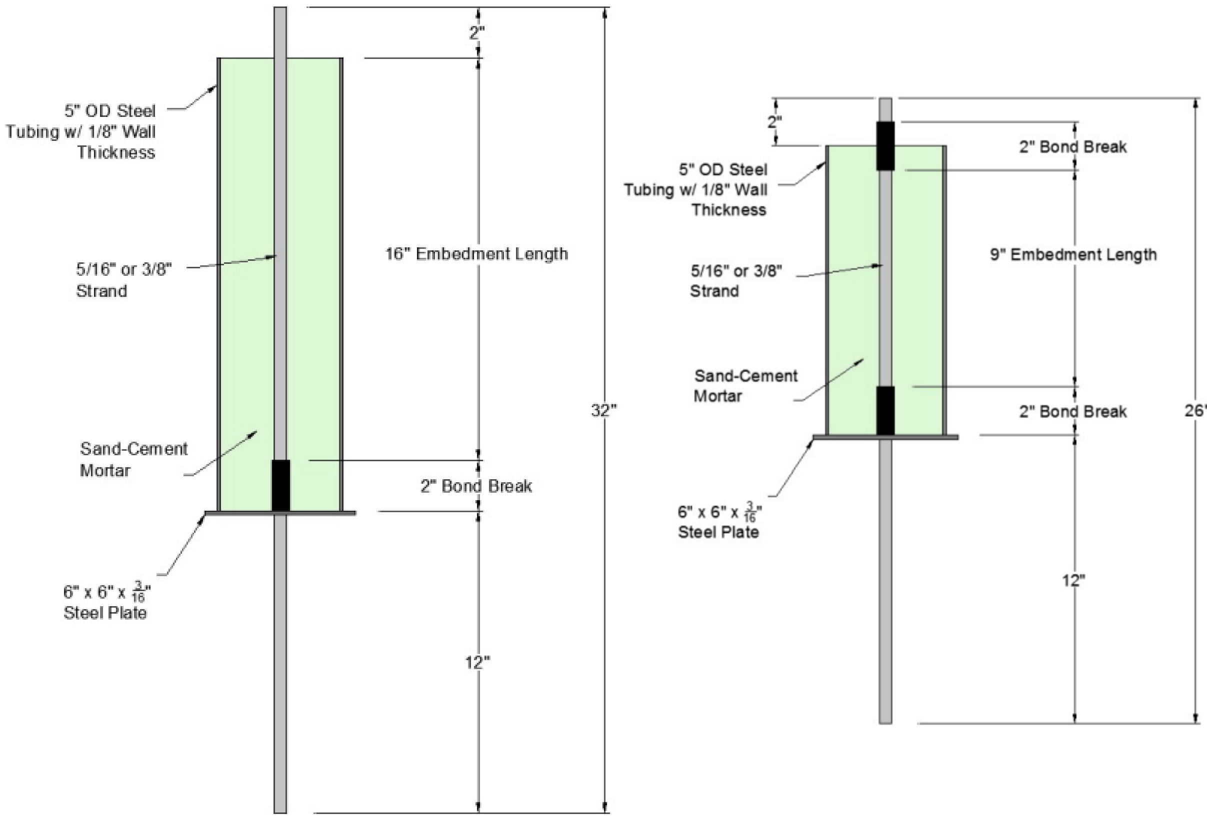

Figure 2.5: Schematics of both the 16-inch and 9-inch Strand Pullout Specimen (Arnold, 2013).

These pullout tests were also performed when the mortar cube strength reached 4,500 psi and before the cube strength reached 5,000 psi. Strands were loaded at a displacement-controlled loading rate of 0.1 inch/minute, while monitoring and recording end slip data and the applied load.

Similar tests were then performed in the plant at CXT Concrete Ties and compared to the results obtained at KSU. Along with pullout tests of fifteen reinforcements from seven different steel manufacturers (the same that were used at KSU), transfer lengths were measured in actual, non-prismatic concrete railroad ties. Approximately fifty transfer length measurements and six pullout specimens were obtained for each type of reinforcement (Arnold, 2013). Testing at CXT followed the same general testing protocol that was followed at KSU, however 4-in x 8-in cylinders were used in place of the 2-in. mortar cubes. Specimens with wire utilized a bond length of 6-in. and the specimens with strand utilized a 4-in. bond length. Rather than a mortar mix, a type III cement conforming to ASTM C150 with a water-to-cement ratio typical of most railroad tie plants was used.

From the results, Arnold was able to conclude that his un-tensioned wire pullout test developed at Kansas State University was able to distinguish between higher and lower bonding wires and showed great correlation with bond performance, especially the transfer length when recording the pullout force at or before 0.10 inches of end-slip. This test demonstrated high repeatability, yielding consistent pullout strengths for six different mortar batches, and was later accepted as ASTM 1096 – "Standard Test Method for Evaluating Bond of Individual Steel Wire, Indented or Plain, for Concrete Reinforcement". For the smaller diameter prestressing strand, several tests resulted in strand rupture. It was found that the Standard Test for Strand Bond can be used for smaller diameter strands by shortening the embedment length to 9 inches and overall specimen length to 12 inches.

It was also found that surface condition of the wires, such as rust, is not a dominant factor in bond, but that the indent geometry plays a large role. The testing results showed that strand pullout tests performed in mortar had poor correlation with transfer lengths found in actual concrete railroad ties. However, there was an excellent correlation between the wire pullouts in mortar and transfer lengths measured from concrete railroad ties. Equation 1 below was recommended for predicting the transfer length of concrete railroad ties using prestressed wires.

$$TL = -0.00080\ (Max\ Force) + 15.2 \qquad \text{(Equation 1)}$$

Where: $TL =$ expected transfer length in concrete railroad ties using pretensioned wires in inches

$Max\ Force =$ maximum force ≤ 0.10 in. end slip

2.2.3 Existing Analytical Models for Calculating Transfer and Development Length

Transfer length is believed to be one of the most important details used when analyzing the bond characteristics of a prestressed specimen. Several analytical models have been developed in efforts to more accurately predict transfer lengths in members.

In 1953, Yves Guyon proposed that the transfer length of a member was directly proportional to the draw-in of the prestressing reinforcement, and inversely proportional to the initial prestressing strand stress.

$$L_t = \alpha \cdot \delta \cdot \frac{E_p}{f_{pi}} \qquad \text{(Equation 2)}$$

Guyon's proposed formula, shown in Equation 2, relates the transfer length, L_t, to the reinforcement draw-in, δ, where E_p represents the modulus of elasticity of the prestressing reinforcement, and f_{pi} represents the prestressing reinforcement stress immediately before transfer of prestress forces. The Guyon coefficient, α, is implemented to consider the stress distribution profile of the concrete in the transfer length ($\alpha = 2$ for a constant bond stress distribution, $\alpha = 3$ for a linear bond stress distribution). It should be noted that Equation 2 was formulated assuming that the flat sections of the member remain flat within the transfer length, which is not completely true due to most of the transfer length being affected by shear lag and the Saint-Venant effect (Vasquez-Herrero, 2013).

In 1993 Gyorgy L. Balaz presented another equation for estimating transfer length that related the same variables used in Guyon's theory. Balaz's proposed formula is shown in

Equation 3, where b represents an experimental or assumed bond stress-slip relational coefficient between zero and one which depends on the concrete type and type of prestressing strand.

$$L_t = 2 \cdot \delta \cdot \frac{E_p}{\left[f_{pi}(1-b)\right]} \qquad \text{(Equation 3)}$$

The draw-in of the prestressing reinforcement immediately after force transfer can be calculated by Equation 4, assuming that the pretensioning stress obeys Hooke's Law and remains elastic.

$$\delta = \int_0^{Lt} \frac{f_{pi} - \sigma_p(x)}{E_p} dx - \int_0^{Lt} \varepsilon_c(x) dx \qquad \text{(Equation 4)}$$

where: $\varepsilon_c(x)$ = Instantaneous longitudinal strain of the concrete due to the release of prestressing forces at a distance "x" from the member's end (positive compressive strain).

$\sigma_p(x)$ = Stress in prestressing reinforcement after force transfer, located at a distance "x" from the member's end.

f_{pi} = Initial strand stress immediately before transfer of prestress forces. (Vasquez-Herrero, Martinez-Lage, & Martinez-Abella, 2013).

End slip measurements can also be used to estimate transfer length by applying Hooke's law and assuming a straight-line stress variation from the end of beam to full prestress at the transfer length.

$$\Delta = \frac{PL}{AE} = \frac{fL}{E} = \frac{(0.5 f_{si} L_{tr})}{E_{ps}} \qquad \text{(Equation 5)}$$

Where: Δ = Measured end slip, in inches

$0.5f_{si}$ = Average initial strand stress over the transfer length after release, in ksi (assuming a straight-line stress variation from end of beam to full prestress at the transfer length)

L_{tr} = Transfer length, in inches

E_{ps} = Modulus of elasticity of prestressing strand, in ksi

By rearranging the equation, the end slip measurement can be used to infer a transfer length:

$$L_t = \frac{\Delta * E_{ps}}{0.5f_{si}} \qquad \text{(Equation 6)}$$

Transfer length and development length have also been found to be directly related to the strand diameter. In 1959, researchers Hanson and Kaar conducted an experimental program which resulted in recommended minimum embedment lengths for different sizes of strand diameter (¼ , ⅜, and ½ inch). Later, in 1962, Alan Mattock used these results to propose Equation 7 and Equation 8 for estimating transfer length and development length.

$$L_t = \left(\frac{f_{se}}{3}\right)D \qquad \text{(Equation 7)}$$

$$L_d = (1.11f_{su} - 0.77f_{se})D \qquad \text{(Equation 8)}$$

where: f_{se} = the effective stress in prestressing strand, in ksi

f_{su} = the average stress in prestressing strand at ultimate load, in ksi

D = the nominal strand diameter, in inches

Dr. Mattock's expression for development length was later modified by the ACI committee in 1963 and is shown in Equation 9 (Tabatabai & Dickson, 1995).

$$L_d = \frac{1}{3} f_{se} D + (f_{su} - f_{se}) D \qquad \text{(Equation 9)}$$

This updated development length equation and Mattock's transfer length equation appear in today's ACI code. Since ACI's adoption of these equations in 1963, and later adoption by the American Association of State Highway and Transportation Officials (AASHTO) in 1973, numerous researchers have made efforts to improve the accuracy of the equations by studying the effects of higher strength concrete and differing prestressing strand material properties.

In 1976, after studying a bond related failure in a pretensioned member, researchers Martin and Scott determined that the recently adopted equations needed to be reassessed. In Hanson and Kaar's initial study, on which the current code equations were based, pretensioned strands were released gradually. While gradual release is used in some prestressed applications, the most common release methods used in the industry are saw cutting and flame cutting, which result in a much more sudden release of prestress forces (Martin & Scott, 1976).

Martin and Scott pointed out that 270 ksi ultimate strength prestressing strand was also becoming more common, giving even more reason to reexamine the adopted equations for transfer and development length. Further investigation into Hanson and Kaar's findings inferred that in structural members containing less than 0.31 percent steel, strand bond slip would likely occur before the section reached 90 percent of its design strength. (Martin & Scott, 1976).

Martin and Scott's re-evaluation of the transfer length equation was based on the transfer length study published by Kaar, LaFraugh, and Mass in 1963, where strands were released by flame cutting (Martin & Scott, 1976). Their research resulted in a much more conservative equation for transfer length, equal to 80 times the diameter of the strand when using 270 ksi strand, compared to the original expression for transfer length which could be estimated to be around 50 times the diameter of the strand when assuming an effective prestress of 150 ksi. Martin and Scott’s more conservative approach to calculating transfer length is shown in Equation 10.

$$L_t = 80D \qquad \text{(Equation 10)}$$

In 1977 Zia and Mostafa also published their recommendations for transfer length and development length equations. Their approach resulted from a linear regression analysis from data available at the time, ranging from concrete compressive strengths of 2 ksi to 8 ksi. The proposed equations, shown in Equation 11 and Equation 12, incorporated the concrete compressive strength at time of prestress release f'_{ci}, along with the strand diameter and initial prestressing forces. These equations were later discovered by Cousins et al. to be a more conservative expression for larger diameter strands, when compared to the equations adopted by ACI (Balazs, 1992).

$$L_t = 1.5\left(\frac{f_{si}}{f'_{ci}}\right)D - 4.6 \qquad \text{(Equation 11)}$$

$$L_d = 1.5\left(\frac{f_{si}}{f'_{ci}}\right)D - 4.6 + 1.25(f_{su} - f_{se})D \qquad \text{(Equation 12)}$$

After the introduction of epoxy-coated strands, Cousins et al. (1986) conducted a study comparing the code accepted equations to the transfer and development lengths of rectangular beams prestressed with un-coated and epoxy-coated strand. In their study, transfer lengths were taken on square beam sections prestressed with a single concentric strand and rectangular beam sections prestressed with a single prestressing strand located towards the bottom of the beam. Results of this study showed that three types of uncoated prestressing strand required higher transfer lengths than what was predicted by the code, inferring that the ACI transfer length equation at the time underestimated the expected transfer length (Cousins, Johnson, & Zia, Transfer Length of Epoxy-Coated Prestressing Strand, 1990).

Cousins' findings alarmed the FHWA, leading them to place restrictions on prestressing strand and enforce a minimum strand spacing distance of 4 times the strand diameter, along with a 1.6 multiplier to the development length of fully bonded strands and a 2.0 multiplier to the development length of de-bonded strands (Akhnoukh, 2008), (Russell & Burns, 1993). The FHWA modified their equation for development length of fully bonded strands in 1988, which can be seen in Equation 13.

$$L_d = 1.6\left[\frac{1}{3} f_{se} D + (f_{su} - f_{se}) D\right] \qquad \text{(Equation 13)}$$

In an attempt to relieve any uncertainty toward the recommended transfer length and development length expressions, the FHWA decided to review the existing data from studies performed throughout the United States. Dr. Dale Buckner was chosen to review the data on behalf of the FHWA. During his investigation, it was found that the ACI/AASHTO transfer length equation underestimated the mean transfer lengths for Grade 270, seven-wire, low-relaxation uncoated strand. Buckner recommended that the equation proposed by Shahawy et al. (1992) found during a study funded through the Florida Department of Transportation (FDOT) be used. Shahawy's proposed equation replaced the term for the effective prestress with the initial stress in the strands before prestress losses, and is shown in Equation 14.

$$L_t = \frac{1}{3} f_{si} D \qquad \text{(Equation 14)}$$

Buckner recommended that for strands, either straight or draped, that end in the upper one-third of the member depth and have at least 12 inches or more of concrete cast below, that a factor of 1.3 be applied to Equation 14. Strands ending in other locations need not be factored. Equation 14 shown above is about 20 percent longer than what was currently accepted in the ACI/AASHTO code. This 20 percent increase in transfer length, mainly coming from switching from Grade 250 strand to Grade 270 low relaxation strand, changes the recommended transfer length approximation in code for shear criteria from $50d_b$ to $60d_b$ (Buckner, 1995).

Dr. Buckner also recommended revising the current development length equation after reviewing previously proposed development length equations and his findings from his transfer length study. Buckner proposed a more conservative expression than that seen in ACI code, stating that conservatism is necessary to reduce the potential for web shear cracks propagating through the strand transfer zone, inducing sudden failures without warning in shear related bond failures. The recommended strand development length expression is shown in Equation 15.

$$L_d = \frac{1}{3} f_{si} D + \lambda (f_{su} - f_{se}) D \qquad \text{(Equation 15)}$$

For general applications, Buckner defined λ as ($0.6 + 40\varepsilon_{ps}$), where ε_{ps} is the strain at f_{ps}. As recommended with transfer length, a factor of 1.3 should also be applied to the development length calculation when the strand end is located in the upper one-third of the member with 12 inches of concrete beneath it. For strands ending in other regions, this factor need not be included (Buckner, 1995).

In 1997, Donald R. Logan assembled a team of prominent individuals with extensive background in bond research, which included Roger Becker, Robert Mast, Saad Moustafa, Donald Pellow, Bruce Russell, and Norman Scott, to investigate the transfer and development lengths of strand samples sourced from different regions in North America. In his research, Logan noted that despite reliance on ACI equations for estimation of transfer and development lengths, the capability of strand to bond to concrete varies considerably depending on the source of supply of the strand. The objectives of this study were to attempt to correlate the pull-out capacity of prestressing strand to its transfer and development lengths in flexural beam tests, establish minimum acceptable pull-out capacities that reliably predict satisfactory performance in flexural beam tests, evaluate the reliability of end slip measurements at release of prestress as a predictor of bond behavior, and determine if there were obvious strand surface properties or dimensional variations that are indicative of strand bond quality (Logan, 1997). For the pull-out test specimens (using the Moustafa Method previously mentioned), six 34-inch samples of each of the six 0.5-inch diameter, 270 ksi strand, were tied to light reinforcing bar cages in two, 6'-8" long, 2'-0" wide by 2'-0" deep, test blocks. Strands were embedded 18 inches into Stress-con's standard 7.0-sack cement, sand and crushed gravel mix designed to reach 4,000 psi overnight and 6,000 psi after 28 days. Results of the pull-out test showed that 4 of the groups tested above 36 kips average maximum pull-out capacity, while the other 2 groups only reached average maximum loads of 11.2 and 10.7 kips, 30 percent of the 1974 benchmark level.

Along with the block-pullout tests, 6 – 90 ft transfer/development length prestressed test beams were cast. Once concrete compressive strength reached 4,254 psi, both ends of the prestressing reinforcement were flame-cut simultaneously to simulate common production conditions. Beams were then saw-cut into 18 ft sections, allowing for a development length test at each end for a total of 60 tests. Four different test load arrangements were used, varying the embedment length (length from the end of the beam to the point of maximum moment) between the calculated strand development length using ACI Code for both the simple beam and cantilever beam test conditions, calculated strand transfer length using ACI Code tested in the cantilever condition, and 80 percent of the calculated strand development length in the simple beam condition. The beams, which were designed to fail in flexure, had a cross section of 6.5 inches wide by 12 inches deep, with a single strand centered 2 inches from the bottom of the beam.

Transfer lengths were obtained indirectly from measurement of end slip of the strand into the concrete at the end of the beams using the following equation:

$$L_t = \frac{\Delta * E_{ps}}{0.5 f_{si}} \qquad \text{(Equation 2)}$$

Initial end slip measurements were used to estimate transfer lengths for the beams in Logan's study resulting in lower transfer lengths at release of prestress for all strand groups but one when compared to the ACI transfer length formula of $L_{tr} = d_b f_{se}/3$. As subsequent end slip measurements were taken, it became evident that the transfer lengths of two groups were increasing significantly over time, whereas the remaining four groups remained below the ACI prediction.

Development testing resulted in four of the wire groups, the same wire groups that showed pull-out capacities exceeding 36-kips and end slip-derived transfer lengths lower than those found using ACI equations, testing extremely well, failing in flexure with no end slip. Conversely, the two wire groups that exhibited pullout capacities of less than 12 kips and transfer lengths that increased significantly over time performed very poorly in flexural testing. All failures during testing of these two groups of wires were due to loss of bond between the steel and the concrete. There was no obvious warning deflection prior to failure in these flexural tests, which made the failure mode of these two strand groups very undesirable.

In 1980, Robert Mast suggested to Logan that the factors which affect the transfer length upon transfer of prestress forces may also have a proportional effect on the flexural bond length (Logan, 1997). If correct, strand slip can then be used to modify the ACI development length equation for both transfer length and the flexural bond length by creating bilinear strand development diagrams, enabling computation of a bilinear moment capacity diagram for any specific member. Mast's "slip theory" was tested and verified in the mid 1980's, and was used again in this study to evaluate the efficacy of this concept. Advisory group member Roger Becker, who conducted research on Mast's slip theory at the University of Wisconsin, analyzed the results of this study and found great correlation with Mast's concept through modification of the ACI development length equation using transfer lengths derived using end slip. Analysis of the results showed that Mast's slip theory correctly predicted flexural failures in the 4 strands with minimal end slip, whereas the ACI equation predicted bond failure prior to reaching the full test load. Mast's slip theory also correctly predicted that the two strand groups that displayed poor bond quality would fail in bond prior to reaching the full test load, whereas the ACI code predicted flexural failures.

Later, in 2008, researchers Ramirez and Russell from Purdue and Oklahoma State University released another report regarding the estimation of bond properties. After their recent publication of the National Cooperative Highway Research Program Report 603 following NCHRP Project 12-60, the researchers became concerned that the current equation used in the code for transfer length did not consider the influence of concrete compressive strengths. The data from this report confirmed several findings from publications prior to the NCHRP study, reinforcing the importance of including concrete material properties in the equation for transfer length.

This study used a modified version of the NASP Bond test. As previously mentioned, the NASP Bond test, which was developed by Russell before execution of the NCHRP study, consisted of casting prestressing strand into mortar and performing pullout tests. For the purposes of the NCHRP study, mortar was replaced with concrete of different strengths. Ramirez and Russell examined 0.5 in. diameter and 0.6 in. diameter strand, with concrete strengths ranging from 4 ksi to 10 ksi.

Ramirez and Russell's research confirmed that the current AASHTO transfer length equation was adequate for predicting the transfer length of prestressing strands with "normal strength concrete", with concrete release strengths of around 4 ksi. Their data also confirms their speculations that variation of concrete release strengths does largely affect the transfer length, showing that the bond strength improves in proportion to the square-root of the concrete strength (Ramirez and Russell, 2008). When a concrete strength of 4 ksi is used, the proposed equation results in a transfer length of 60 strand diameters, concordant with the current design code. Using a higher concrete compressive strength results in shorter transfer lengths, with a minimum length limit of 40 strand diameters. Higher concrete release strengths have also been shown to result in shorter development lengths. The proposed equations for transfer length and development length including consideration of concrete strengths can be seen in Equation 16 and Equation 17, respectively (Ramirez & Russell, 2008).

$$L_t = \frac{120D}{\sqrt{f'ci}} \geq 40D \qquad \text{(Equation 16)}$$

$$L_d = \left[\frac{120}{\sqrt{f'_{ci}}} + \frac{225}{\sqrt{f'_c}}\right] D \geq 100D \qquad \text{(Equation 17)}$$

Several other experiments not mentioned in this study have been performed over the years in efforts to improve the accuracy of transfer length and development length estimations.

2.2.4 Existing Experimental Methods for Measuring Transfer Length

There are currently three techniques that are commonly used to measure transfer length in prestressed specimens. These techniques are based on measurements of the end slip of the prestressing reinforcement, the longitudinal surface strain profile of the concrete specimen, or the prestressing reinforcement stress.

The first method uses the Guyon theory, previously mentioned in Section 2.2.3. This method relates the transfer length of the specimen to the end-slip of the reinforcement during the transfer of prestress forces. Guyon proposed the following equation from his theoretical analysis in 1953 (Guyon, 1953).

$$L_t = \alpha \cdot \frac{\delta}{\varepsilon_{pi}} \qquad \text{(Equation 18)}$$

where: L_t = Transfer length

α = Coefficient representing the shape of the bond stress distribution over the transfer length ($\alpha = 2$ for constant uniform bond distribution, $\alpha = 3$ for linear descending bond stress distribution)

δ = End-slip of the prestressing reinforcement during prestress transfer

ε_{pi} = Initial tensile strain in the prestressing reinforcement

Alternatively, the other two methods relating end-slip to transfer length that were mentioned in Section 2.2.3, Balaz's theory and Hooke Law, can also be used.

The second method involves measuring the surface displacement of the concrete member to determine the surface strain profile of the pretensioned member. This surface strain profile can then be used to determine the transfer length of the specimen. One way to measure the change in surface displacement of the member is to apply measurable inserts along the length of the prestressed beam. Once the member is detensioned, the surface strain of the member will change in accordance with the strain profile. A mechanical gauge can then be used to measure changes between inserts. Comparing the recorded surface measurements in the concrete before detensioning with the surface displacement after release of prestress forces will show the variation of surface strains along the beam. A faster, non-contact method that also can be used to measure the strain in the concrete is Laser-Speckle Imaging (LSI). LSI was introduced by researchers at Kansas State University in 2012. This new method uses laser-speckle patterns that are generated and digitally recorded at various points along the prestressed concrete member. From this data, accurate measurements of transfer length can be rapidly obtained (Zhao, W., Murphy, R.L., Peterman, R. J., Beck, B., & Wu, C.-H., 2012). These strain profiles determined through the previously mentioned methods show strain values increasing along the transfer length until the concrete strains reach a plateau, similar to that shown in Figure 2.6.

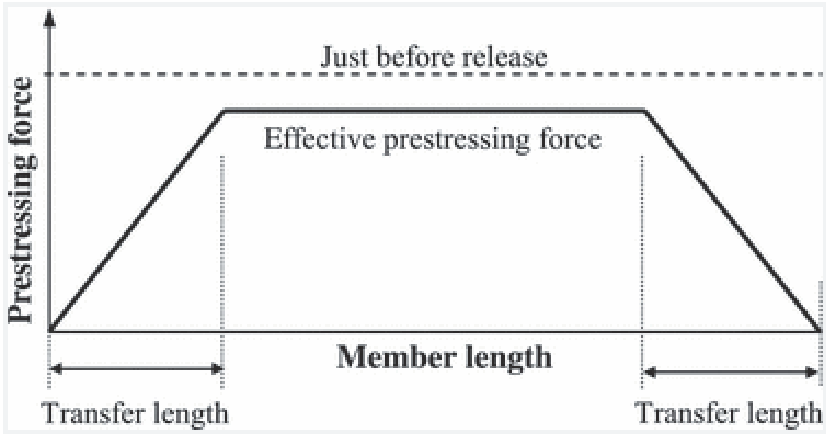

Figure 2.6: Idealized Strain Profile Depicting Transfer of Prestress Forces (Marti-Vargas, J., Caro, L., & Serna, P., 2013).

This strain plateau represents the location at which full transfer of prestress forces in the beam is present. The transfer length can then be determined from the strain profiles by using the slope-intercept method (Deatherage, Burdette, & Chew, 1994), the 95% Average Maximum Strain (AMS) method (Russel & Burns, 1996), or the Zhao-Lee method (Zhao, Beck, Peterman & Lee, 2013). It is common for researchers to use smoothing techniques for these profiles in order to produce more accurate transfer length predictions, while other researchers prefer to use raw data (Lu Z., Boothby, Bakis, & Nanni, 2000).

The third method used to determine the transfer length is to attach electrical-resistance strain gauges or vibrating wire gauges to the surface of the prestressing reinforcement. Electrical-resistance strain gauges determine the strain of the reinforcement upon detensioning by detecting changes in electrical resistance of the gauge, converting the mechanical strain of the gauge into an electronic signal. Vibrating wire gauges determine strain by detecting changes in the natural frequency of the wire after stress is applied to it (Zhao, 2011). This method and the application of these types of gauges is less common due to the susceptibility of the strain gauges to damage during strain gauge application and the beam casting process (Marti-Vargas, J., Caro, L., & Serna, P., 2013).

2.2.5 Existing Experimental Methods for Measuring Development Length

The most common way to accurately measure the development length of a member is through three-point bending. This is performed by incrementally loading the specimen over the development length. When the member is loaded in flexure, a flexural crack will form on the bottom of the beam coincident with the loading point at the top. As the crack grows, the tensile reinforcement is pulled to its ultimate stress, not unlike in a block pullout test. If a member is loaded in flexure outside of the development length, the member will reach its full capacity and fail in flexure as a result of strand rupture. When a member is loaded inside its development length, the strand will lose bond with the concrete and slip into the beam, denoting a failure in bond. The minimum length at which the beam is loaded that still results in a flexural failure is the development length. This method has been used in numerous studies investigating the bond mechanics of different prestressing materials and is still confidently used today.

2.3 Modeling Stress-Strain Curve for Wires – Power Formula

In the past, PCI stress-strain equations that were developed primarily for seven-wire prestressing strand were used to estimate the stresses in prestressing wire. However, through tensile testing of the materials, differences in the wire properties have been discovered, showing the PCI equations underestimate the true strength of prestressing wire. In 2016, researchers at Kansas State University (Chen, 2016) set out to find an appropriate equation that accurately estimates the linear and post-yield behavior of prestressing wire. In this research, regression analysis equations were developed to generalize certain constants in the PCI equation. These equations were based on experimental fitting results for various types of 5.32-mm prestressing wire. The ultimate tensile strength, f_{pu}, and the Elastic modulus, E_p, were determined through testing of each wire used in the study. Wire strength parameters were obtained from manufacturer Mill Test Reports. The minimum elongation at ultimate strain was increased from 3% to 4%, since experimental data showed all wires elongated to strain of .04 or more. From this information, a design-oriented power formula was developed that could estimate stress for a range of specific wire grades, from 250 ksi to 300 ksi (1,724 MPa to 2,068 MPa). Current PCI equations only assume ultimate wire strengths of 250 ksi (1.724 MPa) and 270 ksi (1,862 MPa).

To calculate the stress in prestressing wire using these equations, first a constant K had to be found. The constant K is used to relate f_{py} to f_{pu} and was found through regression analysis of the experimental results. The equation for this linear regression relationship is as follows:

$$Kf_{py} = 1.1607f_{pu} - 60.0118 \qquad \text{(Equation 19)}$$

To account for any differences in wire properties and corresponding variance in ultimate strength, an additional linear regression relationship for yield strength (f_{py}) was derived:

$$f_{py} = 1.0017f_{pu} - 25.7794 \qquad \text{(Equation 20)}$$

$$Q = \frac{f_{pu} - Kf_{py}}{\varepsilon_{pu}E_p - Kf_{py}} \qquad \text{(Equation 21)}$$

The constant Q was then found by applying Equation 19 to Equation 21, and assuming an ultimate strain (ε_{pu}) of .04. Furthermore, setting f_{ps} equal to f_{py} in Equation 22 we can iterate to solve for the constant R.

$$f_{py} = E_p \varepsilon_{py} \left[Q + \frac{1-Q}{\left(1 + \left(\frac{\varepsilon_{py} E_p}{K f_{py}}\right)^R\right)^{\frac{1}{R}}} \right] \quad \text{(Equation 22)}$$

In Equation 22, the yield strain, εpy, is set equal to .01. The wire properties and the values calculated from the above equations, along with the new R parameter, can then be plugged into Equation 23 to find the stress in the prestressing wire at any given strain.

$$f_{ps} = E_p \varepsilon_{ps} \left[Q + \frac{1-Q}{\left(1 + \left(\frac{\varepsilon_{ps} E_p}{K f_{py}}\right)^R\right)^{\frac{1}{R}}} \right] \quad \text{(Equation 23)}$$

The equations used in the initial research of the power formula were not used in this study as this was proven only for 5.32-mm prestressing wire. A modified version of the power formula specifically fitted for larger diameter wires was used and is shown in Appendix A (Chen, Y., Peterman, R. J., 2016).

Chapter 3 - Methodology

3.1 Overview of Study

In this study, pretensioned concrete beams were fabricated using 3 different types of large diameter, chevron-indented prestressing wire. Prestressing wire end-slip and surface displacement measurements were taken before and after the detensioning process to determine the corresponding transfer length of each wire at different concrete release strengths. Once construction of the beams was complete, the specimens were load tested to estimate the development lengths for each wire. During loading of the beams, wire end-slip and vertical displacement of the beam at the loading point were recorded. The transfer and development length measurement procedures used in this study were referenced from previous studies investigating bond performance of prestressing reinforcement.

3.2 Specimen Design and Fabrication

3.2.1 Concrete Mixture

The concrete mixture used in this study included a Type III Portland cement provided from Ash Grove Cement Company, along with a Class F fly ash in accordance with ASTM C618, to achieve a desired slump of 8-inches and water-cement ratio of 0.36. Adva 140M, a mid-to-high range water-reducing agent meeting the requirements of ASTM C494 as a Type A and F and ASTM C1017 Type I, was used to assist in achieving proper workability without largely affecting the desired concrete properties. Aggregates used in this study consisted of a special granite coarse aggregate approximately ¾” - 1 ¼”, along with a coarse sand with approximately ¼” diameter and 100% passing the 3/8” sieve. A locally sourced fine sand from Midwest Concrete Materials was provided as the fine aggregate. Since the beams were to be stored outside until testing, air entrainment was also included to account for any potential freeze-thaw damage. This high early-strength concrete was selected to closely resemble the concrete mixture used by prestressed concrete crosstie manufacturers. Typical water-cement ratio used by crosstie manufacturers is 0.32 or less and the mixture was modified in this study to enhance workability. The concrete mixture was ordered from Midwest Concrete Materials, a local concrete supplier. The mixture design is shown in Table 3.1 below.

Table 3.1: Concrete Mixture Design (Mixture Code 85691100A)

Material	Weight (lb)
Type-III Cement	564 lb
Sand (Fine Aggregate)	1,125 lb
Granite Aggregate	1,390 lb
Water	30.0 gal
Sand (Coarse Aggregate)	290 lb
Air-Entrainment	6.5 oz
Fly Ash (Class F)	141 lb
Adva 140M	42 oz

Concrete strength was tested throughout the experiment, and again at the end to obtain strength curves for the concrete. The concrete strengths and curing temperatures for each wire are shown in Figures 3.1-3.3 and Tables 3.2-3.5 below.

Table 3.2: Concrete Strengths and Temperature Throughout Curing Process of HSM-1 Members.

HSM-1 Members		
Concrete Strength (psi)	Days	Temperature (°F)
0	0.0	80
1,732	0.6	105
2,519	0.7	103
3,176	0.8	89
2,209	0.9	82
3,100	1.0	82
3,432	1.1	81
3,563	1.4	78
4,203	1.9	76
3,818	2.1	75
4,435	2.4	75
4,712	4.1	75
4,774	7.1	75
5,497	9.3	75
6,300	11.1	75
8,877	23.0	74
9,185	24.0	74

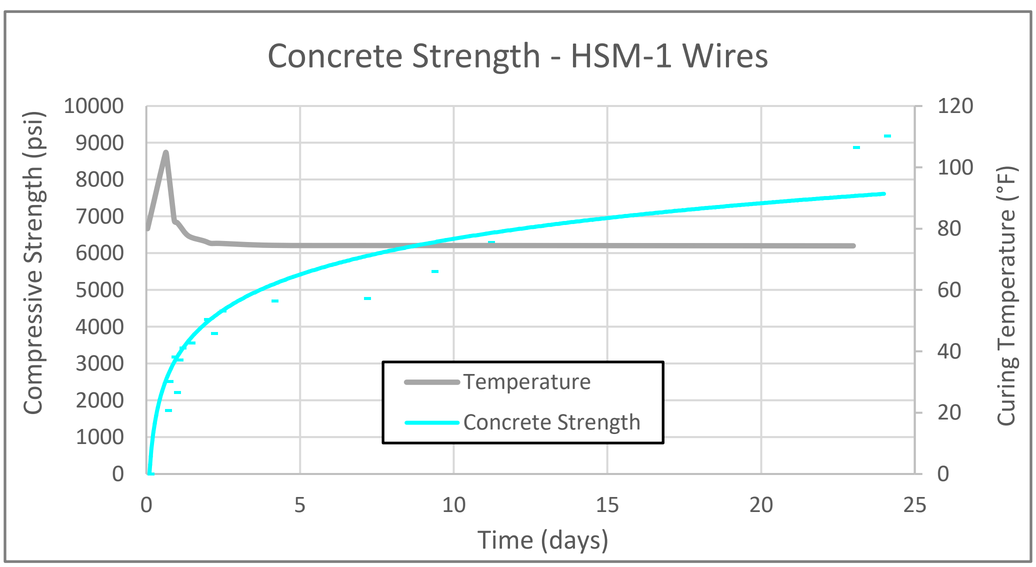

Figure 3.1: Concrete Compressive Strength Curve for Beams with HSM-1 Wire.

Table 3.3: Concrete Strengths and Temperature Throughout Curing Process of HSM-3 Members.

HSM-3 Members		
Concrete Strength (psi)	Days	Temperature (°F)
0	0.0	80
1,349	0.4	104
2,057	0.5	104
3,027	0.8	80
3,275	1.0	77
3,282	1.1	77
3,418	1.2	76
3,729	2.0	76
3,600	2.3	76
3,770	3.3	76
4,188	6.0	76
4,300	7.3	76
5,650	13.0	75
7,066	24.0	74

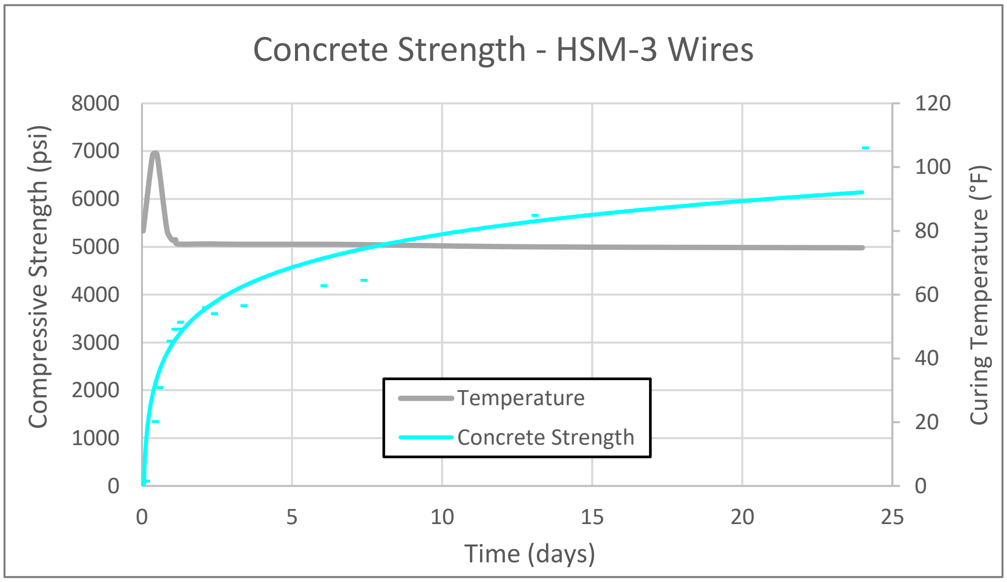

Figure 3.2: Concrete Compressive Strength Curve for Beams with HSM-3 Wire.

Table 3.4: Concrete Strengths and Temperature Throughout Curing Process of voestalpine Members.

V1 Members		
Concrete Strength (psi)	Days	Temperature (°F)
0	0.0	80
1,915	0.4	104
3,686	1.0	82
3,629	1.2	80
3,511	1.3	78
4,587	1.8	77
4,859	3.1	75
5,296	4.3	75
4,651	5.2	74
4,892	6.3	74
5,500	11.2	74
6,092	16.3	74
7,746	23.0	74
8,450	24.0	74

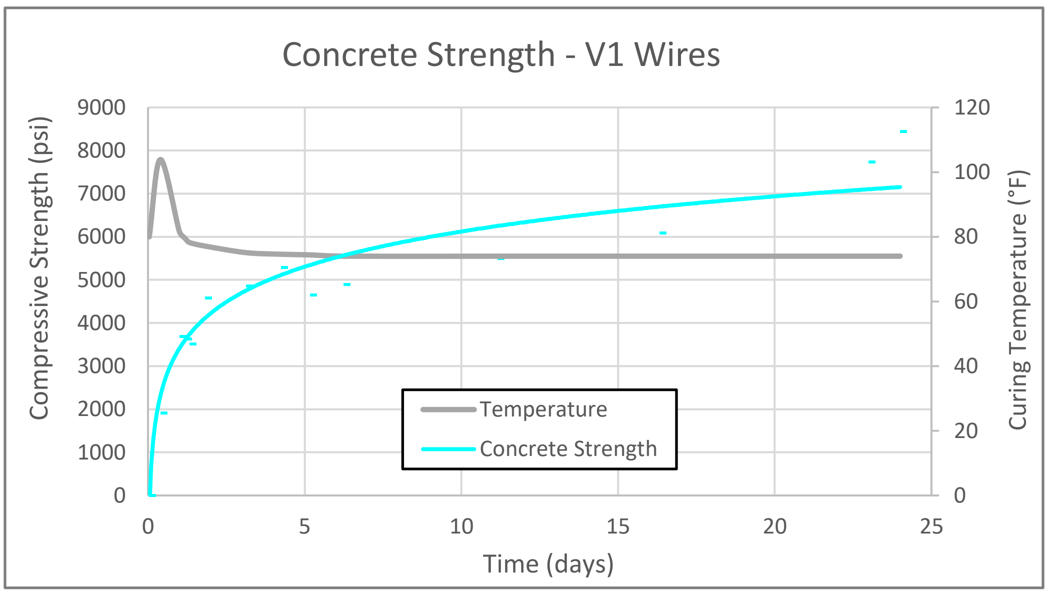

Figure 3.3: Concrete Compressive Strength Curve for Beams with voestalpine Wire.

3.2.2 Prestressing Wire

The prestressing reinforcement was comprised of three different types of 270-ksi large-diameter, chevron-indented low-relaxation prestressing wire. These wires consisted of two different 7.8-mm wires, HSM-1 and HSM-3, provided by the wire manufacturer HSM, and a 7.5-mm wire provided by the prestressed tie manufacturer voeastalpine Railway Systems Nortrak. These indented wires are manufactured by pulling prestressing wire through a set of three indenting rollers, oriented at 120 degrees apart. An example of the indenting rollers, and the indenting pattern and resulting indented wire, are shown in Figure 3.4 and 3.5.

Figure 3.4: Indentation Rollers During Manufacturing of Indented Prestressing Wire (Beck et al., 2019).

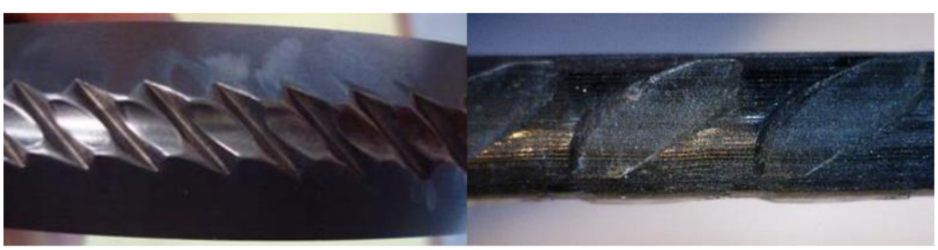

Figure 3.5: Wire Roller and Prestressing Wire After the Indentation Process (Beck et al., 2019).

Through previous studies performed on indented prestressing wire, the indentation geometry has been found to have a significant impact on the bond between the steel and concrete and the splitting stresses present in pretensioned concrete railroad ties. Until recently, research data regarding surface geometry had been limited, resulting in a finite amount of information available to determine the effect indentation had on bond and the corresponding stresses. To resolve this issue, researchers at Kansas State University recently developed a high-resolution non-contact optical wire indent scanner to determine wire indent geometric properties quickly and accurately (Beck et al., 2021). These scanning systems, shown in Figure 3.6 and Figure 3.7, can measure segments of wire up to 36 inches in length, allowing for the determination of important parameters that can be used in predicting bond behavior.

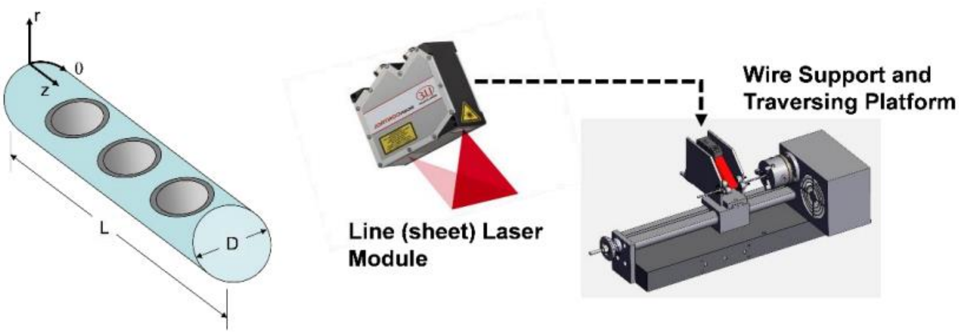

Figure 3.6: Schematic of Indent Profiling System (Beck et al., 2021).

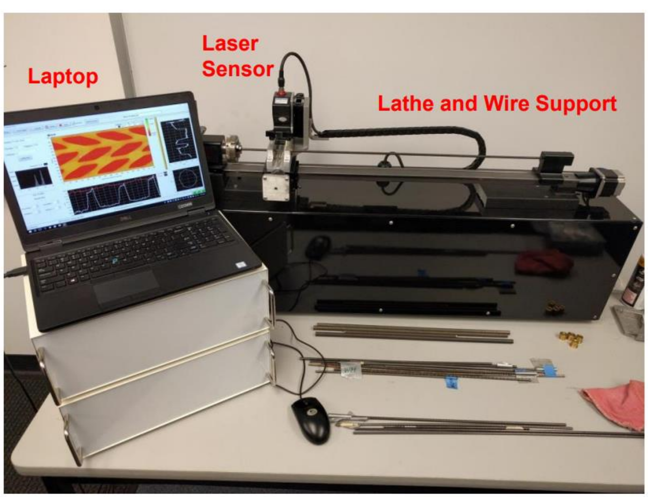

Figure 3.7: Layout of Indent Profiling System (Beck et al., 2021).

This device also presents a method of measuring and performing quality control on the geometrical design, relying on principles of datuming and measurement as defined by ASME Y14.5-2009 standard for Dimensioning and Tolerancing (Beck et al., 2021). With the precision provided through these wire scanners (resolution of one micron), theoretical and empirical models have been developed combining reinforcement wire geometry and release strength of the concrete member to create an all-inclusive model to predict transfer length given conditions of the member (Beck et al, 2021). Key wire indent features obtained from wire scanning are shown in Figure 3.8 below.

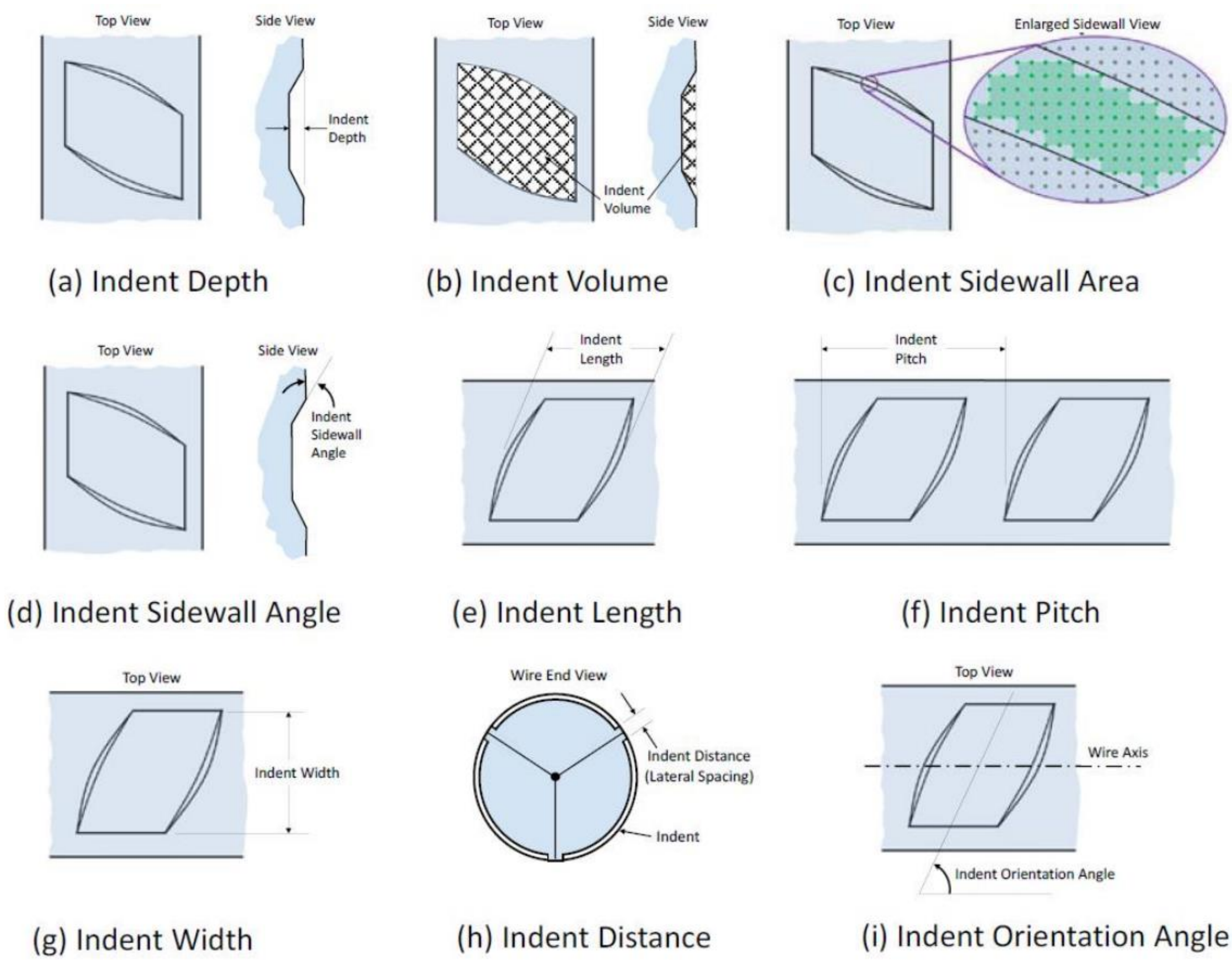

Figure 3.8: Key 3D Wire Indent Geometrical Features Obtained During Scan (Beck et al., 2021).

For this study, all 7.8-mm and 7.5-mm wires were scanned at Kansas State University to obtain accurate surface properties for each wire. A summary of these scans and other mechanical properties can be found in Appendix B.

All wires were cleaned with Dawn dish soap and wiped dry prior to being placed in the forms to remove any oil residue remaining from the manufacturer. Prestressing wire was tensioned to approximately 75 percent of each wire's respective ultimate capacity prior to casting of concrete. The pretensioning methods process used in this study are covered in Section 3.2.3.1. Both HSM-1 and HSM-3 wires were prestressed to 30,000 lbs (15,000 lbs per wire) and voestalpine wires were pretensioned to 26,000 lbs (13,000 lbs per wire). Prestress forces in the wires at time of detensioning are shown in Table 3.5 below.

Table 3.5: Prestress Force in Wires Immediately Prior to Release.

Member	Prestress at Release (lb)
3500-H1	14,930
4500-H1	14,740
6000-H1	14,640
3500-H3	14,970
4500-H3	14,740
6000-H3	15,070
3500-V1	13,200
4500-V1	13,120
6000-V1	13,520

3.2.3 Beam Fabrication

The 27 pretensioned members used in this study included three 5.5 ft beams, three 6.5 ft beams, and three 7.5 ft beams for each of the three types of prestressing wire. The beams had a cross-section of 6”x10”, with the prestressing wire placed 2 inches from the bottom of the beam and each spaced an inch from centerline. Figure 3.9 below shows the cross-section of the flexural members.

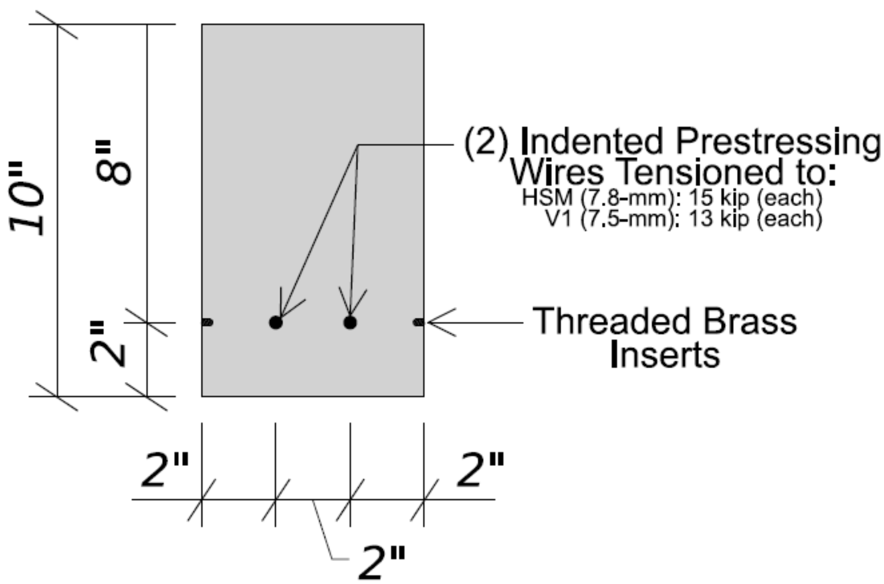

Figure 3.9: Cross-Section of Pretensioned Members with Low-Relaxation Prestressing Wire.

One wire type was used for each pour, with three beam lengths for each desired concrete release strength. Formwork also included two steel channels precision-drilled at one-inch increments along the length of the beam and placed on both sides of the beams in line with the prestressing wire. Threaded brass inserts, as seen in Figure 3.12 were screwed into the channels and cast into the sides of the beam as a means of measuring surface displacement in the concrete.

Figure 3.10: Formwork for Specimen Fabrication and After Curing.

Figure 3.11: Covered Beams During Concrete Curing.

Figure 3.12: Top of Formwork Showing Prestressing Wire and Brass Inserts Spaced at One Inch on Center.

Each pour included nine beams plus 4”x8” concrete compressive strength cylinders. Lifting loops were made from prestressing strand and inserted near the ends of the beams. After the beams were cast, tarps were placed over the forms during curing. Temperatures of the beams were monitored during the curing process using thermocouples. This information was used to control the temperature of the cylinders through a commercial Sure Cure system. The concrete strength cylinders were tested using a Forney hydraulic press, as shown in Figure 3.13. Concrete compressive strengths were closely monitored to ensure pretension forces in the wire were released at compressive strengths of 3500 psi, 4500 psi, and 6000 psi.

Figure 3.13: Forney Hydraulic Press Used to Perform Cylinder Tests.

Concrete compressive strengths at the time of release of prestress forces are shown in Table 3.6.

Table 3.6: Strength at Release of Prestress Forces.

Members	Concrete Release Strength (psi)
3500-H1	3430
4500-H1	4435
6000-H1	6300
3500-H3	3420
4500-H3	4300
6000-H3	5650
3500-V1	3690
4500-V1	4590
6000-V1	6090

3.2.3.1 Prestressing System

The prestressing bed consisted of three rows of wooden formwork with floor mounted steel anchors at the ends of each of the three rows. Load cells were bolted onto one end of the rows and threaded into a chuck which held the prestressing wire, as shown in Figure 3.14Figure 3.14. At the other end, prestressing wire was placed through a hollow threaded bolt and into prestressing wire chucks. Chucks at this end were set into a steel bracket, as depicted in Figure 3.15. A longer threaded rod bolted to the bracket was extended through the end of the anchor, placed through a steel bracket and hydraulic jack, and capped off with a nut.

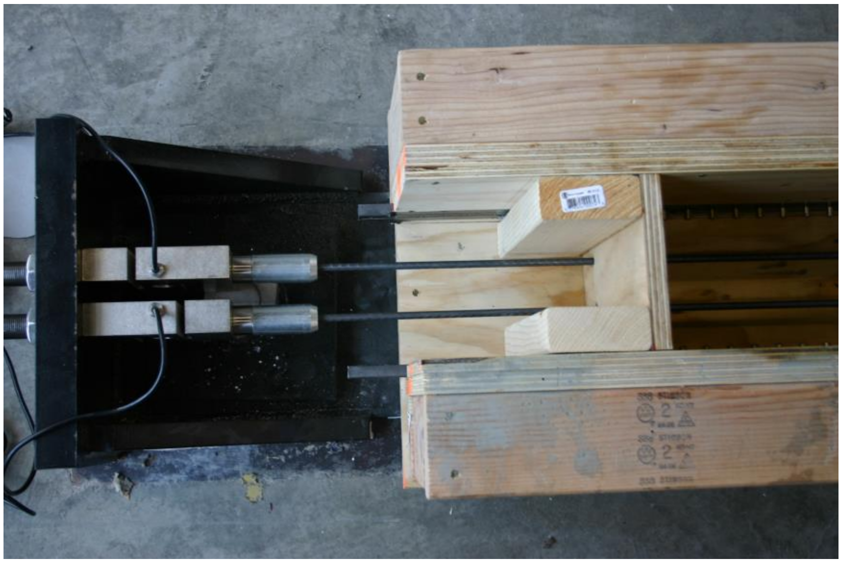

Figure 3.14: Prestressing Configuration with Load Cells at "Dead End" of Prestressing Bed.

Figure 3.15: Prestressing Configuration at the Jacking End, or "Live End" of the Prestressing Bed.

The hydraulic jack was gradually loaded until forces reached 2,000 pounds, at which point the force in each wire was balanced by adjusting the hollow threaded bolts supporting the chucks. Forces in the wires were monitored throughout the prestressing process using a Keithley Model 2700 Data Acquisition System which was connected to the load cells. The jack was slowly loaded until each wire reached 75% of its ultimate tensile strength. The 7.8-mm HSM-1 and HSM-3 wires were both prestressed to 30,000 lbs, while the 7.5-mm voestalpine wire was pulled to 26,000 lbs. Once the wires reached the desired tensile forces, the nut on the threaded rod was tightened against the jacking end of the anchor plate to maintain the pretensioning force. The wooden forms were stripped when the concrete strengths reached 3,500 psi and left uncovered to continue curing until the desired concrete strengths, as determined from the match-cured concrete compressive cylinders, were reached.

3.2.3.2 Beam Nomenclature

Each of the 27 beams were categorized using the beam nomenclature shown in Figure 3.16. This naming system helped to keep track of each beam's respective properties during the measuring and testing processes. Beam lengths, concrete strengths at time of detensioning, and the type of prestressing wire used were written at the top left corner of each beam.

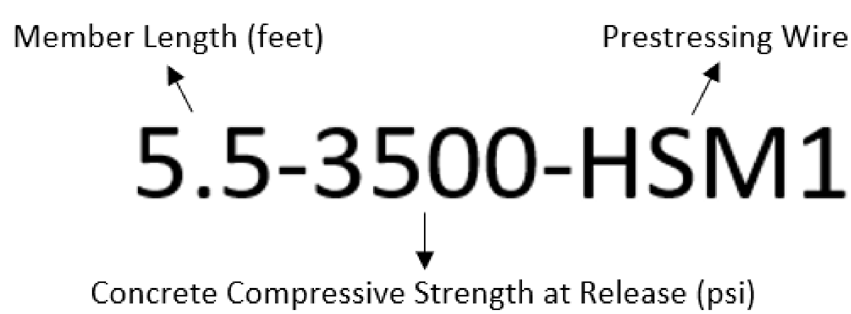

Figure 3.16: Beam Nomenclature Used in This Study.

3.3 Transfer Length Measurements

3.3.1 Methodology

Transfer lengths were determined by measuring the changes in displacement on the beam surface and measuring the wire end-slip into the beam after release of prestress forces. Initial measurements were made after the wooden forms were removed but prior to detensioning. Surface displacement measurements were made before and after release of prestressing forces, 1 week after detensioning, and again immediately before flexural testing to analyze the change in transfer lengths over time. Surface strains calculated by dividing the surface displacement by the gauge length of 8-inches were then plotted.

3.3.2 Wire End Slip Readings

Wire end-slip readings were obtained with a dial indicator as shown in Figure 3.17. The dial gauges were mounted to cylindrical sleeves, which were clamped to the prestressing wire using three screws. The dial gauges chosen for this study had a precision of .0001 inches. Once the gauges were properly mounted and placed against the beam ends, the dial gages were zeroed out.

Figure 3.17: Dial Gauges Used to Measure Wire Slip During the Release of Prestress Forces.

Tensile forces in the wires were gradually lowered using the same jacking system employed in the initial prestressing process. Readings from the load cells were closely monitored during the detensioning process to ensure the wire was not pulled past the initial prestressing force while loosening the nut on the threaded rod. As tensile forces were released, the dial gauges recorded the distance into the section that each wire moved. Data collected from the dial gauges was then used to estimate transfer lengths based on Guyon's, Balaz's and applying Hooke's Law which related end-slip to transfer length. The wire elongation between the clamping point of the dial gauge and the end of the beam was subtracted from the end-slip measurements to provide accurate end-slip data.

3.3.3 Surface Displacement Measurements

Surface displacements over the length of the beam were measured using a Whittemore Gauge having an 8” gauge length. The use of this manual measuring system allowed for precise and convenient measurements between the three lines of beams, and ensured that long-term measurements would be attained. Although more efficient and precise measurement tools exist, such as the non-contact laser speckle imaging (LSI) device used by Peterman (Zhao, Beck, Peterman & Lee, 2012), these rely on digital image correlation of surface features and have been found to be less reliable when obtaining long-term data. Using a manual Whittemore Gage was sufficient for this study as only three beams were detensioned at a time and time constraints were not an issue. A Mitutoyo Absolute Digimatic Indicator was attached to the Whittemore gauge so that strain readings could be automatically recorded at the click of a button, greatly reducing the time required for the collection of displacement data. Images of both the Whittemore Gauge, and the Digimatic Indicator are shown below.

Figure 3.18: Whittemore Gauge Used in Surface Displacement Data Collection.

Figure 3.19: Mitutoyo Absolute Digimatic Indicator Used in Surface Displacement Data Collection.

Transfer lengths were calculated from the plots of surface strain through two methods of analysis. The first method of analysis, which is commonly used in transfer length studies, is the 95% AMS method (Russell & Burns, 1996). In this method, smoothed surface strain data is plotted over the length of the beam. From the strain profile, the average maximum strain value can be determined by taking the average of all surface strain data that lie within the plateau. This average maximum strain value is then multiplied by 0.95 to find the “95% Average Maximum Strain (AMS)”. The distance from the end of the beam where the 95% AMS intersects the smoothed strain profile is determined to be the transfer length. (Russell & Burns, 1993). The software used in this study to calculate the 95% AMS surface profile used raw strain data and took human error into account.

The second method used in this study is the Zhao-Lee (ZL) method proposed by the inventors of the Laser Speckle Imaging device at Kansas State University. This unbiased process of strain profile analysis uses a least-squares algorithm to minimize any variation between a best-fit bi-linear strain profile and a profile using raw strain data. The ZL method incorporates software that calculates the values automatically, taking random error due to the strain sensor into account and eliminating bias and human error involved in the determination of the strain profile plateau, whereas the 95% AMS method requires manual implementation in order to yield the transfer length values. (Zhao, Beck, Peterman, Murphy, Wu, & Lee, 2013).

3.4 Flexural Load Testing

3.4.1 Methodology

All beams constructed in this study were tested under three-point bending until failure. An iterative testing process was implemented to estimate the development lengths associated with each type of prestressing wire. As mentioned earlier in this report, the development length of the prestressing wire is the length of embedment required to fully develop the ultimate strength of the tensile reinforcement. Therefore, the beams could be loaded using different support lengths, converging to an approximate development length through analysis of the corresponding failure mechanism. Test specimens that were able to be loaded to the beam ultimate capacity, failed in wire rupture indicating fully developed reinforcement. Members failing through slippage of the wire into the beam are said to have failed in bond, indicating the reinforcement is not fully developed at the point of loading.

3.4.2 Load Frame, Instrumentation, and Testing Procedures

All testing performed in this study was conducted at the Kansas State University Structural Testing Laboratory. A prestressed concrete testing frame, as shown in Figure 3.20, was mounted to the strong floor of the laboratory using Hydrocal Gypsum Cement and a steel rod threaded into the existing steel floor base mounts and capped with a steel washer and nut at the frame's base. The frame was equipped with a Hydraulic Actuator with a 40,000 lb capacity connected to the concrete frame using a steel built-up member. A load cell connected to the actuator was used to monitor the loading force during testing. Two steel channels were attached to the prestressed loading frame at the base of the actuator to prevent any lateral displacement of the actuator during loading. Concrete blocks with dimensions of 2.5'x2.5'x3.0' were placed on both sides of the loading frame using Hydrocal gypsum cement, to serve as end supports for the beams.

Figure 3.20: Prestressed Concrete Loading Frame Used for Flexural Testing of Specimens.

Steel plate supports measuring 3.5” wide and 1” thick were secured to the ends of the concrete loading blocks using Hydrocal. These supports, shown in Figure 3.21 and Figure 3.22, were used to replicate the typical “pin and roller” connections used in idealized three-point bending. Wooden boxes were placed between the concrete loading blocks and the load frame to support the failing beams and protect the frame.

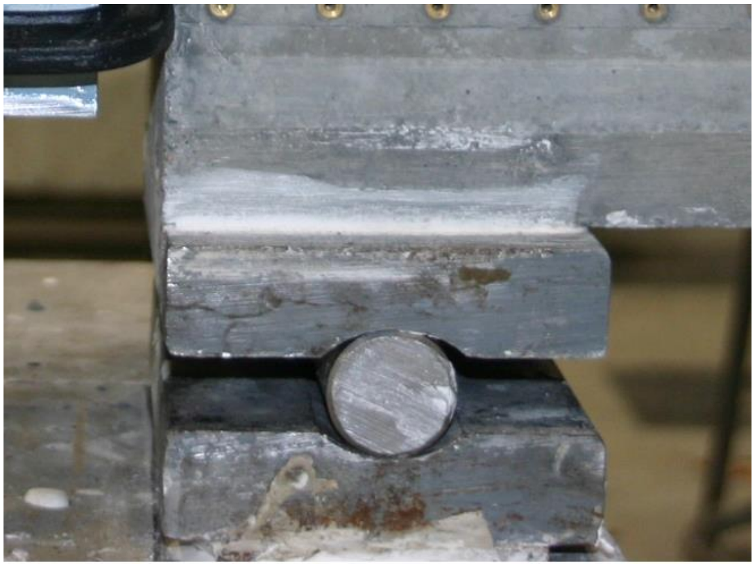

Figure 3.21: “Pinned” Connection Used at Beam Support.

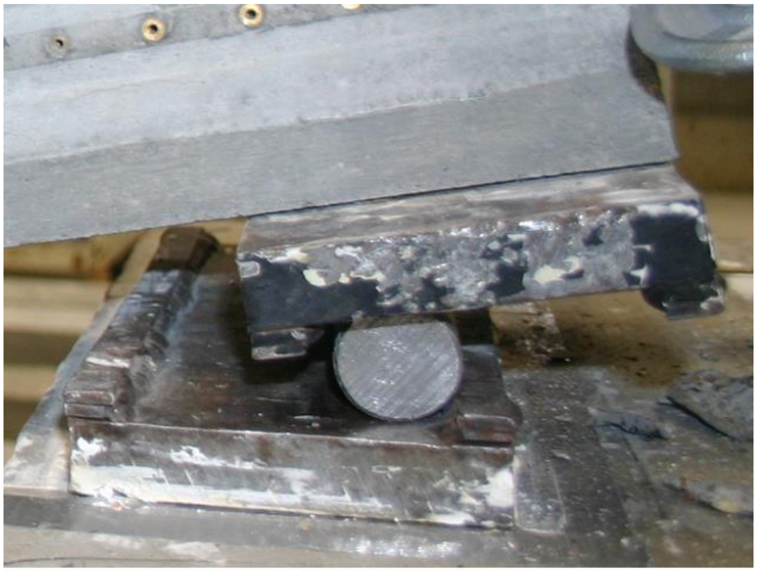

Figure 3.22: “Roller” Connection Used at Beam Support.

Instrumentation used during testing allowed for continuous recording of end-slip and midspan deflections concurrent with the load being applied to the beam. Once the beams were positioned into the desired loading location, the ends of the prestressing wires were ground flat and equipped with the end-slip Linear Variable Differential Transformer (LVDT) assembly, shown in Figure 3.23 and Figure 3.24.

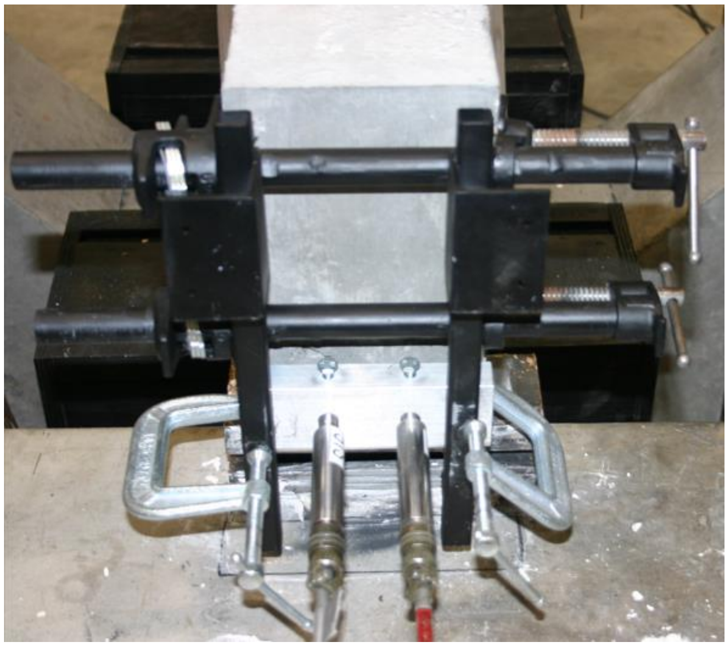

Figure 3.23: End-slip LVDT Assembly for Monitoring Wire Slip During Testing.

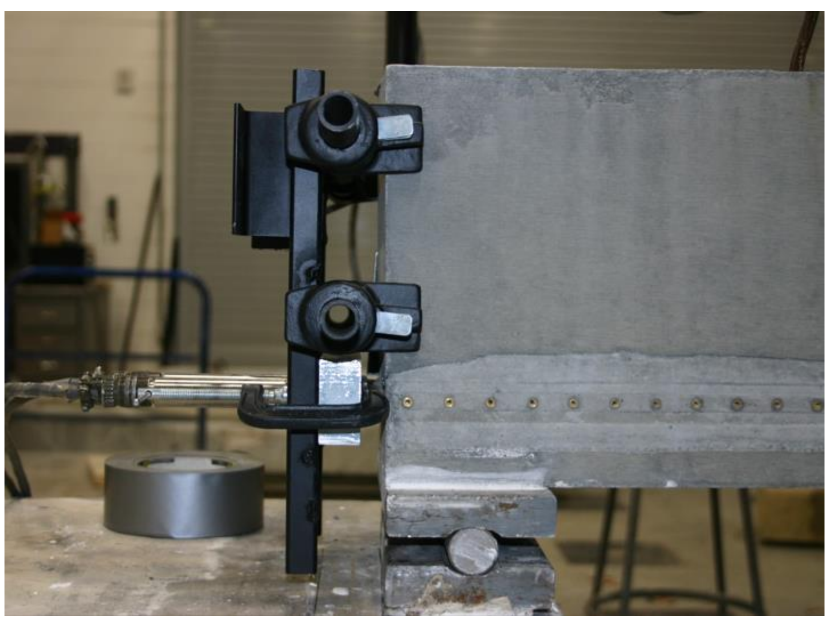

Figure 3.24: Side View of the End-Slip LVDT Assembly.

A 1”x3/4” aluminum bar was then epoxied to the bottom of the specimen directly under the point of loading. This aluminum bar extended laterally past the edges of the beam and was equipped with vertically positioned LVDT’s to measure the deflection of the beam. A 3-inch-wide neoprene bearing pad was inserted between the hydraulic actuator and the beam to provide a more uniform bearing surface. All LVDT data was recorded using a Keithley Model 2700 Data Acquisition System. The load testing frame set-up with the deflection LVDT’s described above is shown in Figure 3.25.

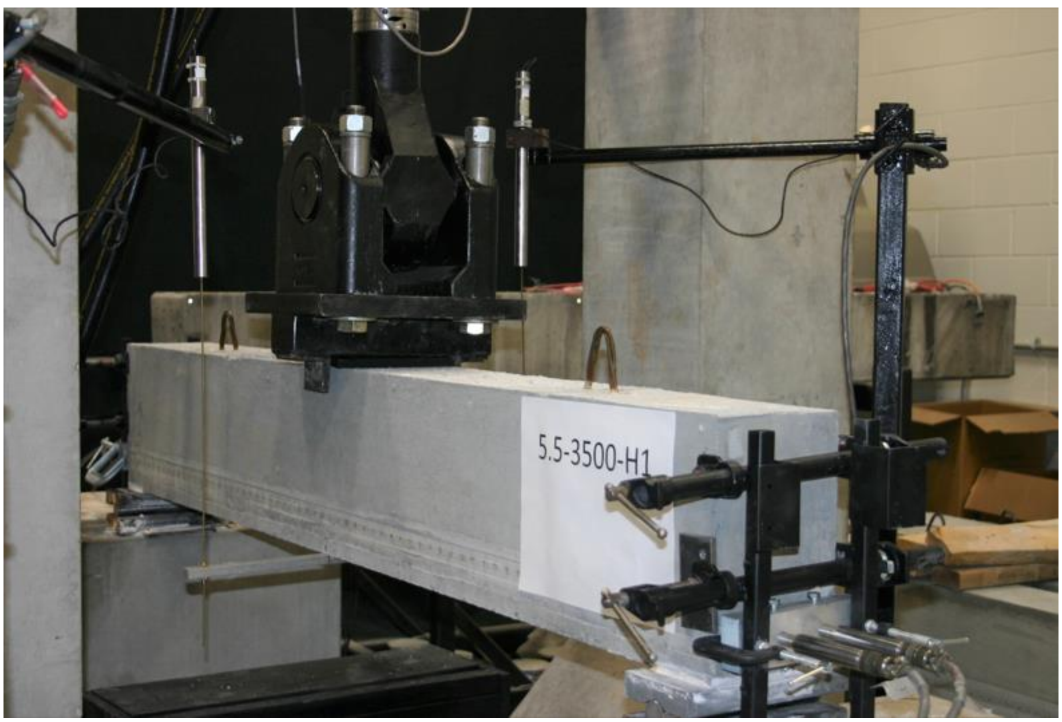

Figure 3.25: Flexural Testing Frame With Deflection and End-Slip LVDT’s.

Once test specimens were positioned correctly and equipped with the aforementioned monitoring system, a Flextest servo-hydraulic controller with closed loop control loaded the beam at a rate of 1000 lbs/min. Beams were loaded until failure and each test video-recorded.

3.4.3 Section Flexural Capacities

All data collected from flexural testing results was interpreted by comparing the maximum moment of beams during testing with the theoretical nominal moment capacity of the section. Nominal Moment Capacities were calculated using the ACI 318 Building Code Requirements for Structural Concrete, paired with the Power Formula modified for larger diameter prestressing wire. An example showing the calculation of the nominal moment capacity is shown in Appendix A. Section flexural capacity calculations for performance evaluation of the beams use the actual as-measured beam properties, also accounting for prestress losses using surface strains before testing. A summary of the maximum concrete strains (obtained from the Whittemore readings prior to testing) is shown in Table 3.7.

Table 3.7: Maximum Concrete Strains Used for Calculating Prestress Losses.

	5.5 ft		6.5 ft		7.5 ft	
R.S. = 3,500 psi	Avg. Live End	Avg. Dead End	Avg. Live End	Avg. Dead End	Avg. Live End	Avg. Dead End
HSM-1	730	800	680	660	720	810
HSM-3	730	820	640	720	740	810
V1	870	980	780	870	870	900

	5.5 ft		6.5 ft		7.5 ft	
R.S. = 4,500 psi	Avg. Live End	Avg. Dead End	Avg. Live End	Avg. Dead End	Avg. Live End	Avg. Dead End
HSM-1	780	740	610	570	680	700
HSM-3	690	680	580	560	610	610
V1	810	740	760	740	770	760

	5.5 ft		6.5 ft		7.5 ft	
R.S. = 6,000 psi	Avg. Live End	Avg. Dead End	Avg. Live End	Avg. Dead End	Avg. Live End	Avg. Dead End
HSM-1	610	630	610	660	630	690
HSM-3	590	610	480	560	570	550
V1	610	620	660	630	730	650

Chapter 4 - Results

4.1 Transfer Length

The transfer length values for the 27 prestressed members were evaluated to compare the bond characteristics of HSM-1, HSM-3, and voestalpine (V1) wires. Two methods were used to estimate the transfer lengths of the wires; measuring end-slip of the prestressing wire into the beams during release of prestress forces, and evaluating the change in surface strain of the beams due to transfer of prestress forces.

4.1.1 End-Slip Results

Prestressing wire end-slip was recorded during the initial release of prestress forces and again at one week for all 6.5-ft beams. Elongation due to prestressing forces were subtracted from end-slip readings, providing an end-slip measurement which could be used to estimate the transfer length associated with each prestressing wire through application of Guyon's and Balaz's proposed end-slip theories and also Hooke's Law of Elasticity.

Properties from the wire used in this study were applied to Hooke's Law to estimate transfer lengths using Equation 2. For HSM wires, E_{ps} was determined to be 28,205 ksi and f_{si} was set equal to 202.5 ksi. For the voestalpine wires, E_{ps} was determined to be 29,490 ksi, with f_{si} equal to 190 ksi. This resulted in a transfer length approximation of $L_t = 279\Delta$ in. for HSM wires, and $L_t = 311\Delta$ in. for the voestalpine wires. End-slip values and the corresponding transfer length estimations using the aforementioned methods, are shown in Table 4.1, Table 4.2, and Table 4.3.

Table 4.1: Transfer Length Estimations Using Guyon's Theory for End-Slip Measurements.

Guyon's theory :

	End Slip Measurement		Alpha=2		Alpha=3	
	At Release	1-week	TL at Release	TL at 1-week	TL at Release	TL at 1-week
HSM-1-3500	0.0691	---	19.4	---	29.0	---
HSM-1-4500	0.0407	---	11.6	---	17.3	---
HSM-1-6000	---	---	---	---	---	---
HSM-3-3500	0.0594	0.0683	16.6	19.1	24.8	28.6
HSM-3-4500	0.0547	0.0573	15.5	16.3	23.2	24.4
HSM-3-6000	0.0525	0.0554	14.6	15.4	21.8	23.0
V1-3500	---	---	---	---	---	---
V1-4500	0.0522	0.0535	16.1	16.5	24.1	24.7
V1-6000	0.0471	0.0483	14.1	14.5	21.2	21.7

Table 4.2: Transfer Length Estimations Using End-Slip Measurements Assuming a Linear Increase of Force Over the Transfer Length.

Hooke's Law:

	End Slip Measurement			
	At Release	1-week	TL at Release	TL at 1-week
HSM-1-3500	0.0691	---	19.3	---
HSM-1-4500	0.0407	---	11.3	---
HSM-1-6000	---	---	---	---
HSM-3-3500	0.0594	0.0683	16.5	19.0
HSM-3-4500	0.0547	0.0573	15.2	16.0
HSM-3-6000	0.0525	0.0554	14.6	15.4
V1-3500	---	---	---	---
V1-4500	0.0522	0.0535	16.2	16.6
V1-6000	0.0471	0.0483	14.6	15.0

Table 4.3: Transfer Length Estimations Using Balaz's Theory for End-Slip Measurements.

Balaz's Theory:

	End Slip Measurement			
	At Release	1-week	TL at Release	TL at 1-week
HSM-1-3500	0.0691	---	20.4	---
HSM-1-4500	0.0407	---	12.2	---
HSM-1-6000	---	---	---	---
HSM-3-3500	0.0594	0.0683	17.5	20.1
HSM-3-4500	0.0547	0.0573	16.3	17.1
HSM-3-6000	0.0525	0.0554	15.4	16.2
V1-3500	---	---	---	---
V1-4500	0.0522	0.0535	17.0	17.4
V1-6000	0.0471	0.0483	14.9	15.2

As seen in the tables above, some measurements were not recorded due to slipping or breaking of the dial gage mount during prestress release.

4.1.2 Transfer Lengths Using Surface Displacement Measurements

Surface displacement measurements recorded with the Whittemore Gage were entered into Excel to produce strain profiles for each test specimen. Surface displacement measurements were recorded before and after the release of initial prestressing forces, one week after detensioning, and again immediately before flexural testing of the specimen. All strain data was smoothed by taking a 5-point average of the measured strain, providing much smoother strain profiles for visual presentations. Strain at the dead and live end of the beam were analyzed separately using the Zhao-Lee and 95% Average Maximum Strain (AMS) methods. Graphs for each of the two methods used in this study are shown in Figure 4.1 and Figure 4.2 below.

.

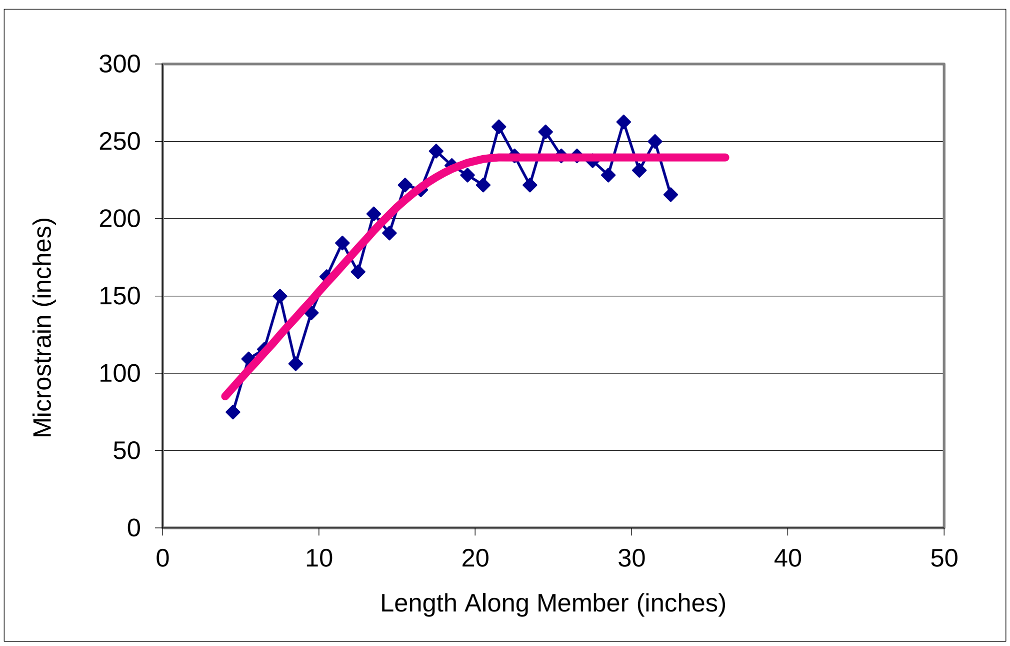

Figure 4.1: Graph Showing Surface Strain Data Analyzed Using the Zhao-Lee Method.

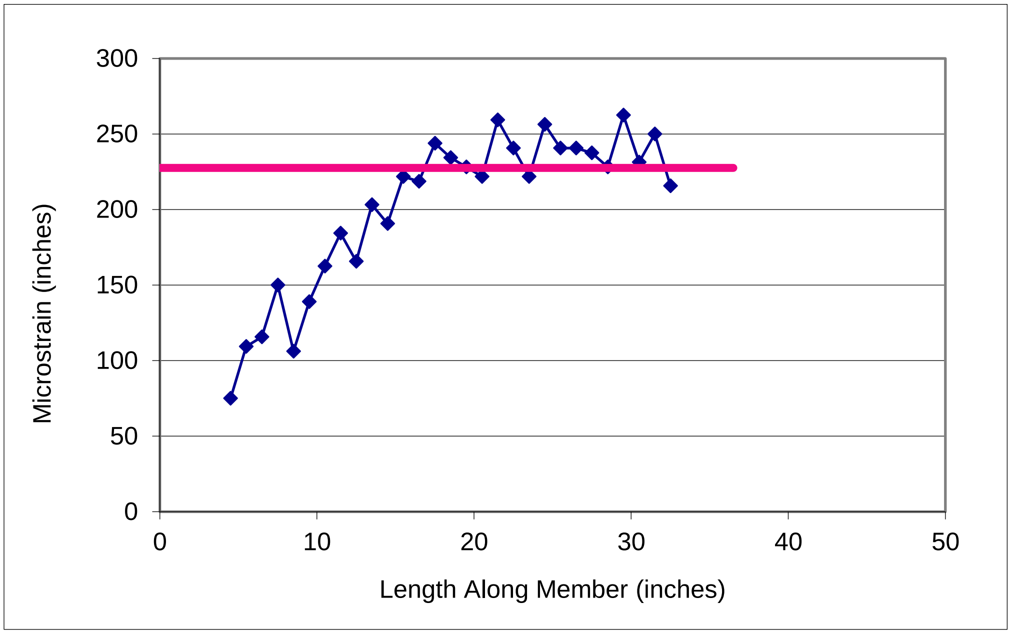

Figure 4.2: Graph Showing Surface Strain Data Analyzed Using the 95% AMS Method.

Transfer lengths for all beam sizes were then averaged and tabulated for each respective concrete release strength and are shown in Table 4.4. The resulting strain profiles for each specimen at the three different times of measurement, along with the calculated transfer lengths using the 95% AMS method and the Zhao-Lee method, are included in Appendix C.

Table 4.4: Average Transfer Length for All Wire Types, Organized by Concrete Release Strength.

Zhao-Lee:

f'ci	HSM-1	HSM-3	V1
3500	17.3	20.1	19.5
4500	16.7	17.4	18.9
6000	13.8	16.9	14.5

AMS:

f'ci	HSM-1	HSM-3	V1
3500	17.0	20.1	19.6
4500	18.9	17.2	19.4
6000	14.2	16.0	14.3

Zhao-Lee (1-week):

f'ci	HSM-1	HSM-3	V1
3500	18.8	19.8	19.6
4500	18.6	16.9	18.8
6000	16.0	19.3	15.1

AMS (1-week):

f'ci	HSM-1	HSM-3	V1
3500	18.2	20.0	19.7
4500	19.3	16.4	18.9
6000	15.4	18.6	14.9

Zhao-Lee (Before Test):

f'ci	HSM-1	HSM-3	V1
3500	17.6	18.7	14.7
4500	17.6	16.0	14.3
6000	16.6	18.3	12.3

AMS (Before Test):

f'ci	HSM-1	HSM-3	V1
3500	18.6	19.3	18.6
4500	18.9	17.3	17.8
6000	16.9	18.0	15.0

Comparing the transfer length predictions determined by the two methods used in this study resulted in variance ranging from 0.2% to 21.0%, with an average difference of 5.0% between the two methods. This variance is most likely due to human error during the collection of surface displacement data, paired with differences between the two methods of calculation. Figure 4.3 below compares the transfer length results for all wire types, organized via the concrete compressive strength at release of prestress forces.

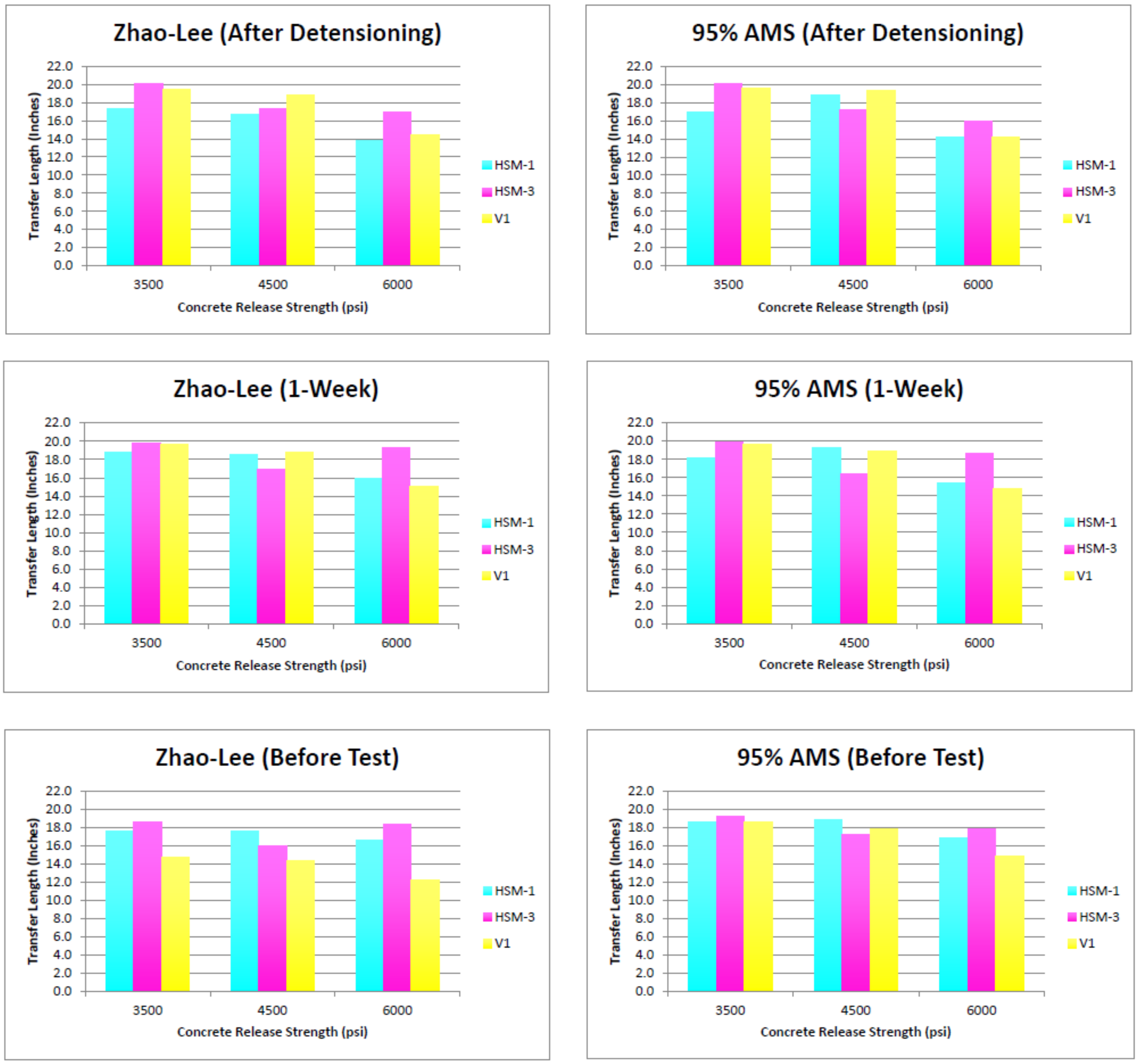

Figure 4.3: Transfer Length Measurements for HSM-1, HSM-3, and Voestalpine (V1) Wires.

As expected, most initial transfer lengths decreased with increasing concrete release strength. However, release of pretension forces at a concrete strength of 6,000 psi resulted in increasing transfer lengths over time for both the HSM-1 and HSM-3 wires. The results also indicate that going from a release strength of 3,500 psi to a release strength of 4,500 psi does not have significant impact on long-term transfer length for HSM-1 and voestalpine wires. However, detensioning at 6,000 psi resulted in considerably lower transfer lengths for HSM-1 and voestalpine wires.

The results show that the voestalpine wire (V1) was most largely affected by changes in concrete release strengths. Voestalpine wires had the lowest transfer lengths at a release strength of 6,000 psi for both methods of transfer length analysis. According to the Zhao-Lee method, voestalpine wires had the lowest long-term transfer lengths for all concrete release strengths when compared to the other two wires used in the study.

HSM-1 wires on average had the lowest transfer lengths at the time of detensioning. However, the results indicate that the transfer lengths for the HSM-1 wires rose the most over time. As seen in Figure 4.3, concrete release strengths for the HSM-1 wire were 130 psi and 650 psi higher for the 4,500 psi and 6,000 psi release strengths, respectively, when compared to that of the HSM-3 wire. Taking this into account, it is not surprising to see shorter initial transfer lengths and higher growth over time for the more lightly-indented HSM-1 wire.

The HSM-3 wire had the largest transfer lengths out of the three wires, except for at a release strength of 4,500 psi where it performed the best when using the 95% AMS method. This wire also appeared to have the least amount of change in transfer length over time, making it the most effective wire for long-term predictability. These results confirm that the mechanical interlocking action of concrete with the wire indentation plays a large role in developing and maintaining bond between the concrete and prestressing steel. The HSM-3 transfer lengths were considerably higher than those of other wires when detensioned at concrete strengths of 3,500 psi and 6,000 psi.

4.1.3 Correlation Between End-Slip and Surface Strain Transfer Lengths

Estimated transfer lengths calculated in Table 4.1 using Guyon's theory show an average absolute error of 11.3% when compared to transfer lengths recorded using surface strain. The HSM-1 wire showed the largest error between the wires, with a maximum error of 38.8%. The estimated transfer lengths shown in Table 4.2 show a maximum error 39.9%, and an average absolute error of 11.5%, when compared to the transfer lengths found using surface strain. Transfer lengths from Table 4.3, estimated using Balaz's proposed equation, showed maximum error of 35.5% for the HSM-1 wire, and an average absolute error of 9.6%. Deviation of transfer length estimations using experimental end-slip from those found using surface strain data are shown in Table 4.5, Table 4.6, and Table 4.7.

Table 4.5: Deviation of End-Slip Estimations Using Guyon's Theory from Surface Strain Transfer Lengths.

Surface Strain (Zhao-Lee Method):

3500	HSM-1	HSM-3	V1
Release	12%	18%	---
1-week	---	5%	---

4500	HSM-1	HSM-3	V1
Release	31%	11%	15%
1-week	---	6%	15%

6000	HSM-1	HSM-3	V1
Release	---	5%	3%
1-week	---	4%	1%

Surface Strain (95% AMS Method):

3500	HSM-1	HSM-3	V1
Release	14%	18%	---
1-week	---	5%	---

4500	HSM-1	HSM-3	V1
Release	39%	10%	17%
1-week	---	1%	13%

6000	HSM-1	HSM-3	V1
Release	---	9%	1%
1-week	---	18%	3%

Table 4.6: Deviation of End-Slip Estimations Using Hooke's Law from Surface Strain Transfer Lengths.

Surface Strain (Zhao-Lee Method):

3500	HSM-1	HSM-3	V1
Release	11%	18%	---
1-week	---	5%	---

4500	HSM-1	HSM-3	V1
Release	32%	12%	14%
1-week	---	7%	14%

6000	HSM-1	HSM-3	V1
Release	---	6%	1%
1-week	---	3%	5%

Surface Strain (95% AMS Method):

3500	HSM-1	HSM-3	V1
Release	13%	18%	---
1-week	---	5%	---

4500	HSM-1	HSM-3	V1
Release	40%	11%	16%
1-week	---	2%	12%

6000	HSM-1	HSM-3	V1
Release	---	8%	3%
1-week	---	17%	1%

Table 4.7: Deviation of End-Slip Estimations Using Balaz's Theory from Surface Strain Transfer Lengths.

Surface Strain (Zhao-Lee Method):

3500	HSM-1	HSM-3	V1
Release	18%	13%	---
1-week	---	0%	---

4500	HSM-1	HSM-3	V1
Release	27%	6%	10%
1-week	---	0%	10%

6000	HSM-1	HSM-3	V1
Release	---	11%	3%
1-week	---	1%	7%

Surface Strain (95% AMS Method):

3500	HSM-1	HSM-3	V1
Release	20%	13%	---
1-week	---	1%	---

4500	HSM-1	HSM-3	V1
Release	35%	5%	12%
1-week	---	5%	8%

6000	HSM-1	HSM-3	V1
Release	---	4%	4%
1-week	---	13%	3%

Attempting to relate end-slip of the wire to the transfer length resulted in a moderate amount of error when using the equations mentioned in the prior section. Figure 4.4 below compares the transfer lengths calculated using the most accurate equation, Balaz's end-slip equation, to those found using surface strain.

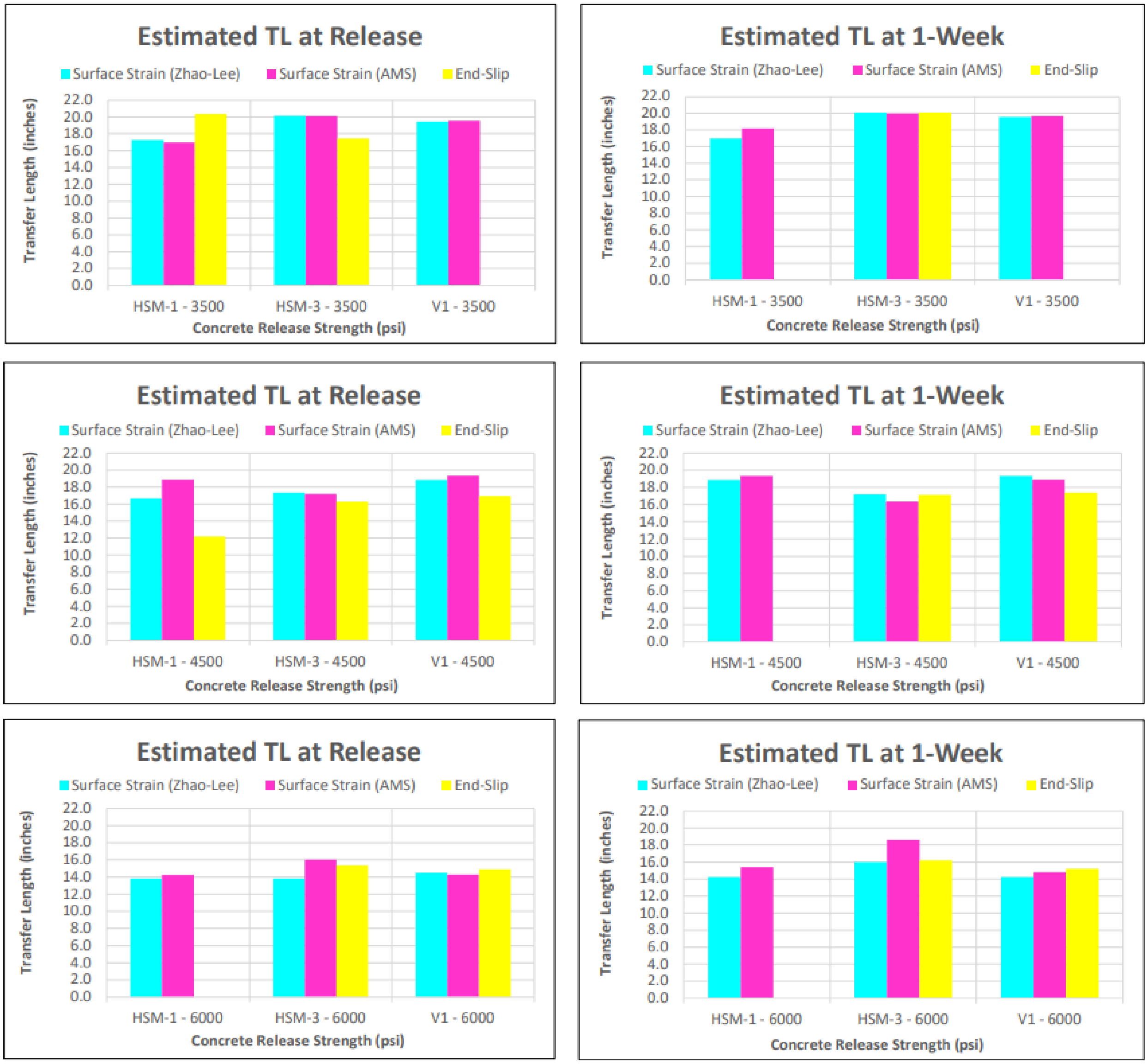

Figure 4.4: Comparison of Transfer Length Estimations Using Balaz's End-Slip Theory to Estimations Using Surface Strain for All Concrete Release Strengths.

While some transfer length estimations were relatively close to what was shown through surface strain data, the results from the theories used in this study lacked precision and overall underestimated the transfer lengths shown through surface displacement measurements. Therefore, the equations used in this portion of the study should only be used to approximate the actual transfer lengths. Further research is recommended to confirm the reliability of these formulas, as there is limited data provided through this research.

4.1.4 Transfer Length Analysis for 7.8-mm and 7.5-mm Prestressing Wire

The resulting transfer lengths for each specimen calculated using surface strain data were compared to transfer length estimations using the formulas recommended in previous studies. The equation proposed by Martin and Scott (1976) resulted in more than 50% error when compared to the transfer lengths found through surface strain data. Because of this significant error, transfer length estimations using Martin and Scott's equation are not included in these results. Equations proposed by Ramirez and Russell (2008), Alan Mattock (1962), Zia and Mostafa (1977), and through the NCHRP Study resulted in less than 26.0% error when compared to the transfer lengths found using surface strain data. Transfer lengths using these previously proposed equations, though not specifically designed for large-diameter prestressing wire, are shown below in Table 4.8.

In efforts to provide more accurate transfer length estimations of large diameter prestressing wire, a multiple-regression analysis was performed using data from this study. The proposed equation, Equation 24 shown below, resulted in an average error of 0.62% and an absolute average error of 6.34%, also shown in Table 4.8.

Table 4.8: Comparison of Transfer Length Estimations from the Proposed Equation vs. Previously Recommended formulas.

		Alan Mattock (1962)		NCHRP Study		Zia and Mostafa (1977)		Ramirez and Russell (2008)		Proposed Equation	
Specimen	Experimental Results	$\frac{1}{3} f_{si} D$	Error (%)	60D	Error (%)	$1.5\left(\frac{f_{si}}{f_{ci}}\right) D - 4.6$	Error (%)	$\frac{120D}{\sqrt{f'_{ci}}} > 40D$	Error (%)	Equation 24	Error (%)
5.5-3500-H1	15.5	20.6	34%	18.4	19%	22.5	45%	19.9	29%	17.2	11%
5.5-3500-H3	18.6	20.7	12%	18.4	-1%	22.6	22%	19.9	7%	17.2	-7%
5.5-3500-V1	14.5	19.0	31%	17.7	22%	18.6	28%	18.5	27%	13.4	-8%
5.5-4500-H1	16.7	20.4	22%	18.4	11%	16.1	-4%	17.5	5%	16.5	-1%
5.5-4500-H3	14.7	20.4	39%	18.4	25%	16.7	14%	17.8	21%	16.6	13%
5.5-4500-V1	13.5	18.9	40%	17.7	31%	13.9	3%	16.5	23%	12.8	-5%
5.5-6000-H1	15.1	20.2	34%	18.4	22%	9.9	-35%	14.7	-2%	15.8	5%
5.5-6000-H3	16.2	20.8	29%	18.4	14%	12.0	-26%	15.5	-4%	16.0	-1%
5.5-6000-V1	12.1	19.4	61%	17.7	47%	9.7	-19%	14.4	19%	12.3	2%
6.5-3500-H1	18.3	20.6	13%	18.4	1%	22.5	23%	19.9	9%	18.1	-1%
6.5-3500-H3	18.2	20.7	14%	18.4	2%	22.6	25%	19.9	10%	18.1	0%
6.5-3500-V1	15.8	19.0	20%	17.7	12%	18.6	17%	18.5	17%	14.3	-10%
6.5-4500-H1	15.7	20.4	30%	18.4	17%	16.1	2%	17.5	11%	17.4	11%
6.5-4500-H3	16.8	20.4	21%	18.4	10%	16.7	0%	17.8	6%	17.5	4%
6.5-4500-V1	14.6	18.9	29%	17.7	21%	13.9	-5%	16.5	13%	13.7	-6%
6.5-6000-H1	16.2	20.2	25%	18.4	14%	9.9	-39%	14.7	-9%	16.7	3%
6.5-6000-H3	19.9	20.8	5%	18.4	-7%	12.0	-40%	15.5	-22%	16.9	-15%
6.5-6000-V1	13.1	19.4	49%	17.7	36%	9.7	-25%	14.4	10%	13.3	2%
7.5-3500-H1	18.8	20.6	10%	18.4	-2%	22.5	20%	19.9	6%	19.0	1%
7.5-3500-H3	19.4	20.7	7%	18.4	-5%	22.6	17%	19.9	3%	19.0	-2%
7.5-3500-V1	13.9	19.0	37%	17.7	28%	18.6	34%	18.5	33%	15.2	10%
7.5-4500-H1	20.5	20.4	0%	18.4	-10%	16.1	-21%	17.5	-14%	18.3	-11%
7.5-4500-H3	16.6	20.4	23%	18.4	11%	16.7	1%	17.8	7%	18.4	11%
7.5-4500-V1	14.9	18.9	27%	17.7	19%	13.9	-6%	16.5	11%	14.7	-1%
7.5-6000-H1	18.5	20.2	9%	18.4	0%	9.9	-47%	14.7	-21%	17.6	-5%
7.5-6000-H3	19.0	20.8	10%	18.4	-3%	12.0	-37%	15.5	-18%	17.8	-6%
7.5-6000-V1	11.7	19.4	66%	17.7	51%	9.7	-17%	14.4	23%	14.2	21%
		Avg. Error:	26%	**Avg. Error:**	14%	**Avg. Error:**	-2.6%	**Avg. Error:**	7.4%	**Avg. Error:**	0.6%
		Absolute Avg. Error:	25.8%	**Absolute Avg. Error:**	16.4%	**Absolute Avg. Error:**	21.2%	**Absolute Avg. Error:**	14.1%	**Absolute Avg. Error:**	6.3%

$$T_L = .05212\frac{f_{pi}}{f'_{ci}} + 294.729D + .0757L - 81.36 \qquad \text{(Equation 24)}$$

The regression analysis resulted in an R^2 value of 0.837, which can be seen with the other regression analysis results in below.

Table 4.9: Statistical Parameters for Transfer Length Model - Equation 24

Regression Statistics	
Multiple R	.8369
R Square	.7004
Adjusted R Square	.6614
Standard Error	1.386
Observations	27

	Coefficients	Standard Error	t Stat	P-value
Intercept	-81.36	14.76	-5.512	.000
f_{pi}/f'_{ci}	0.052	0.027	1.897	.070
D	294.729	48.77	6.043	.000
L	0.076	0.027	2.781	.011

Figures 4.5 through 4.7 show the transfer lengths from Table 4.8, compared to the experimental transfer lengths, sorted by concrete release strengths. As can be seen in Figure 4.5, Equation 24 results in accurate transfer lengths for all members except for those including voestalpine wires, and the 5.5-ft HSM-1 and HSM-3 members.

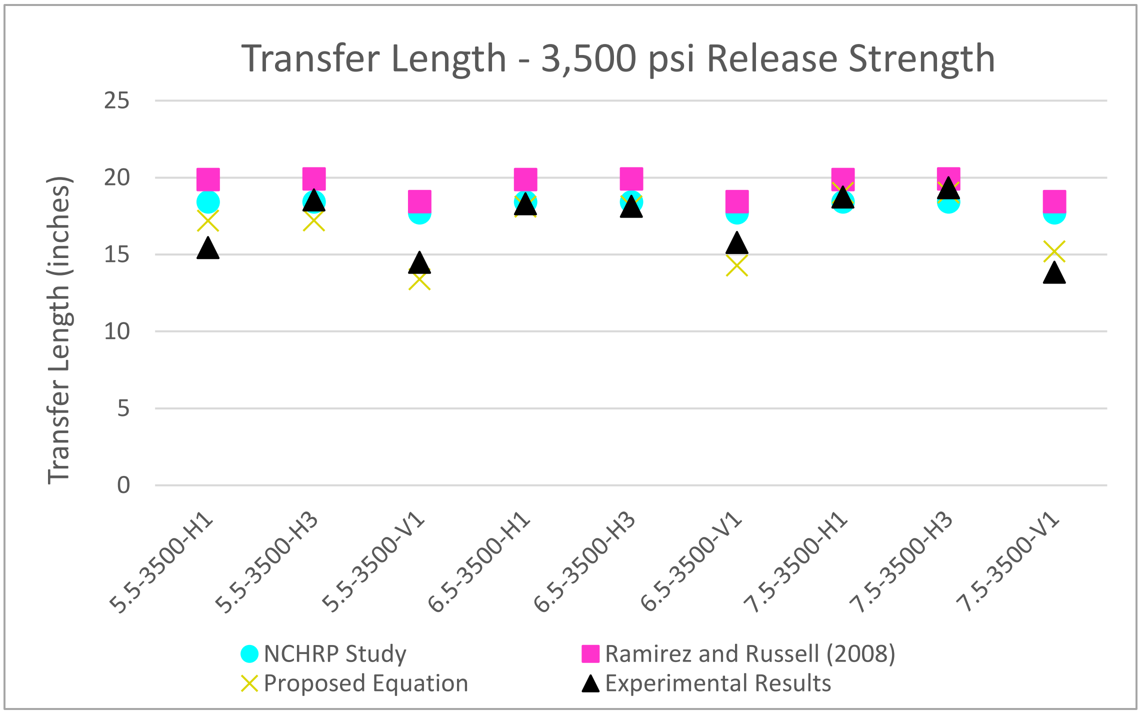

Figure 4.5: Transfer Length Comparison for 3,500 psi Concrete Release Strength.

Using the proposed equation to estimate transfer length for members detensioned at a concrete release strength of 4,500 psi resulted in more error than estimations for concrete release strengths of 3,500 psi and 6,000 psi. While most estimations were conservative for both HSM-1 and HSM-3 wires, the equation slightly underestimated the transfer length of members fitted with voestalpine wires.

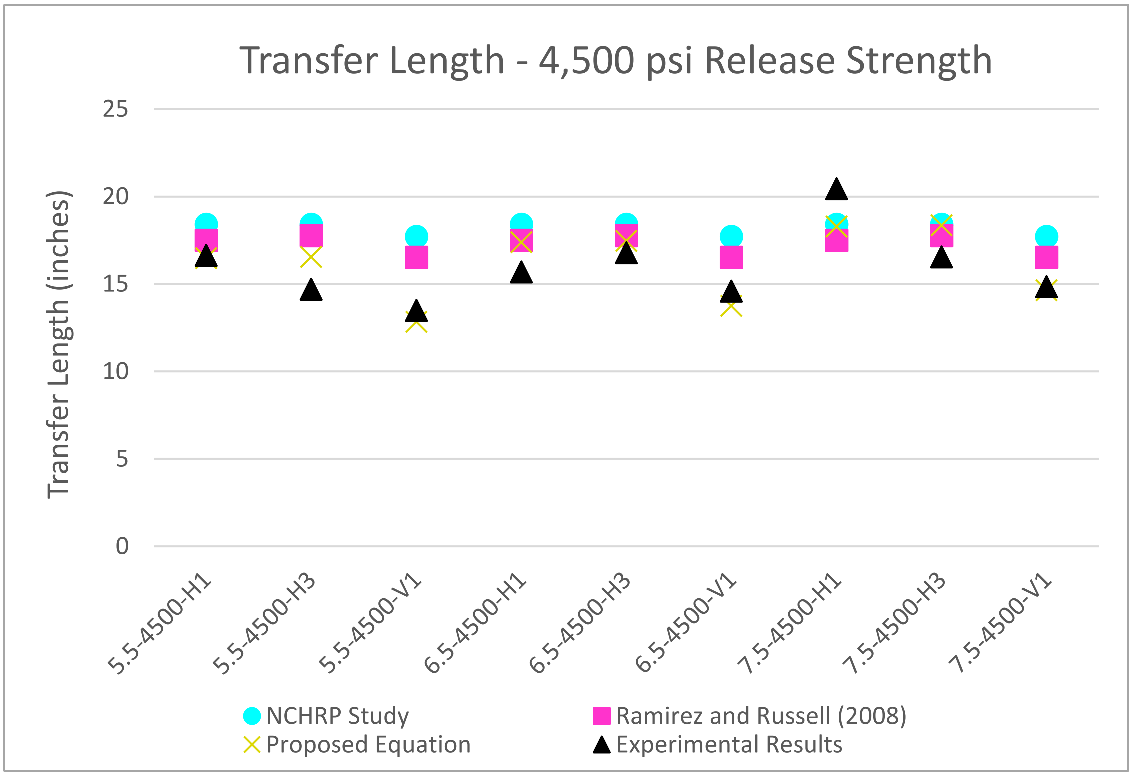

Figure 4.6: Transfer Length Comparison for 4,500 psi Concrete Release Strength.

Transfer length estimations for members prestressed with voestalpine wires with a concrete release strength of 6,000 psi were more accurate when compared to estimations at other release strengths. However, the 7.5-ft beam pretensioned with voestalpine wire showed much lower transfer lengths than what was predicted through the proposed equation. While estimated transfer lengths using Equation 24 were more accurate than those using previously proposed equations for prestressing strand, there were still estimations that over and underestimated the transfer lengths shown through surface strain. The comparison for transfer lengths for members with a release strength of 6,000 psi is shown in Figure 4.7 below.

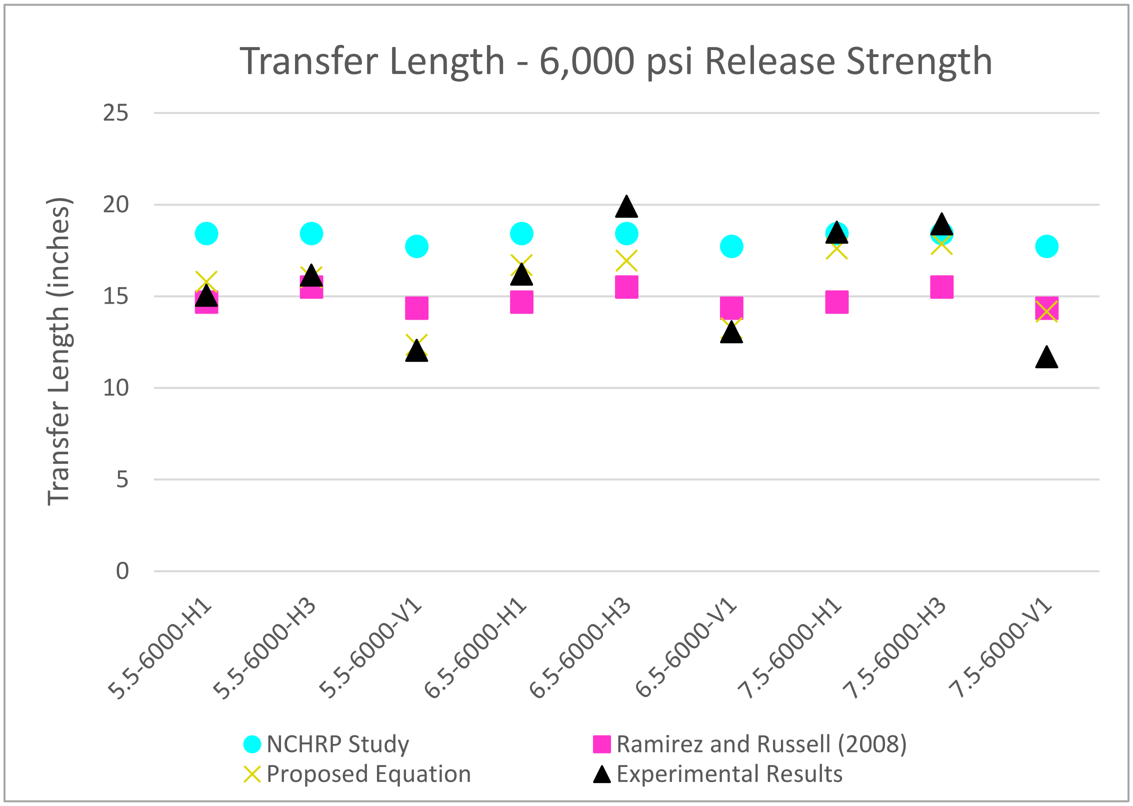

Figure 4.7: Transfer Length Comparison for 6,000 psi Concrete Release Strength.

While the proposed formula does provide significantly less error when trying to predict transfer length in these prestressing wires, it is recommended that further research be done to confirm these results. It is also recommended that a multiplication factor of 1.2 be applied to Equation 24 when used in the field to provide more conservative estimations of transfer length for large-diameter chevron indented prestressing wire.

Transfer Lengths from surface strain data show an average transfer length approximation shown in Table 4.10 below.

Table 4.10: Transfer Length Approximations for HSM and voestalpine Prestressing Wires.

HSM-1	HSM-3	V1
59D	61D	63D

4.2 Development Length

All specimens were tested in three-point bending to determine the mode of failure associated with each prestressing wire. The prestressing wire was said to have reached its ultimate tensile capacity, and therefore its full development length, when the experimental moment capacity reached the calculated nominal moment capacity for the section. Members that failed via slipping of the wire into the member were said to have failed in bond, thus indicating insufficient length for development of the prestressing reinforcement.

In order to home in on development lengths for the three types of wires, the beams were tested at different lengths from the end of the beam supported by the "roller" connection. If wire rupture was noted as the cause of beam failure, the loading point was moved closer towards the end of the beam, thus shortening the embedment length of the wire. This process was continued until bond was denoted as the failure mechanism; in which case the loading point was moved away from the beam end. Data obtained from the testing was used to converge to approximate development lengths for all three wire types.

4.2.1 Flexural Testing Results

The first members tested were the 5.5-ft beams. Beams with a concrete release strength of 3,500 psi and 4,500 psi were tested at midpoint providing an embedment length of 33 inches from the ends of the beams, as shown in Figure 4.8.

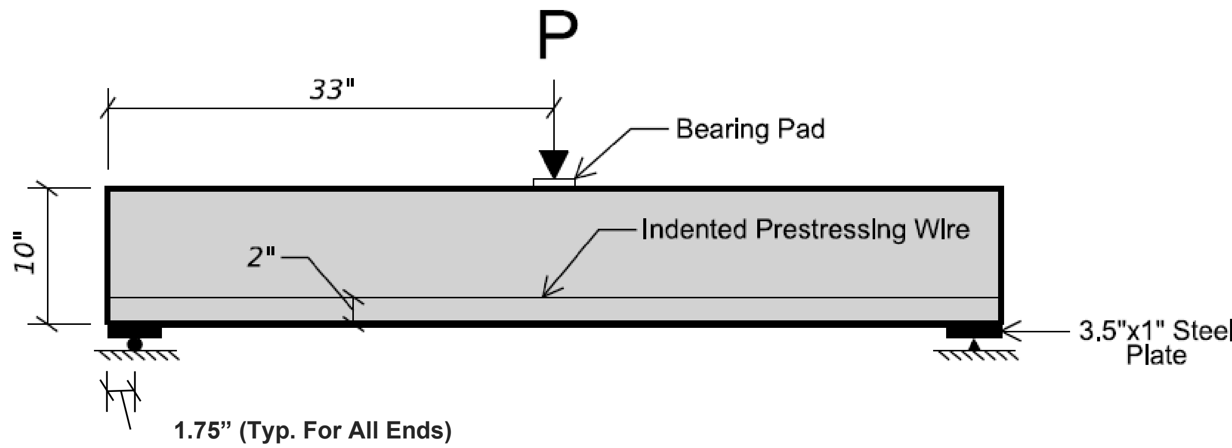

Figure 4.8: Flexural Testing Set-up for all 5.5-ft Members with 3,500 psi and 4,500 psi Release Strengths.

All tests at this length resulted in rupture of the prestressing wire. Since testing at this length was determined to provide sufficient embedment length for development, the loading point was decreased to an embedment length of 27 inches and beams with a concrete release strength of 6,000 psi were tested.

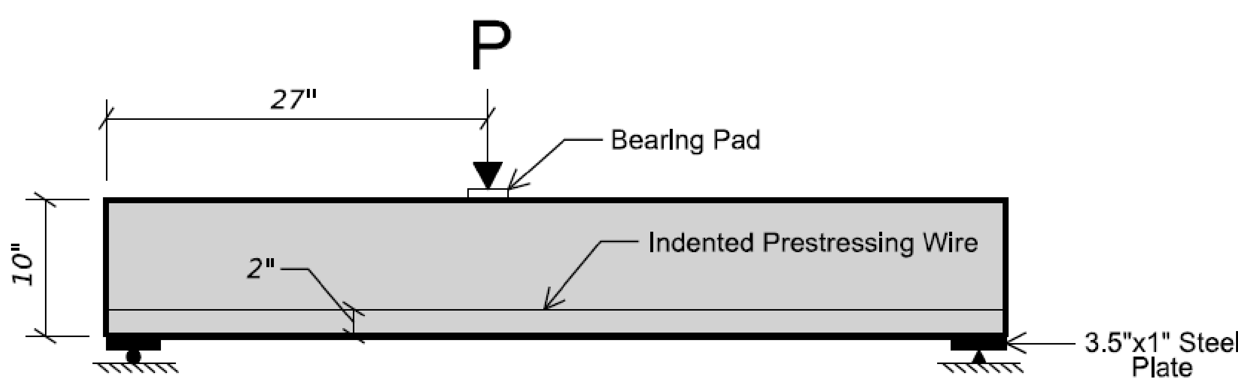

Figure 4.9: Flexural Testing Configuration for 5.5-ft Members with Concrete Release Strengths of approximately 6,000 psi.

These wires also failed in rupture, concluding that all reinforcement had been fully developed at embedment lengths of 27 inches. Figure 4.10 shows the typical loading vs. deflection for beams failing in wire rupture, with no end slip.

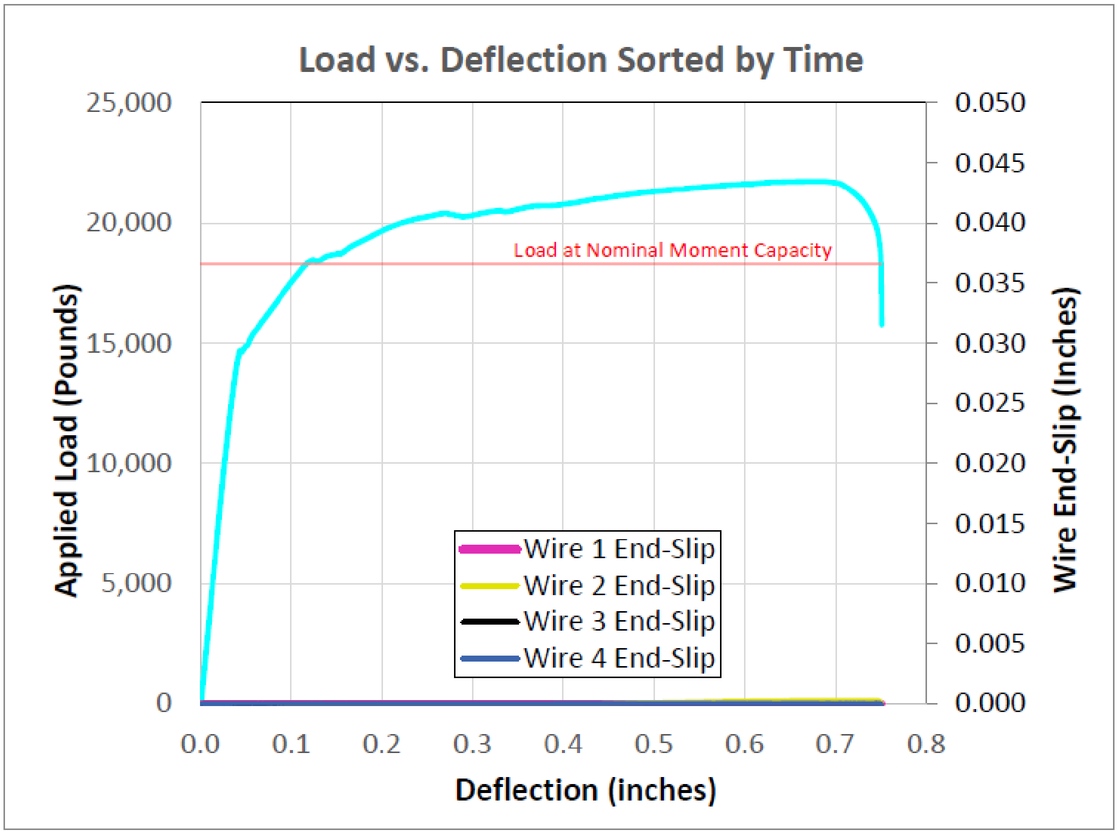

Figure 4.10: Graph Showing the Load, Deflection, and End-Slip Results from Flexural Testing of a Specimen.

Next the 6.5-ft specimens were tested. Beams with a concrete release strength of 3,500 psi were tested first, with the load placed 24 inches from the beam ends. All tests for this release strength resulted in rupture of the prestressing wire. However, the beam prestressed with HSM-1 wire saw wire slip of approximately .0065 inches during testing. For this reason, the HSM-1 beam with a concrete release strength of 4,500 psi was also tested at 24 inches. This test resulted in wire rupture, with no slipping of the HSM-1 wire during testing, confirming the wire was fully developed. The testing configuration for embedment lengths of 24 inches is shown below.

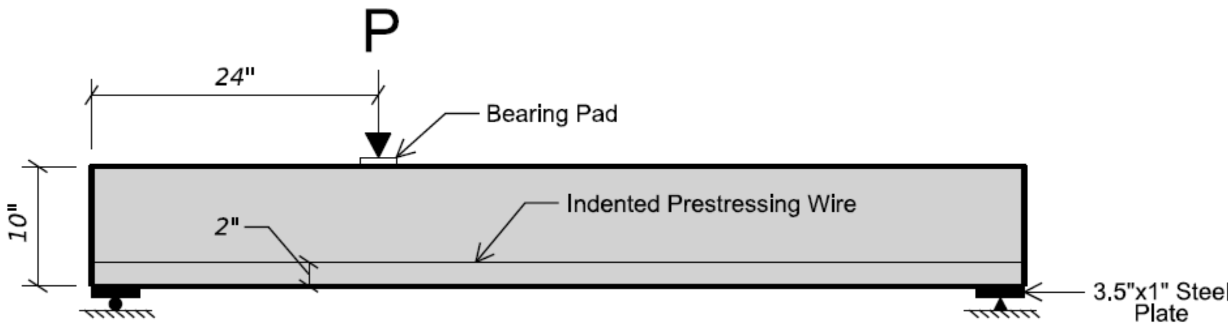

Figure 4.11: Flexural Testing Configuration for all 6.5-ft Members with a Concrete Release Strength of 3,500 psi, and the 6.5-ft, HSM-1 Beam with A Concrete Release Strength of 4,500 psi.

The loading point was then reduced to a test length of 21 inches. Beams prestressed with HSM-3 and voestalpine (V1) wires with concrete release strengths of 4,500 psi were tested at this length.

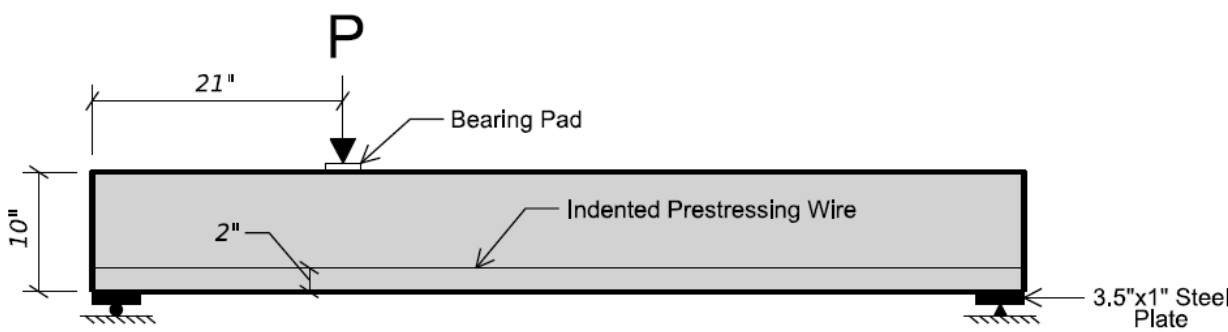

Figure 4.12: Flexural Testing Configuration for HSM-3 and voeastalpine Wires with Concrete Release Strength of 4,500 psi.

The beam fitted with HSM-3 wire resulted in wire rupture, whereas the V1 wire resulted in full slip of the reinforcement. During V1 testing, a flexural-shear crack developed approximately 13 inches from the end of the beam, shown in Figure 4.13. This crack resulted in spalling of the concrete surrounding the prestressing wire, reducing the available bond and leading to slipping of the wire.

Figure 4.13: Development of Flexural-Shear Crack During Testing of Specimen 6.5-4500-V1.

The remaining 6.5-ft beams, having a concrete release strength of approximately 6,000 psi, were then tested at 21 inches as shown below.

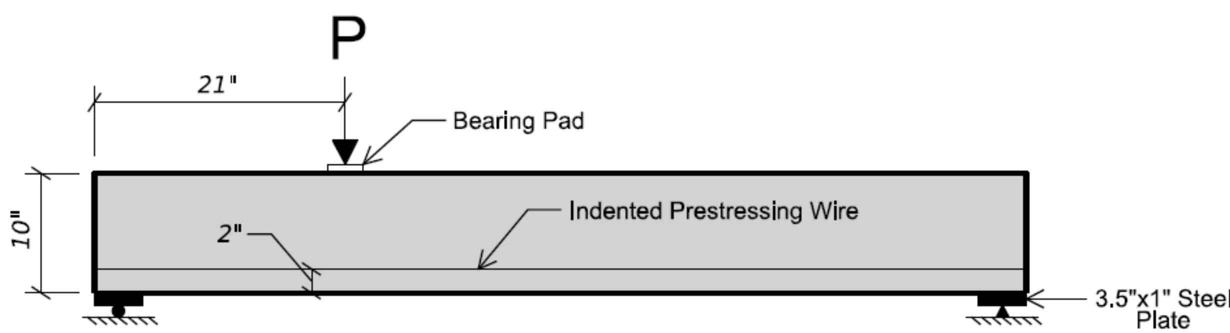

Figure 4.14: Flexural Testing Configuration for 6.5-ft Members with Concrete Release Strengths of 6,000 psi.

Both the HSM-3 wire and V1 wire failed via wire rupture, with the HSM-3 wire experiencing only minor slippage (around .005 inches). The beam fitted with HSM-1 wire experienced full wire slip. During testing, a flexural crack propagating down to the bottom of the beam, approximately 17 inches from the beam end, caused significant spalling of concrete below the prestressing wire, as shown in Figure 4.15.

Figure 4.15: Spalling of Concrete During Flexural Testing of Specimen 6.5-6000-H1.

The 7.5-ft beams were tested next. The beams with a concrete release strength of 3,500 psi were placed into the loading frame with a point of loading located 21 inches from the end of the specimen.

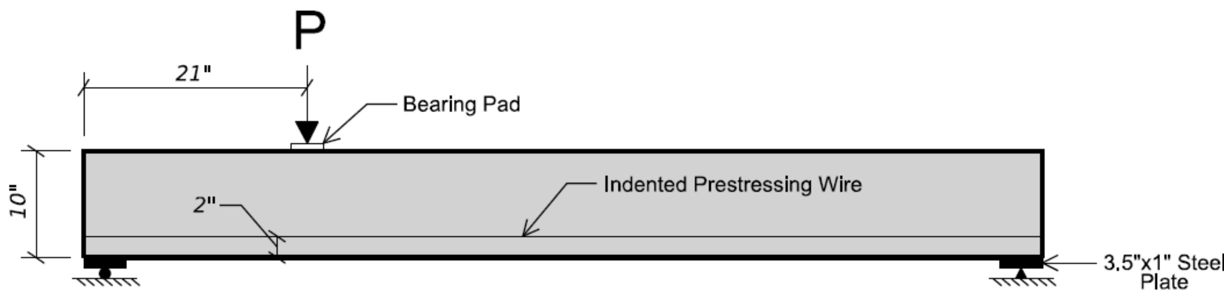

Figure 4.16: Flexural Testing Configuration for the 7.5-ft Members with a Concrete Release Strength of 3,500 psi.

The member fitted with HSM-1 wire was tested first, resulting in a flexural-shear of the beam approximately 12 inches from the member's end and bond failure. The flexure-shear crack can be seen in Figure 4.17 and Figure 4.18. This shear crack greatly reduced the length available for development of the reinforcement and resulted in heavy concrete spalling between the crack and point of loading.

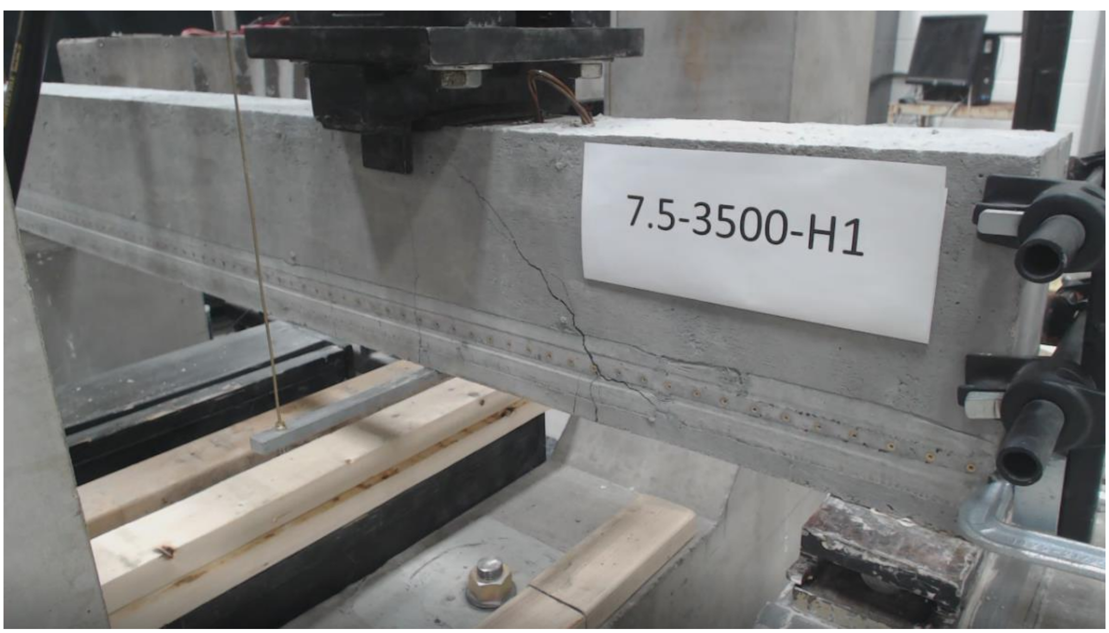

Figure 4.17: Initial Development of Flexural-Shear Crack During Flexural Testing of Specimen 7.5-3500-H1.

Figure 4.18: Full Development of Flexural-Shear Crack Shown After Failure of Specimen.

Testing of the HSM-3 wire also resulted in a flexural-shear crack, which developed approximately 15 inches from the end of the beam. This led to bond failure and full slipping of the wires. This failure is shown in Figure 4.19. The 7.5-mm voestalpine wire was the only test resulting in wire rupture for beams with a concrete release strength of 3,500 psi when tested at 21 inches.

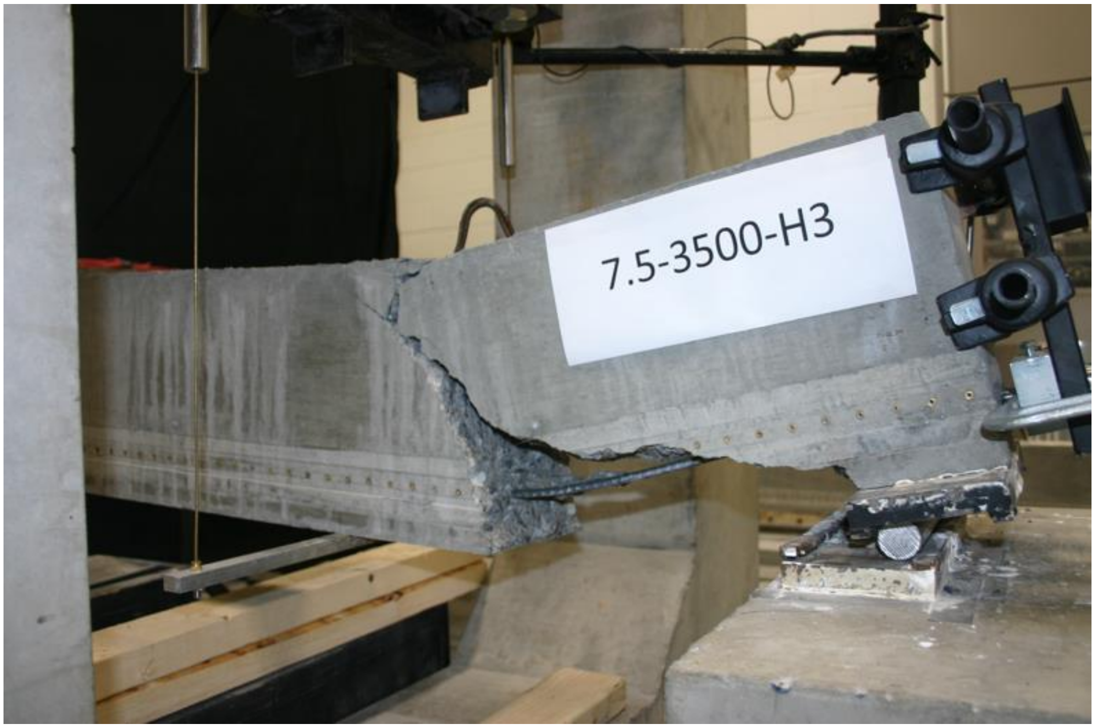

Figure 4.19: Shear Crack During Flexural Testing Leading to Spalling of Concrete and Bond Failure.

The 7.5-ft prestressed members with a release strength of 4,500 psi were tested next, with the point of loading located 18 inches from the end of the beam.

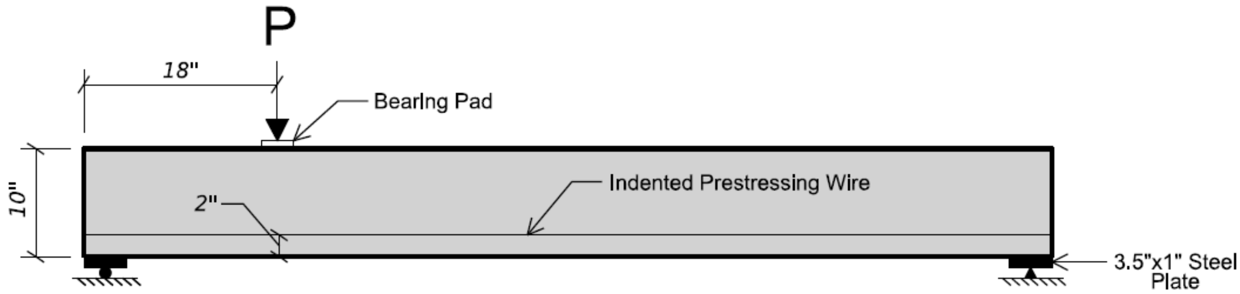

Figure 4.20: Flexural Testing Configuration of the 7.5-ft Members with a Concrete Release Strength of 4,500 psi.

The specimen fitted with HSM-1 wire resulted in a crack which propagated down to the bottom of the member, approximately 15 inches from the beam end. This crack is shown in Figure 4.21. As a result, the HSM-1 wire failed in bond due to insufficient length for proper development. Both the HSM-3 and V1 wires were fully developed, resulting in rupture of the wires.

Figure 4.21: Flexure-Shear Crack During Flexural Testing Leading to Spalling of Concrete and Bond Failure.

Beams with a concrete release strength of 6,000 psi were tested last. For this last series of flexural tests, the testing length was reduced to 16 inches from the ends of the beams as shown below.

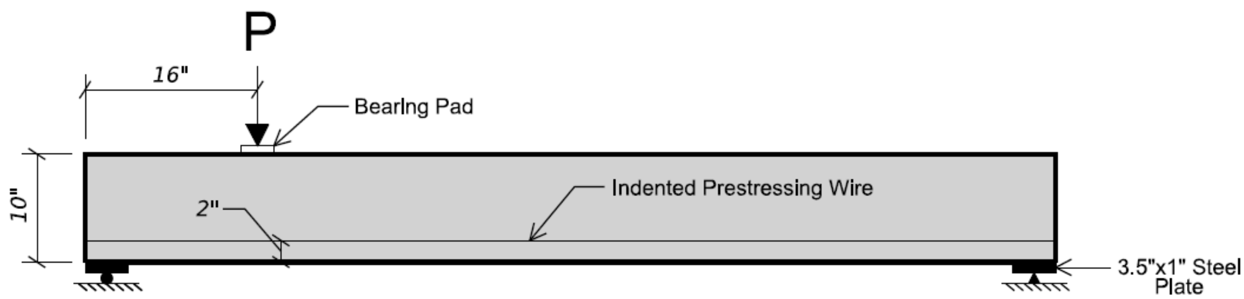

Figure 4.22: Flexural Testing Configuration for the 7.5-ft Members with a Concrete Release Strength of 6,000 psi.

The member equipped with HSM-1 wire was tested first. This beam failed in wire rupture, indicating the wire was fully developed, but did have significant wire slippage of approximately .0125 inches. The beam with HSM-3 wire was tested next, resulting in another crack developing 11 inches from the end of the beam, as shown in Figure 4.23. This beam failed via bond and experienced complete slipping of the wires.

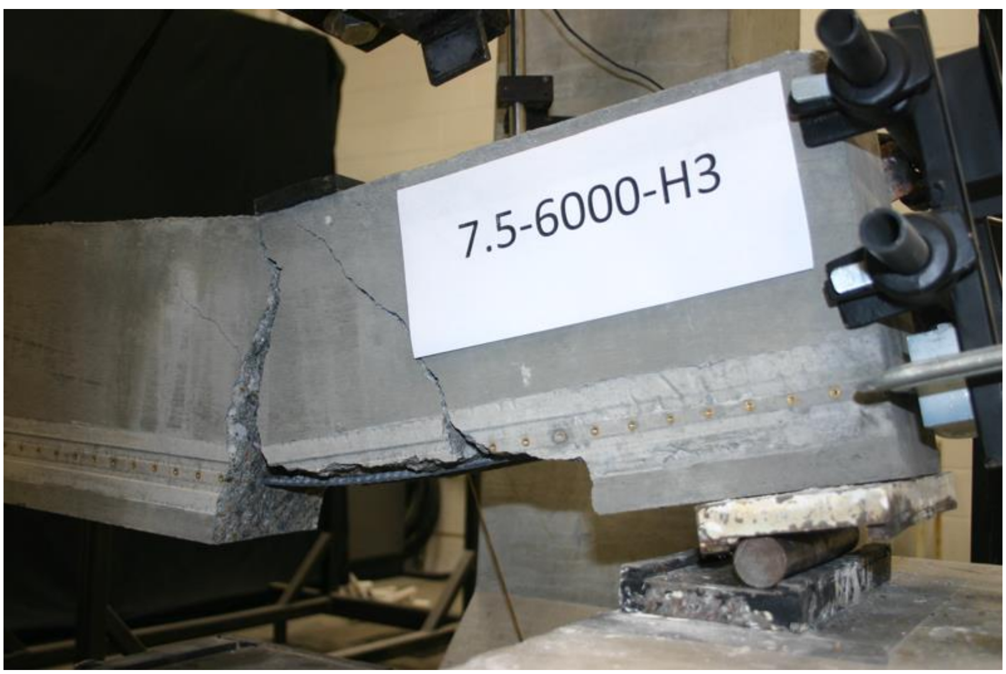

Figure 4.23: Development of Flexural-Shear Crack Leading to Spalling and Bond Failure of Specimen 7.5-6000-H3.

The last test was for the member prestressed with voestalpine wire. The wire in this test was fully developed and failed through rupture, with minimal end slip of approximately .004 inches.

Table 4.11 shows the testing results for all beams. Testing lengths, along with lengths from the beam's end where flexural or shear cracks developed, are included. Data taken from the tests were used to create graphs comparing the applied load, corresponding beam deflection, and wire slip experienced during testing. These graphs, along with additional pictures of beams after testing, are included in Appendix D.

Table 4.11: Flexural Testing Results for All Specimens.

Specimen	Test Length	Length at Crack	Wire Rupture	Theoretical Nominal Moment (k-ft)	Moment Achieved (k-ft)	Wire Slip Recorded
5.5-3500-H1	33	32	Yes	25.2	-	-
6.5-3500-H1	24	27	Yes	25.2	28.5	0.007
7.5-3500-H1	21	12	No	25.2	27.4	0.086
5.5-3500-H3	33	30	Yes	24.6	-	-
6.5-3500-H3	24	23	Yes	24.6	27.3	0.000
7.5-3500-H3	21	15	No	24.6	26.3	0.042
5.5-3500-V1	33	33	Yes	21.3	-	-
6.5-3500-V1	24	24	Yes	21.3	24.3	0.001
7.5-3500-V1	21	21	Yes	21.3	24.6	0.010
5.5-4500-H1	33	33	Yes	25.2	29.9	0.000
6.5-4500-H1	24	24	Yes	25.2	29.8	0.000
7.5-4500-H1	18	15	No	25.2	24.5	0.059
5.5-4500-H3	33	33	Yes	24.6	28.2	0.000
6.5-4500-H3	21	22	Yes	24.6	29.3	0.000
7.5-4500-H3	18	18	Yes	24.6	29.9	0.000
5.5-4500-V1	33	33	Yes	21.3	25.5	0.000
6.5-4500-V1	21	14	No	21.3	25.2	0.046
7.5-4500-V1	18	17	Yes	21.3	25.7	0.006
5.5-6000-H1	27	27	Yes	25.2	28.6	0.000
6.5-6000-H1	21	17	No	25.2	29.4	0.060
7.5-6000-H1	16	16	Yes	25.2	33.2	0.014
5.5-6000-H3	27	27	Yes	24.6	28.0	0.000
6.5-6000-H3	21	21	Yes	24.6	29.3	0.000
7.5-6000-H3	16	11	No	24.6	31.2	0.042
5.5-6000-V1	27	26	Yes	21.3	25.2	0.001
6.5-6000-V1	21	21	Yes	21.3	25.7	0.007
7.5-6000-V1	16	16	Yes	21.3	27.7	0.005

Results from the flexural testing of the specimens give insight into the actual development lengths required for the three types of wire, dependent on the concrete release strength. However, due to the number of beams constructed and tested in this study, along with undesirable flexure-shear failures possibly due to testing at or near the D-region of the members, only approximate recommendations of development lengths can be provided.

For HSM-1 wires with a concrete release strength of 3,500 psi (3,430 psi), an embedment length of 24 inches was shown to be required for full development of said reinforcement. HSM-1 wires with concrete release strengths of 4,500 psi (4,435 psi) also show a required length of 24 inches for development, whereas HSM-1 wires detensioned at 6,000 psi (6,300 psi) showed full development when only 16 inches of wire embedment was provided.

HSM-3 wires detensioned at a concrete release strength of 3,500 psi (3,420 psi) showed full development of the reinforcement at test lengths of 24 inches. The same wire detensioned at 4,500 psi (4,300 psi) was fully developed when provided with 18 inches of embedment length. Due to flexural-shear being the cause of failure in the last load test for the beams with a release strength of 6,000 psi (5,650 psi), the lowest embedment length that resulted in full development of the wire was 21 inches.

The voestalpine wire had the lowest development lengths throughout flexural testing. This wire showed full development at test lengths of 21 inches, 18 inches, and 16 inches for concrete release strengths of 3,500 psi (3,690 psi), 4,500 psi (4,590 psi), and 6,000 psi (6,090 psi), respectively. A summary of the development lengths for all wires and their respective concrete strengths, and flexural bond lengths, independent of member length, is shown below in Table 4.12.

Table 4.12: Development Lengths for All Wires, Based on Flexural Testing Results.

Lowest Embedment Length to Achieve Development				
Member Group	Embedment Length (inches)	f'ci at Release (psi)	Minimum Flexural Bond Length (inches)	f'c Before Testing (psi)
3500-H1	21	3,430	2.3	9,000
4500-H1	24	4,435	7.4	9,000
6000-H1	16	6,300	-2.5	9,000
3500-H3	24	3,420	1.7	7,000
4500-H3	18	4,300	1.2	7,000
6000-H3	16	5,650	-3.9	7,000
3500-V1	21	3,690	5.2	8,100
4500-V1	18	4,590	3.2	8,100
6000-V1	16	6,090	3.0	8,100

Chapter 5 - Conclusion

In this study, the bond properties of three different types of large-diameter indented prestressing wires were studied by analyzing the transfer length and development length results for 27 prestressed members. Through previous research in prestressed concrete, transfer length and development length have been shown to be two critical parameters in evaluating bonding properties of prestressing reinforcement.

In the first part of this experiment, transfer lengths of all 27 members fabricated in this study were calculated by using the surface strain present in the beam after prestress transfer. Previously proposed equations relating wire end-slip to the transfer length were analyzed in this study and showed moderate correlation when compared to transfer lengths found using the surface strain of the concrete members. Due to the lack of accuracy of estimated transfer lengths, these equations are only recommended as a rough approximation for transfer length. Transfer lengths attained through analysis of surface strain data were compared to previously recommended formulas for estimating transfer length. While some of the previously proposed transfer length equations came close in estimating the transfer lengths of the large diameter prestressing wire reviewed in this study, an equation was derived that approximated the transfer length of the wire with much less error.

Through analysis of the transfer length results, it was found that the smaller diameter voestalpine wire (7.5-mm) was the most affected by concrete release strengths. According to the Zhao-Lee method of approximating transfer lengths with strain data, voestalpine also had the lowest long-term transfer lengths for all concrete release strengths between the three wires. The more heavily indented wire, HSM-3 wire, on average showed the longest transfer lengths of all wires. This could be in part due to the lower concrete release strengths when compared to that of the other two wires. HSM-3 wires also had the least amount of change in transfer length over time. It is also worth noting that the majority of beams pretensioned with HSM-3 wire had lower strain values in comparison to beams pretensioned with the other two wires. HSM-1 wires on average had the lowest transfer lengths at the time of detensioning, but had the largest increase in transfer length over time. Overall, the transfer length of the indented prestressing wires showed growth of approximately 1.0” on average according to end-slip data, and decreased an average of 0.3” when using surface strain data. This is extremely minimal growth over time, especially when compared to that of prestressing strand which can show growth of approximately 30% in just 28 days (Lane, 1998). Transfer length for 270-ksi prestressing strand is estimated to be between 40D and 60D depending on concrete compressive strengths (Ramirez and Russell, 2008). The results from this study showed that an estimate of 60D would be a reasonable approximation for these wires.

In the second part of this study, the prestressed beams were loaded in three-point bending to determine development lengths for each member. All beams that reached the nominal moment capacity were said to have obtained full development. Beams that failed in bond most commonly experienced flexural-shear cracks, which propagated to within the development length and resulted in full wire slip. Approximate development lengths for each wire were attained through flexural testing of each specimen at various lengths from the beam’s end, with all members attaining full development at an embedment length of 24 inches. Based on the results of the testing, recommended development lengths were provided for each type of wire, dependent on concrete release strength. For HSM-1 wires, the research showed that the wire was fully developed at lengths of 24 inches for concrete release strengths of both 3,500 psi and 4,500 psi, and 16 inches for a release strength of 6,000 psi. HSM-3 wires were shown to be fully developed at test lengths of 24 inches, 18 inches, and 21 inches for concrete release strengths of 3,500 psi, 4,500 psi, and 6,000 psi, respectively. Voestalpine wires were fully developed at test lengths of 21 inches, 18 inches, and 16 inches for release strengths of 3,500 psi, 4,500 psi, and 6,000 psi, respectively.

These development lengths were compared to calculated development lengths using equations proposed by previous studies on prestressed concrete. These equations, primarily meant for larger prestressing strand, largely overestimated the development lengths found in this study.

Further research is needed to assess the accuracy of the equations proposed in this study, as this study was limited in terms of number of samples. It should also be noted that this study only used one consistent concrete mixture, representative of that commonly used in the manufacturing of concrete railroad ties. Therefore, bond behavior of wires may differ from what is shown in this study for other concrete mixtures. If determining the development length through flexural testing is chosen as a testing method for future research, it is also recommended that saw cutting be implemented in efforts to guide the flexural crack to directly below the loading point. This may result in more desirable cracking and reduce the amount of flexural-shear cracking that was witnessed in this research.

Chapter 6 - References

ACI 318. (2011). Building Code Requirements for Structural Concrete (ACI 318-11) and Commentary. Farmington Hills: American Concrete Institute.

Akhnoukh, A. K. (2008). *Development of high performance precast/prestressed bridge girders. ETD collection for University of Nebraska, Lincoln*.

Arnold, M. L., Peterman, R. J., (2013). Un-tensioned Pullout Tests to Predict the Bond Quality of Different Prestressing Reinforcements Used in Concrete Railroad Ties. Manhattan, KS: Kansas State University.

ASTM A1081. (2012). Standard Test Method for Evaluating Bond of Seven-Wire Prestressing Strand. 5 pp. West Conshohocken, PA: ASTM International.

Balaz, G. (1993, March-April). Transfer Length of Prestressing Strand as a Function of Strand Draw-in and Initial Prestress. *PCI*, 86-93.

Beck, BT, Robertson, AA, Peterman, RJ, Savic, A, Wu, CJ, Riding, KA, & Bloomfield, J. "A High Resolution Automated Prestressing Wire Indent Profiling System for Verification of Wire-Concrete Mix Compatibility." *Proceedings of the 2019 Joint Rail Conference*. *2019 Joint Rail Conference*. Snowbird, Utah, USA. April 9–12, 2019. V001T01A009. ASME.

Beck, B. T., Robertson, A. A., Peterman, R. J., Riding, K. A. (April 2021). A Wire Indent Profiling System for the Assessment of Bond and Splitting Propensity of Prestressing Wires Used in Pretensioned Concrete Railroad Ties. KSU-21-11. U. S. Department of Transportation Federal Railroad Administration.

Beck, B. T., Haynes, M., Wu, C. H., Peterman, R. J. (April 2021). Use of 3D Non-Contact Profilometry to Quantify Indent Characteristics of Prestressing Wires Used in Pretensioned Concrete Railroad Ties. KSU-21-7. U. S. Department of Transportation Federal Railroad Administration.

Buckner, C. D. (1995). A Review of Strand Development Length for Pretensioned Concrete Members. *PCI, 84-105.*

Chen, Y., Peterman, R. J., (2016). Testing and Modeling Tensile Stress-Strain Curve for Prestressing Wires in Railroad Ties. Manhattan, KS: Kansas State University.

Cousins, T. E., Johnson, D., & Zia, P. (July-August 1990). Transfer and Development Length of Epoxy Coated and Uncoated Prestressing Strands. *PCI*, 92-103.

Deatherage, H. J., Burdette, E. G., & Chew, C. K. (January-February 1994). Development Length and Lateral Spacing Requirements of Prestressing Strand for Prestressed Concrete Bridge Girders. *PCI*, 70-83.

Guyon, Y. (1953). *Prestressed Concrete.* John Wiley and Sons.

Hanna, A. (1979). Prestressed concrete Ties for North American Railroads. *PCI*, 32-61.

Hanna, A. (1986). Concrete Ties for U.S Railroads-an Update. *Concrete in Transportation*, 267-286.

Hanson, W. N., & Kaar, P. H. (n.d.). Flexural Bond Tests of Pretensioned Prestressed Beams. Journal of the American Concrete Institute.

Hawkins, N. M., & Ramirez, J. A. (2010). Due Diligence Review of NASP Strand Bond Test Method. Chicago, IL: *PCI*.

Kaar, P., LaFraugh, R. W., & Mass, M. A. (1963). Influence of Concrete Strength on Strand Transfer Length. *PCI*, 47-67.

Lane, S. N. (1998). A New Development Length Equation for Pretensioned Strands in Bridge Beams and Piles. McLean, Virginia: Federal Highway Administration.

Logan, D. R., Gerstle, K. H., Brooks, M. D. (1988). Effect of Initial Strand Slip on the Strength of Hollow-Core Slabs. *PCI*, 90-111.

Logan, D. R. (1997). Acceptance Criteria for Bond Quality of Strand for Pretensioned Prestressed Concrete Applications. *PCI*, 52-90.

Lu, Z., Boothby, T. E., Bakis, C. E., & Nanni, A. (March-April 2000). Transfer and Development Lengths of FRP Prestressing Tendons. *PCI*, 84-95.

Martin, L. D., & Scott, N. L. (1976). Development of Prestressing Strand in Pretensioned Members. 73(8).

Marti-Vargas, J., Caro, L., & Serna, P. (2013). Experimental Technique for Measuring the Long-term Transfer Length in Prestressed Concrete. Strain An International Journal for Experimental Mechanics, 125-134.

Momeni, A. F., Peterman, R. J. (2016). Effect of Concrete Properties and Prestressing Steel Indentation Types on the Development Length and flexural Capacity of Pretensioned Concrete Members. Doctor of Philosophy Dissertation, Kansas State University.

Momeni, A. F., Peterman, R. J., (2016). Effect of Concrete Properties and Prestressing Steel Indentation Types on the Development Length and Flexural Capacity of Pretensioned Concrete Members. Manhattan, KS: Kansas State University.

Polydorou, T., Riding, K. A., Peterman, R. J. (2014). Determination of Acceptance Criteria for Prestressing Strand in Pre-Tensioned Applications. Doctor of Philosophy Dissertation, Kansas State University.

Porterfield, K. B., Volz, J. S., Myers, J. J. Sneed, L. (2012). Bond, Transfer Length, and Development Length of Prestressing Strand in Self-Consolidating Concrete. Master's Thesis, Missouri University of Science and Technology.

Rose, D., & Russell, B. W. (1997). Investigation of Standardized Tests to Measure the Bond Performance of Prestressing Strand.

Russel, B. W., & Burns, N. H. (1993). *Design Guidelines for Transfer, Development and Debonding of Large Diameter Seven Wire Strands in Pretensioned Concrete Girders.* The University of Texas at Austin.

Russel, B. W., & Burns, N. H. (1996). Measured Transfer Lengths of 0.5 and 0.6 in. Strands in Pretensioned Concrete. PCI, 44-65.

Russell, B. W. (2006). *Final Report - NASP Round IV Strand Bond Testing*. Oklahoma State University.

Russell, B. W. (n.d.). *NASP Strand Bond Testing Round III*.

Russell, B. W., & Paulsgrove, G. A. (1999). *NASP Strand Bond Testing Round I*. Norman, OK: The University of Oklahoma.

Russell, B. W., & Paulsgrove, G. A. (1999). *NASP Strand Bond Testing Round II*. Norman, OK: University of Oklahoma.

Russell, B. W., & Ramirez, J. A. (2008). *NCHRP Report 603*. Washington, DC: Transportation Research Board.

Russell, B. W., & Ramirez, J. A. (2008). *NCHRP Report 603*. Washington, DC: Transportation Research Board.

Russell, B. W., and Burns, N. H. (1996). Measured Transfer Lengths of 0.5 and 0.6 in. Strands in Pretensioned Concrete. *PCI*, 41, 44-65.

Tabatabai, H., & Dickson, T. J. (1995). The History of the Prestressing Strand Development Length Equation. McLean, Virginia: US Department of Transportation Federal Highway Administration.

Vadivelu, Jayaprakash, (2009). Impact of Larger Diameter Strands on AASHTO/PCI Bulb-Tees. Master's Thesis, University of Tennessee.

Vadivelu, Jayaprakash, Impact of Larger Diameter Strands on AASHTO/PCI Bulb-Tees. Master's Thesis, University of Tennessee, 2009.

Vazquez-Herrero, C., Martinez-Lage, I., & Martinez-Abella, F. (2013). Transfer Length in Pretensioned Prestressed Concrete Structures Composed of High Performance Lightweight and Normal-Weight Concrete. *Engineering Structures*, 983-992.

Vazquez-Herrero, C., Martinez-Lage, I., & Martinez-Abella, F. (2013). Transfer Length in Pretensioned Prestressed Concrete Structures Composed of High Performance Lightweight and Normal-Weight Concrete. *Engineering Structures*, 983-992.

Vazquez-Herrero, C., Martinez-Lage, I., Aquilar, G., & Martinez-Abella, F. (2013). Evaluation of Strand Bond Properties along the Transfer Length of Prestressed Lightweight Concrete Members. *Engineering Structures*, 1048-1058.

Vazquez-Herrero, C., Martinez-Lage, I., Aquilar, G., & Martinez-Abella, F. (2013). Evaluation of Strand Bond Properties along the Transfer Length of Prestressed Lightweight Concrete Members. *Engineering Structures*, 1048-1058.

Zhao, W. (2011). Development of a Portable Optical Strain Sensor with Applications to Diagnostic Testing of Prestressed Concrete. Manhattan, KS: Kansas State University.

Zhao, W., Beck, B., Peterman, R., Murphy, R., Wu, C.-H., & Lee, G. (2013). A Direct Comparison of the Traditional Method and A New Approach in Determining 220 Transfer Lengths in Prestressed Concrete Railroad Ties. Joint Railroad Conference . Knoxville, TN.

Zhao, W., Beck, B., Peterman, R., Wu, C.-h., Lee, G., & Bodapati, N. (2013). Determining Transfer Length In Pre-Tensioned Concrete Railroad Ties: Is A new Evaluation Method Needed? Rail Transportation Division Fall Technical Conference. ASME, Altoona, PA.

Zhao, W., Murphy, R. L., Peterman, R. J., Beck, B., & Wu, C.-H. (2013, March). A Non-Contact Inspection Method to Determine the Transfer Length in Pre-tensioned Concrete Railroad Ties. *ASCE Journal of Engineering Mechanics*, 139(3), 256-263.

Zhao, W., Murphy, R. L., Peterman, R. J., Beck, B., & Wu, C.-H. (Winter 2012). Development of A Laster Speckle Imaging Device to Determine the Transfer Length in Pretensioned Concrete Members. *PCI*, 135-143.

Appendix A - Example of Moment Capacity Calculation

This example shows the calculation of the nominal moment capacity for Specimen 6.5-3500-H1, tested at a 24-inch embedment length.

Section Properties:

$$f_{pu} = 279\ ksi$$

$$E_{ps} = 28205\ ksi$$

$$Wire\ Diamater = \frac{7.8mm}{25.4} = .30709\ in$$

$$Wire\ Area = \pi \times \frac{.30709^2}{4} = .074065\ in^2$$

$$d_p = 10" - 2" = 8 \text{ in}$$

$$f'_c = 9\ ksi$$

$$Section\ Width = b = 6\ in$$

$$Section\ Height = h = 10\ in$$

$$Section\ Area = A_c = 60\ in^2$$

$$Section\ Moment\ of\ Inertia = \frac{bh^3}{12} = 500\ in^4$$

$$y = \frac{h}{2} = 5\ in$$

Calculating Prestress Losses:

$$Maximum\ Measured\ Strain = 680 \times 10^{-6}$$

$$Prestress\ Loss = 680 \times 10^{-6} \times E_{ps} = 19.180\ ksi$$

$$Initial\ Prestress = 15000\ lb$$

$$f_{pi} = \frac{15000}{.074065 \times 1000} = 202.525\ ksi$$

$$Total\ Prestress\ Loss = \frac{19.180}{202.525} \times 100 = 9.47\%$$

Calculating wire eccentricity and corresponding strains of prestressing wire:

$$e_1 = 3\ in\quad (centroid\ of\ wires\ located\ at\ beam\ center)$$

$$f_{pe} = 202.525 \times \left(1 - \frac{9.47}{100}\right) = 183.346\ ksi$$

$$\varepsilon_1 = \frac{f_{pe}}{E_{ps}} = .0065$$

$$E_c = 57\sqrt{f'_c} = 57 \times \sqrt{9000} = 5407.495\ ksi$$

$$\varepsilon_2 = \frac{p_e}{A_c E_c} + \frac{p_e e^2}{I_c E_c} = \frac{183.346 \times .074065 \times 2}{6 \times 10 \times 5407.495} + \frac{183.346 \times .074065 \times 2 \times 3^2}{500 \times 5407.495} = .000174$$

First, try c = 1 inch:

$$\varepsilon_3 = .003 \times \frac{d_p - c}{c} = .003 \times \frac{8-1}{1} = .021$$

$$\varepsilon_{ps} = \varepsilon_1 + \varepsilon_2 + \varepsilon_3 = .0065 + .000174 + .021 = .02767$$

Next, using the Power Formula calculate the stress in pre-stressing wires (f_{ps}):

1) Assumptions and wire properties:

$$f_{pu} = 279\ ksi$$

$$Strain\ at\ Yield = \varepsilon_y = 0.01 \qquad (assumption\ used\ in\ Power\ Formula)$$
$$Strain\ at\ Ultimate\ Capacity = \varepsilon_{pu} = 0.04 \qquad (assumption\ used\ in\ Power\ Formula)$$

2) Given the data above, we can solve for Kfpy, fpy, and constant Q:

$$Kf_{py} = 1.1665 f_{pu} - 62.4595 = 1.1665 \times 279 - 62.4595 = 262.994\ ksi$$

$$f_{py} = 1.0012 f_{pu} - 25.5406 = 1.0012 \times 279 - 25.5406 = 253.794\ ksi$$

$$Q = \frac{f_{pu} - Kf_{py}}{\varepsilon_{pu} E_p - Kf_{py}} = \frac{279 - 262.994}{.04 \times 28205 - 262.994} = .0185$$

3) Using the values found in Step 2 and setting fps equal to fpy, a constant R will be calculated using the Power Formula equation below:

$$f_{ps} = f_{py} = \varepsilon_{py} E_p \left[Q + \frac{1 - Q}{\left(1 + \left(\frac{\varepsilon_{py} E_p}{Kf_{py}}\right)^R\right)^{\frac{1}{R}}} \right]$$

$$253.794 = .01 \times 28205 \left[.0185 + \frac{1 - .0185}{\left(1 + \frac{.01 \times 28205^R}{262.994}\right)^{\frac{1}{R}}} \right]$$

Iterating to solve for R results in a constant R = 10.4319

4) Calculate fps by substituting Kfpy, Q, R, and prestressing strain (ε_{ps}):

$$f_{ps} = \varepsilon_{ps} E_p \left[Q + \frac{1 - Q}{\left(1 + \left(\frac{\varepsilon_{ps} E_p}{Kf_{py}}\right)^R\right)^{\frac{1}{R}}} \right]$$

$$f_{ps} = .02767 * 28205 \times \left[.0185 + \frac{1 - .0185}{\left(1 + \left(\frac{.02767 \times 28205}{262.944}\right)^{10.4319}\right)^{\frac{1}{10.4319}}} \right] = 272.569\ ksi$$

Checking depth of Neutral Axis (c) by summing forces in the horizontal direction:

$$\sum F_x = 0 = T - C$$

$$T = C$$

$$0.85 \times f'_c \times \beta_1 \times b \times c = A_{ps} \times f_{ps}$$

$$0.85 \times 9 \times 0.65 \times 6 \times 1.0 = 2 \times 0.074065 \times 272.569$$

$$29.835\ kip \neq 40.3756\ kip$$

First, try c = 1.3376 inch:

$$\varepsilon_3 = .003 \times \frac{d_p - c}{c} = .003 \times \frac{8 - 1.3376}{1.3376} = .01494$$

$$\varepsilon_{ps} = \varepsilon_1 + \varepsilon_2 + \varepsilon_3 = .0065 + .000174 + .01494 = .02162$$

$$f_{ps} = .02162 * 28205 \times \left[.0185 + \frac{1 - .0185}{\left(1 + \left(\frac{.02162 \times 28205}{262.944}\right)^{10.4319}\right)^{\frac{1}{10.4319}}} \right] = 269.404\ ksi$$

Checking depth of Neutral Axis (c) by summing forces in the horizontal direction:

$$\sum F_x = 0 = T - C$$

$$T = C$$

$$0.85 \times f'_c \times \beta_1 \times b \times c = A_{ps} \times f_{ps}$$

$$0.85 \times 9 \times 0.65 \times 6 \times 1.3376 = 2 \times 0.074065 \times 269.404$$

$$39.907\ kip = 39.907\ kip$$

$$T = C \ \rightarrow \ Depth\ of\ Neutral\ Axis = 1.3376\ inches$$

Taking the moment about the center of compression block:

$$M_n = A_{ps} f_{ps} \left(d_p - \frac{\beta_1 c}{2} \right)$$

$$M_n = 2 \times .074065 \times 269.404 \times \left(8 - \frac{0.65 \times 1.3376}{2} \right) = 301.9\ \ kip - in$$

Appendix B - Wire Specifications

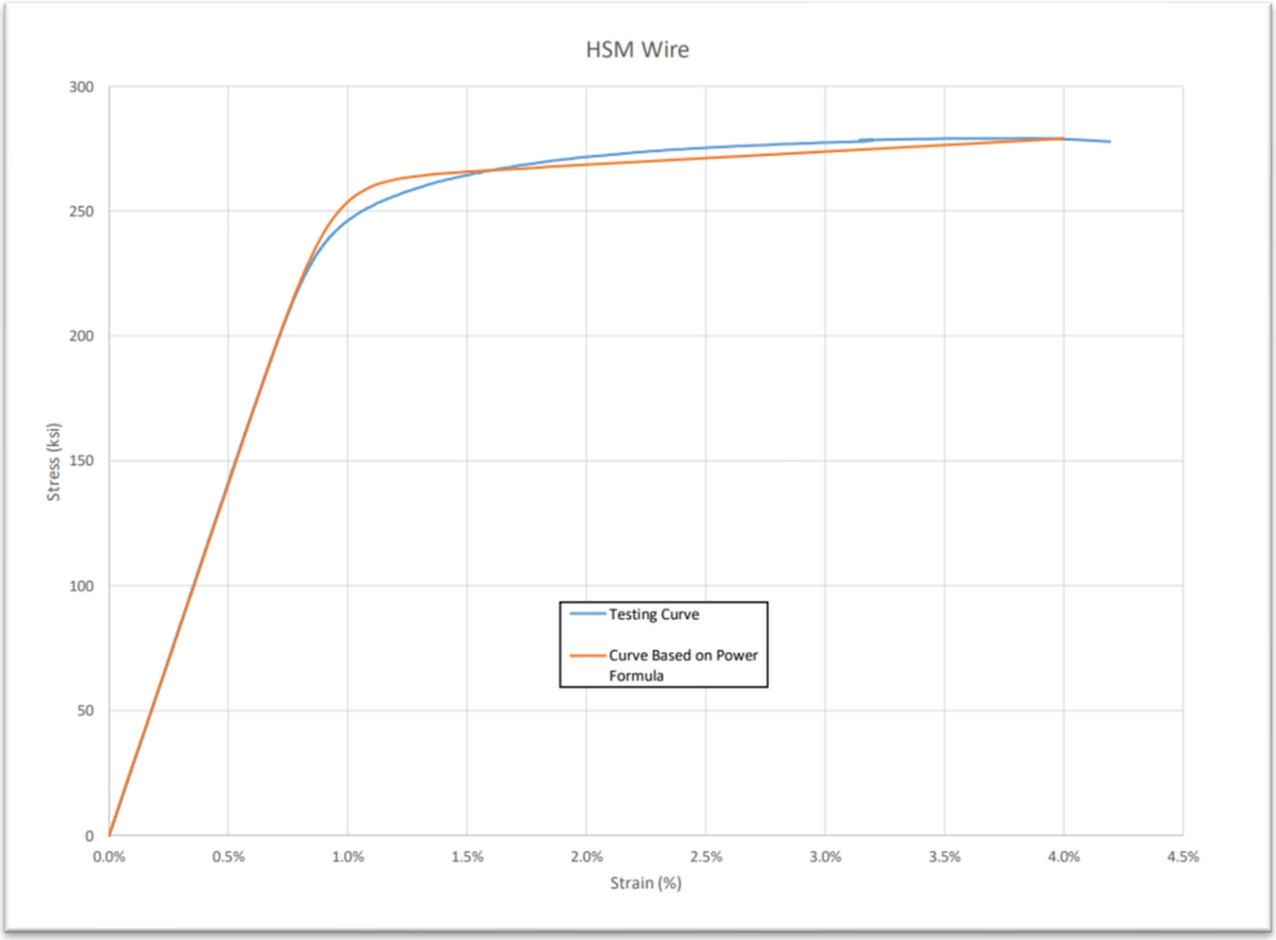

Figure B.1: Stress vs. Strain Curve for HSM-1 Wire.

Table B.1: HSM Indented Wire Properties.

Average Wire Diameter (HSM-1):	7.588 mm
Average Wire Diameter (HSM-3):	7.495 mm
Cross-Sectional Area (HSM-1):	.0700 in^2
Cross-Sectional Area (HSM-3):	.0684 in^2
Yield Strength:	253.8 ksi
Tensile Strength:	279.2 ksi
E	28,205 ksi

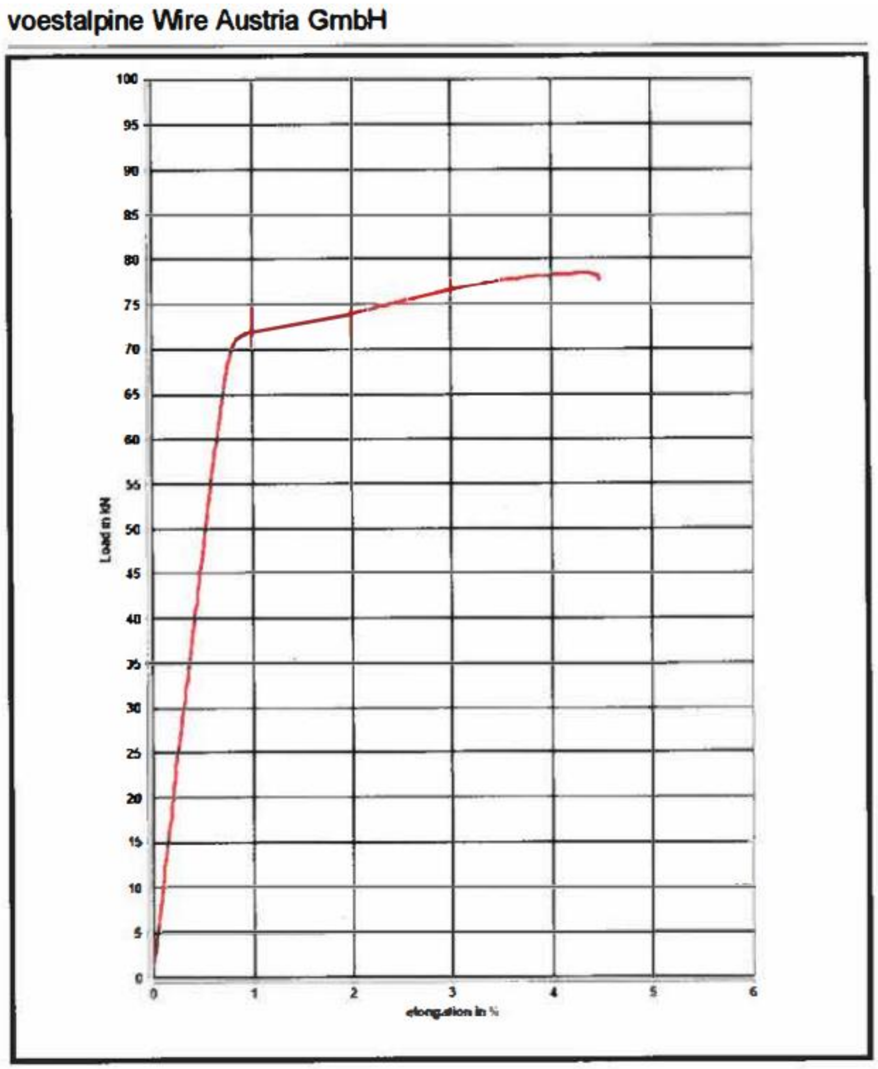

Figure B.2: Stress vs. Strain Curve for Voestalpine Wire.

Table B.2: Voestalpine Indented Wire Properties.

Average Wire Diameter:	7.323 mm
Cross-Sectional Area:	.0653 in^2
Yield Strength:	235.8 ksi
Tensile Strength:	257.3 ksi
E	29,486 ksi

Table B.3: Wire Scan Report for HSM-1 Prestressing Wire Using Non-Contact Wire Scanner.

	Row 1			Row 2			Row 3		
Indents: (99 total)	33			33			33		
Orientation	-44.0			59.5			53.4		
Bite Per Length (2.89)	2.79			2.78			3.10		
	5%	Row 1 Mean	95%	5%	Row 2 Mean	95%	5%	Row 3 Mean	95%
Depth(In)	0.00100	0.00320	0.00453	0.00115	0.00292	0.00434	0.00144	0.00343	0.00468
Length(In)	0.16515	0.20296	0.27559	0.16805	0.19708	0.26332	0.15710	0.19606	0.22761
Sidewall Angle L(Deg)	1.27786	14.30708	21.13355	1.50218	16.41985	26.28572	2.57088	16.98704	24.28294
Sidewall Angle R(Deg)	1.64358	20.51409	29.85940	1.99817	14.96892	22.18071	3.76536	16.20540	21.87701
ProfileArea(sq In)	0.00018	0.00061	0.00090	0.00019	0.00054	0.00084	0.00023	0.00063	0.00088
Sidewall Length L(In)	0.00889	0.01791	0.03470	0.00773	0.01431	0.03466	0.00781	0.01488	0.03389
Sidewall Length R(In)	0.00688	0.01184	0.03466	0.00702	0.01410	0.03466	0.00830	0.01397	0.02662
BasinLengths(In)	0.13325	0.17433	0.20629	0.13932	0.16957	0.19236	0.13108	0.16830	0.18555
Width(In)	0.14337	0.15521	0.18983	0.15935	0.16834	0.17449	0.15257	0.15990	0.17397
Volume(mm3)	1.41333	1.52850	1.67976	1.35338	1.46525	1.58036	1.55170	1.63164	1.72984
Pitch(In)	0.34489	0.34499	0.34523	0.34114	0.34145	0.34158	0.34247	0.34252	0.34265
Sidewall Area L(sq In)	0.00291	0.00388	0.00621	0.00183	0.00273	0.00429	0.00215	0.00289	0.00414
Sidewall Area R(sq In)	0.00205	0.00258	0.00464	0.00190	0.00270	0.00445	0.00223	0.00272	0.00418

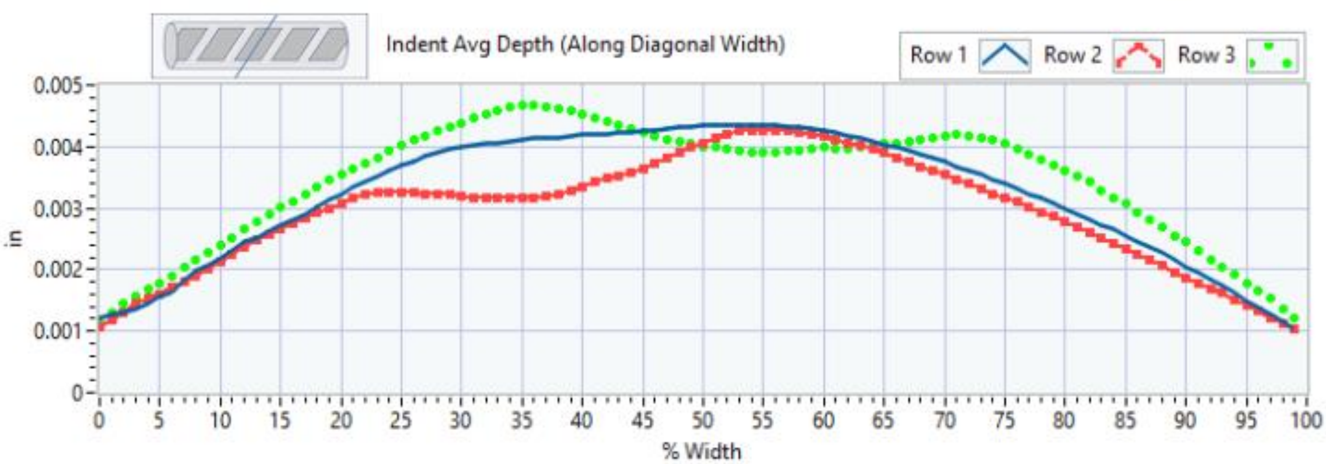

Table B.4: Wire Scan Report for HSM-3 Prestressing Wire Using Non-Contact Wire Scanner.

	Row 1			Row 2			Row 3		
Indents: (99 total)	33			33			33		
Orientation	-53.4			60.0			53.2		
Bite Per Length (5.90)	6.34			5.28			6.08		
	5%	Row 1 Mean	95%	5%	Row 2 Mean	95%	5%	Row 3 Mean	95%
Depth(In)	0.00304	0.00630	0.00856	0.00270	0.00534	0.00772	0.00287	0.00623	0.00802
Length(In)	0.15137	0.20020	0.22109	0.17744	0.20160	0.22067	0.16631	0.19729	0.21532
Sidewall Angle L(Deg)	3.12831	19.12136	25.78430	2.32274	20.46106	30.74127	13.92097	24.78537	33.11132
Sidewall Angle R(Deg)	7.68883	25.23892	36.17754	3.10163	19.59071	25.45133	3.76666	20.93867	27.53990
ProfileArea(sq In)	0.00045	0.00117	0.00173	0.00042	0.00099	0.00155	0.00041	0.00115	0.00159
Sidewall Length L(In)	0.01002	0.02543	0.06511	0.01041	0.02344	0.08744	0.01112	0.01549	0.01945
Sidewall Length R(In)	0.01128	0.01693	0.03070	0.01017	0.01967	0.04921	0.01382	0.02024	0.03902
BasinLengths(In)	0.11138	0.16054	0.18738	0.10333	0.16055	0.18681	0.11773	0.16426	0.18463
Width(In)	0.17693	0.17942	0.18193	0.17381	0.17604	0.17765	0.16731	0.17438	0.21500
Volume(mm3)	3.27240	3.37466	3.46382	2.69170	2.80773	2.92685	3.15038	3.23667	3.44964
Pitch(In)	0.34482	0.34503	0.34538	0.34459	0.34480	0.34519	0.34554	0.34572	0.34607
Sidewall Area L(sq In)	0.00500	0.00558	0.00625	0.00360	0.00465	0.00564	0.00304	0.00333	0.00533
Sidewall Area R(sq In)	0.00329	0.00370	0.00441	0.00361	0.00390	0.00447	0.00366	0.00431	0.00620

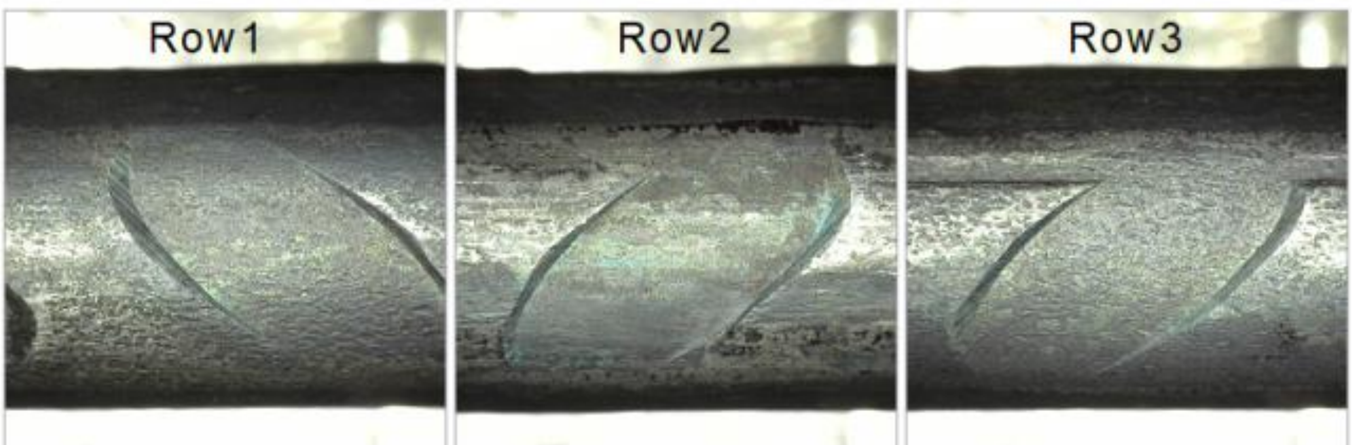

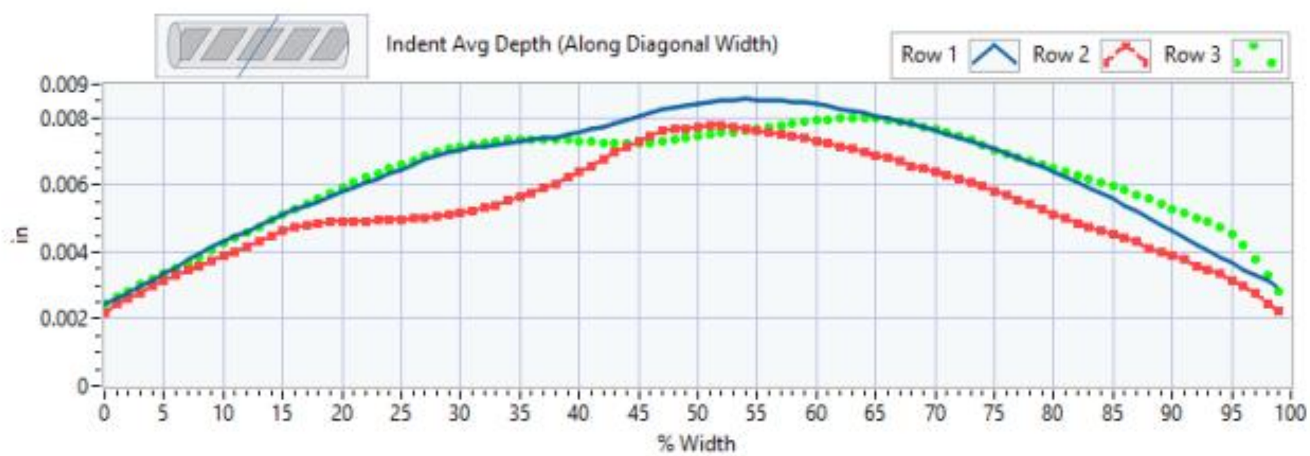

Table B.5: Wire Scan Report for V-1 Prestressing Wire Using Non-Contact Wire Scanner.

	Row 1			Row 2			Row 3		
Indents: (75 total)	25			25			25		
Orientation	-46.1			51.8			45.8		
Bite Per Length (3.65)	3.89			3.77			3.27		
	5%	Row 1 Mean	95%	5%	Row 2 Mean	95%	5%	Row 3 Mean	95%
Depth(In)	0.00155	0.00317	0.00445	0.00151	0.00322	0.00458	0.00141	0.00297	0.00430
Length(In)	0.17897	0.21460	0.26535	0.18373	0.21328	0.23677	0.16536	0.21047	0.26298
Sidewall Angle L(Deg)	1.26554	9.91226	15.31144	2.03514	15.39259	21.99544	1.32574	12.19010	20.61618
Sidewall Angle R(Deg)	1.50316	12.02731	21.64528	1.68590	13.14872	19.24746	1.39073	11.26685	21.71166
ProfileArea(sq In)	0.00025	0.00060	0.00092	0.00026	0.00064	0.00096	0.00023	0.00056	0.00085
Sidewall Length L(In)	0.00939	0.02863	0.10193	0.00730	0.01623	0.05075	0.00815	0.02471	0.08330
Sidewall Length R(In)	0.01006	0.02339	0.06920	0.00854	0.02071	0.05706	0.00875	0.02404	0.06467
BasinLengths(In)	0.08693	0.16325	0.19921	0.12700	0.17723	0.20360	0.10533	0.16240	0.19763
Width(In)	0.20412	0.21073	0.21955	0.19307	0.20026	0.21565	0.17586	0.18737	0.19463
Volume(mm3)	1.93725	2.07143	2.36910	1.83440	2.05679	2.32649	1.59417	1.70484	1.85032
Pitch(In)	0.33122	0.33222	0.33468	0.33011	0.33104	0.33169	0.32777	0.32885	0.33094
Sidewall Area L(sq In)	0.00524	0.00827	0.01140	0.00322	0.00406	0.00566	0.00447	0.00635	0.00816
Sidewall Area R(sq In)	0.00501	0.00671	0.01065	0.00341	0.00517	0.01043	0.00429	0.00615	0.01097

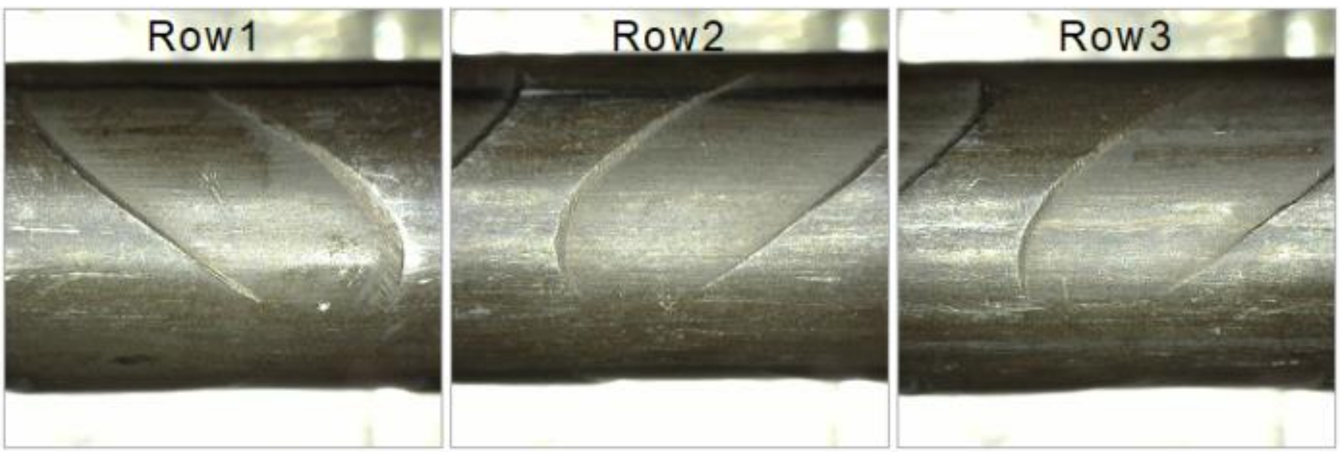

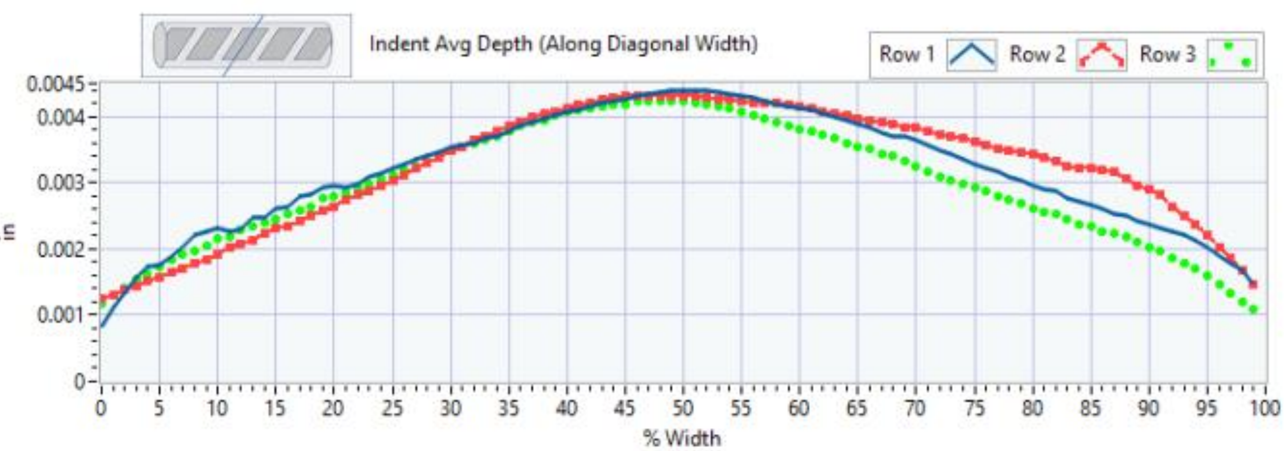

Appendix C - Specimen Transfer Length Results

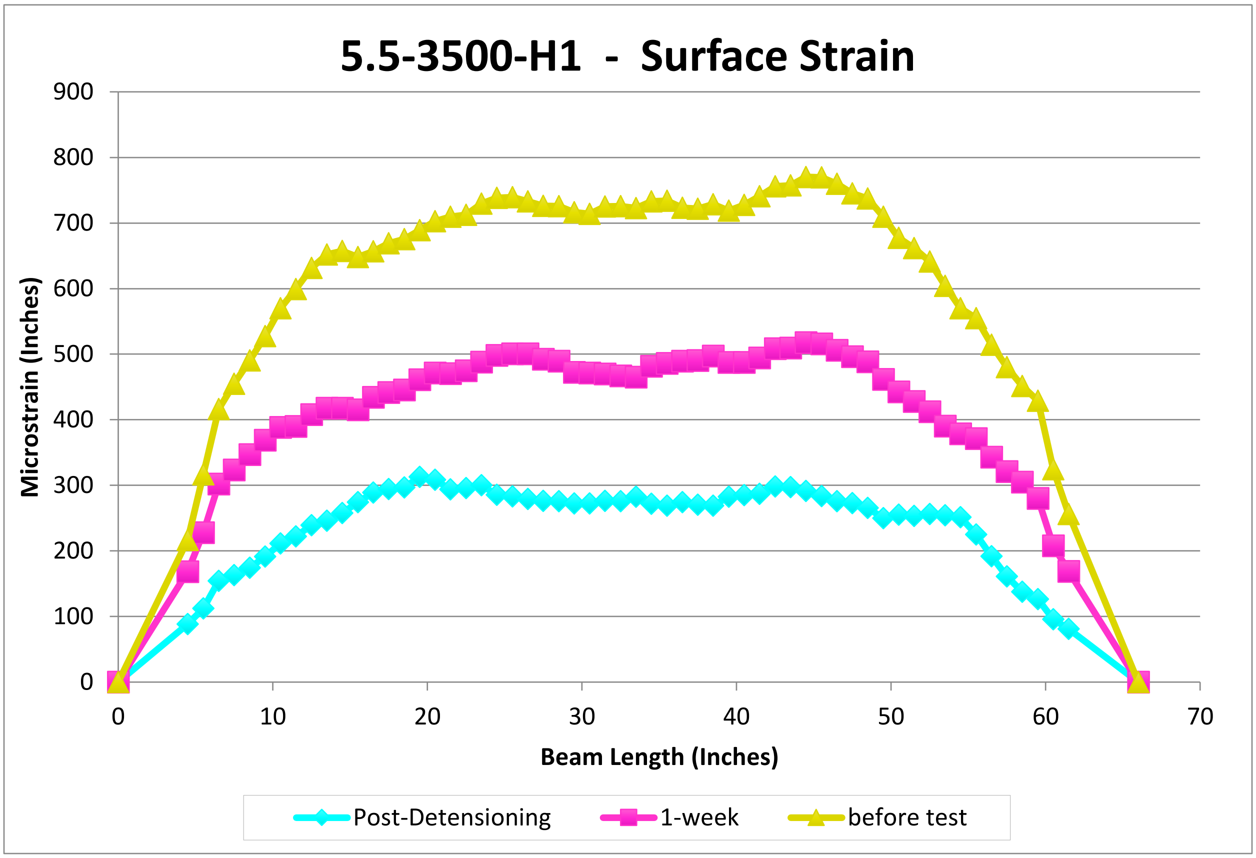

Figure C.1: Surface Strain Measurements for Beam 5.5-3500-H1.

Table C.1: Transfer Length Summary for 5.5-3500-H1.

Transfer Length				
Time of Measurement	**Live End (AMS)**	**Dead End (AMS)**	**Live End (ZL)**	**Dead End (ZL)**
After Detensioning	15.4	17.4	15.6	13.7
1-Week	18.8	16.8	18.0	17.4
Before Testing	17.9	16.3	14.6	16.3

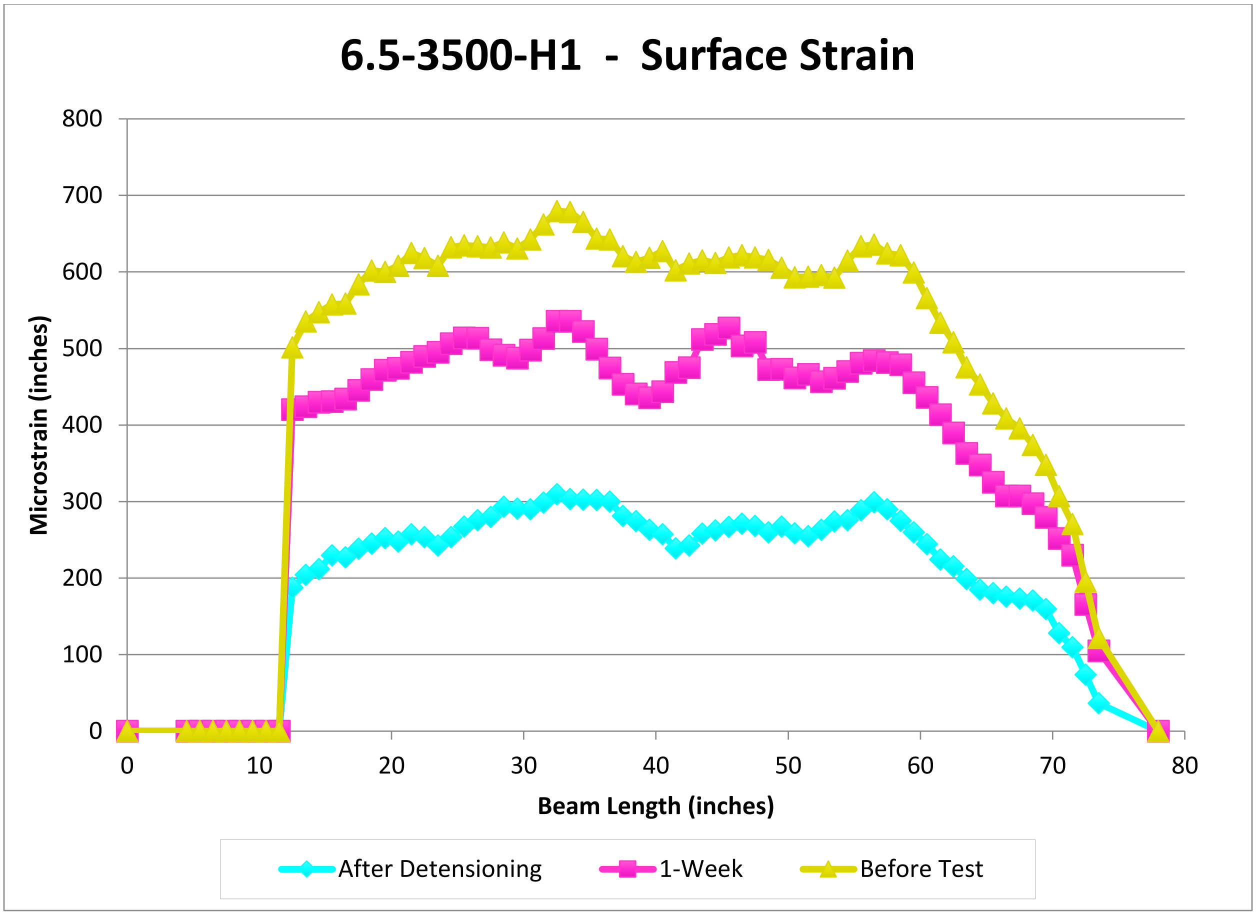

Figure C.2: Surface Strain Measurements for Beam 6.5-3500-H1.

Table C.2: Transfer Length Summary for 6.5-3500-H1.

Transfer Length				
Time of Measurement	**Live End (AMS)**	**Dead End (AMS)**	**Live End (ZL)**	**Dead End (ZL)**
After Detensioning	-	18.1	-	18.3
1-Week	-	18.5	-	19.5
Before Testing	-	18.0	-	18.3

Several brass inserts on the Live End of the beam were damaged during removal of formwork and surface displacement measurements could not be made. Therefore, Transfer Length values for the Live End of the beam were discarded.

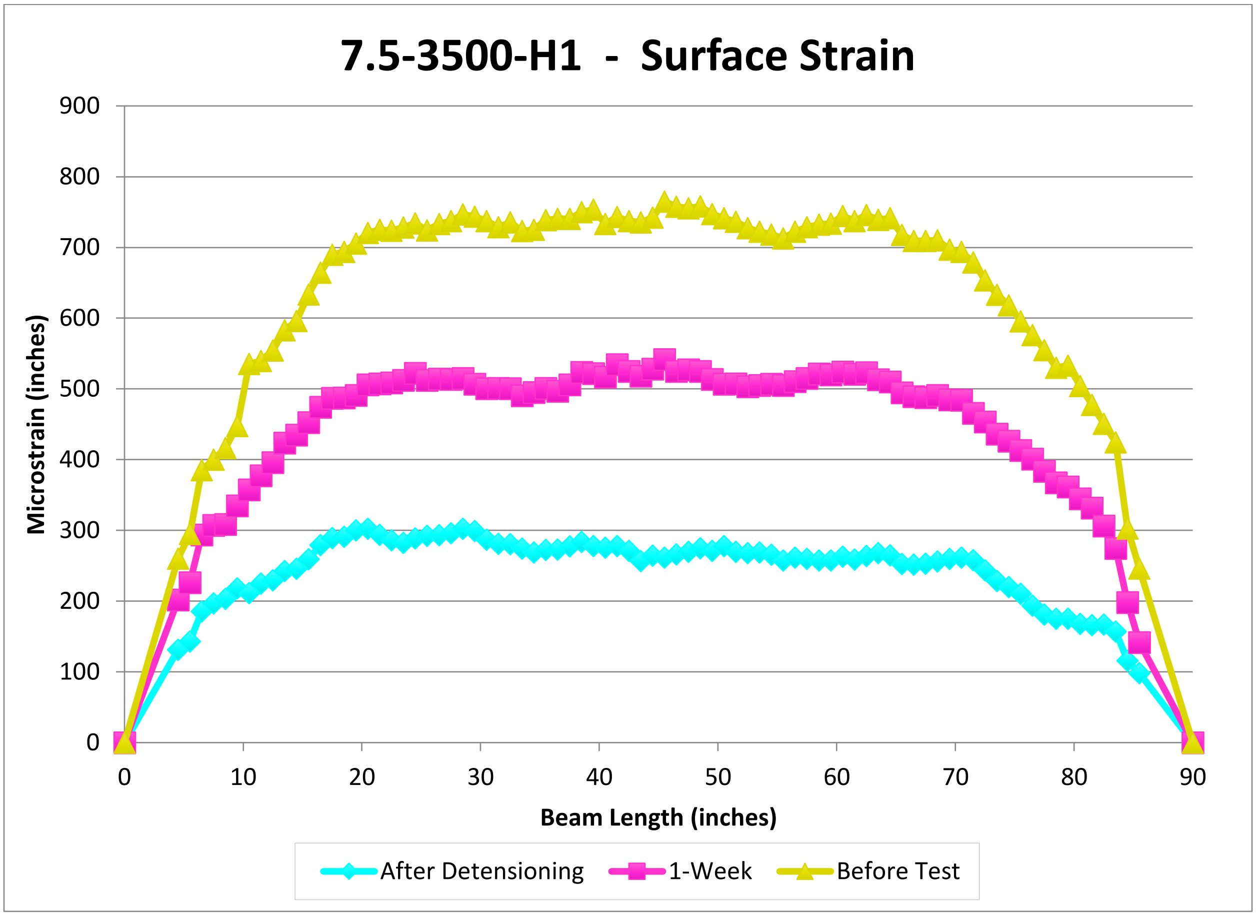

Figure C.3: Surface Strain Measurements for Beam 7.5-3500-H1.

Table C.3: Transfer Length Summary for 7.5-3500-H1.

Transfer Length				
Time of Measurement	**Live End (AMS)**	**Dead End (AMS)**	**Live End (ZL)**	**Dead End (ZL)**
After Detensioning	16.0	18.0	17.6	21.2
1-Week	17.3	19.5	18.8	20.3
Before Testing	18.9	20.3	18.9	18.6

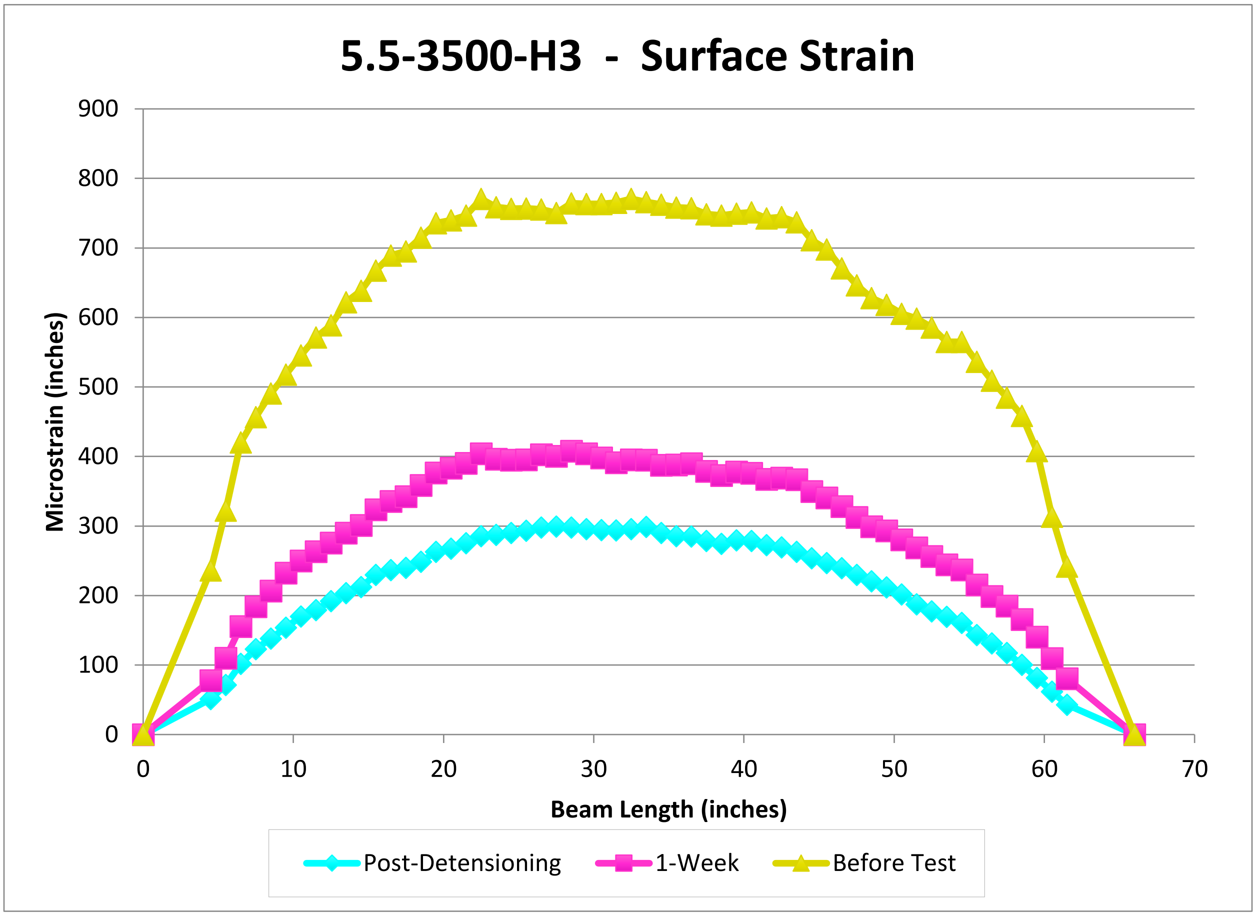

Figure C.4: Surface Strain Measurements for Beam 5.5-3500-H3.

Table C.4: Transfer Length Summary for 5.5-3500-H3.

Transfer Length				
Time of Measurement	**Live End (AMS)**	**Dead End (AMS)**	**Live End (ZL)**	**Dead End (ZL)**
After Detensioning	21.7	23.3	20.7	22.5
1-Week	19.5	22.3	19.3	23.1
Before Testing	18.6	21.2	17.6	19.5

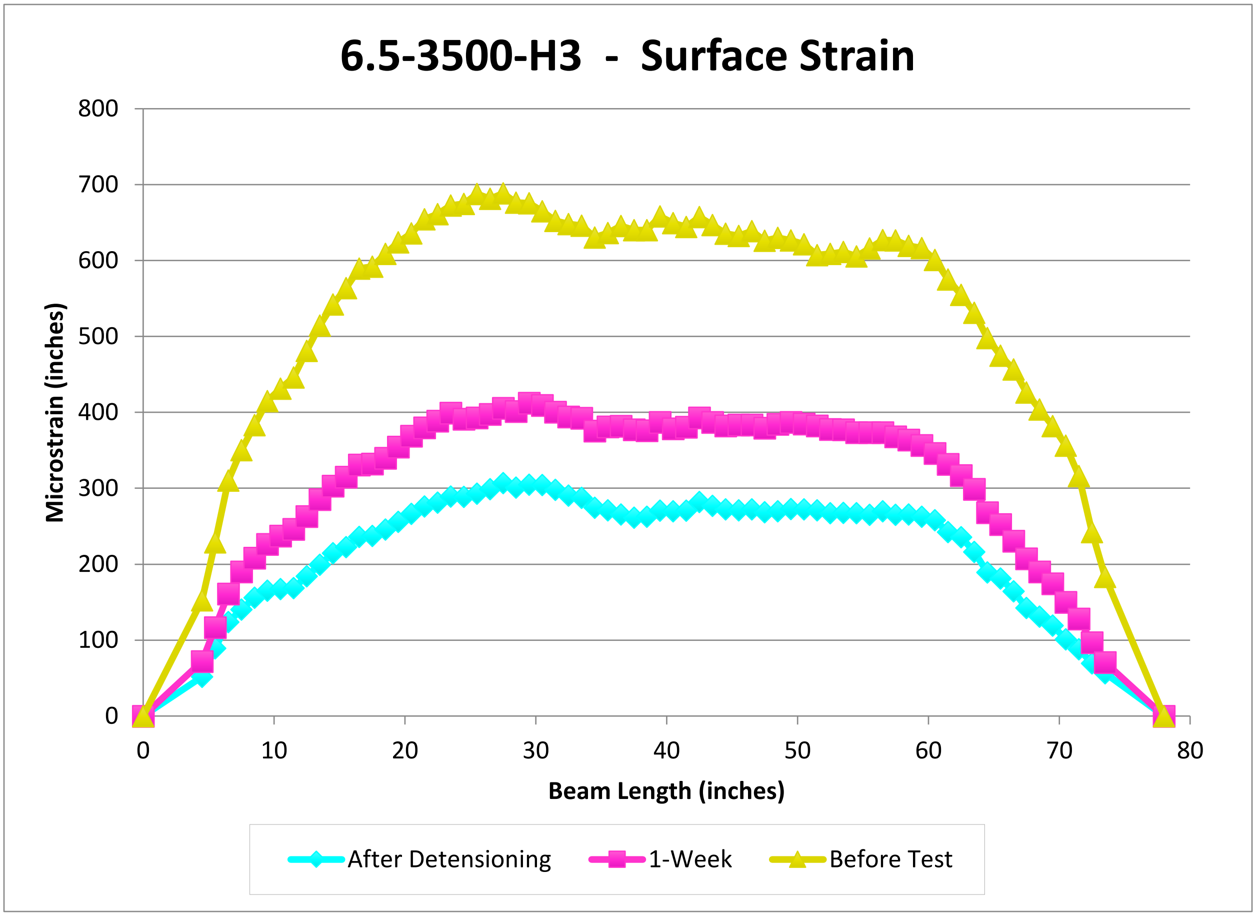

Figure C.5: Surface Strain Measurements for Beam 6.5-3500-H3.

Table C.5: Transfer Length Summary for 6.5-3500-H3.

Transfer Length				
Time of Measurement	**Live End (AMS)**	**Dead End (AMS)**	**Live End (ZL)**	**Dead End (ZL)**
After Detensioning	21.3	17.2	21.7	19.6
1-Week	20.8	18.5	20.2	18.5
Before Testing	19.6	17.4	18.4	17.9

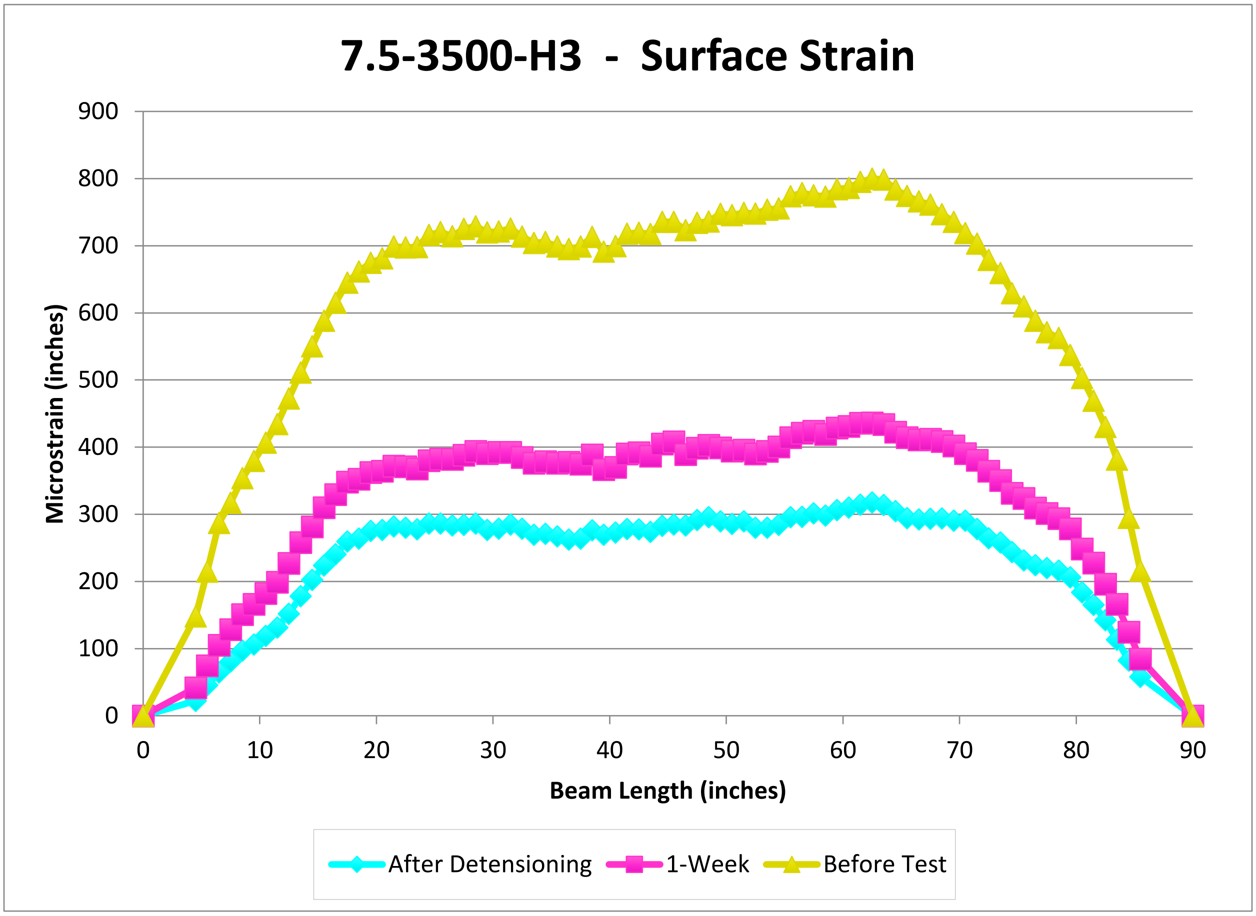

Figure C.6: Surface Strain Measurements for Beam 7.5-3500-H3.

Table C.6: Transfer Length Summary for 7.5-3500-H3.

Transfer Length				
Time of Measurement	**Live End (AMS)**	**Dead End (AMS)**	**Live End (ZL)**	**Dead End (ZL)**
After Detensioning	18.7	18.4	18.6	17.7
1-Week	19.6	19.1	18.9	18.7
Before Testing	19.7	19.5	19.3	19.4

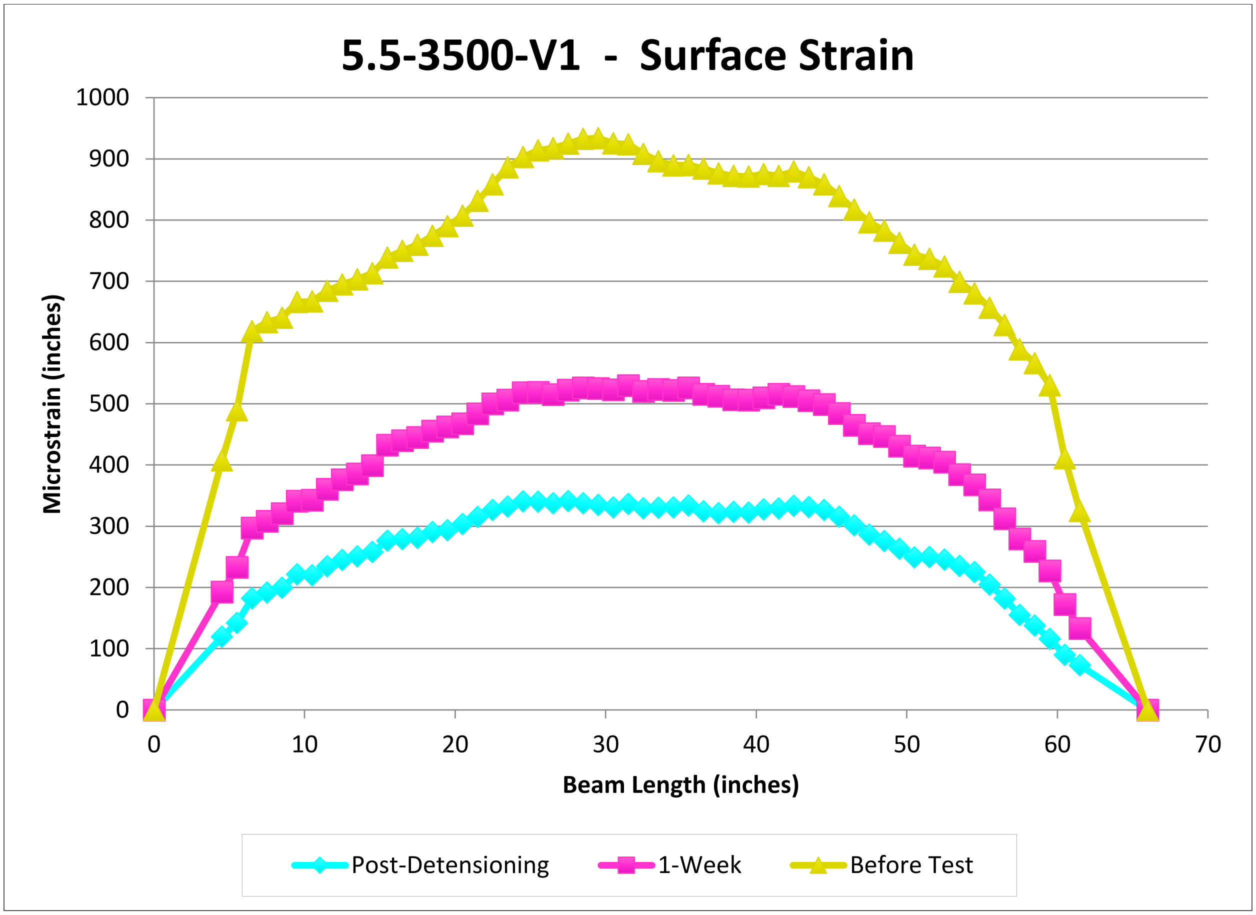

Figure C.7: Surface Strain Measurements for Beam 5.5-3500-V1.

Table C.7: Transfer Length Summary for 5.5-3500-V1.

Transfer Length				
Time of Measurement	**Live End (AMS)**	**Dead End (AMS)**	**Live End (ZL)**	**Dead End (ZL)**
After Detensioning	21.8	20.1	23.3	20.0
1-Week	22.1	20.6	23.1	20.0
Before Testing	21.2	19.6	13.4*	15.6*

* Transfer Length calculated using the software shows a low value when compared to the plotted strain. Use of the 1-week transfer length is recommended.

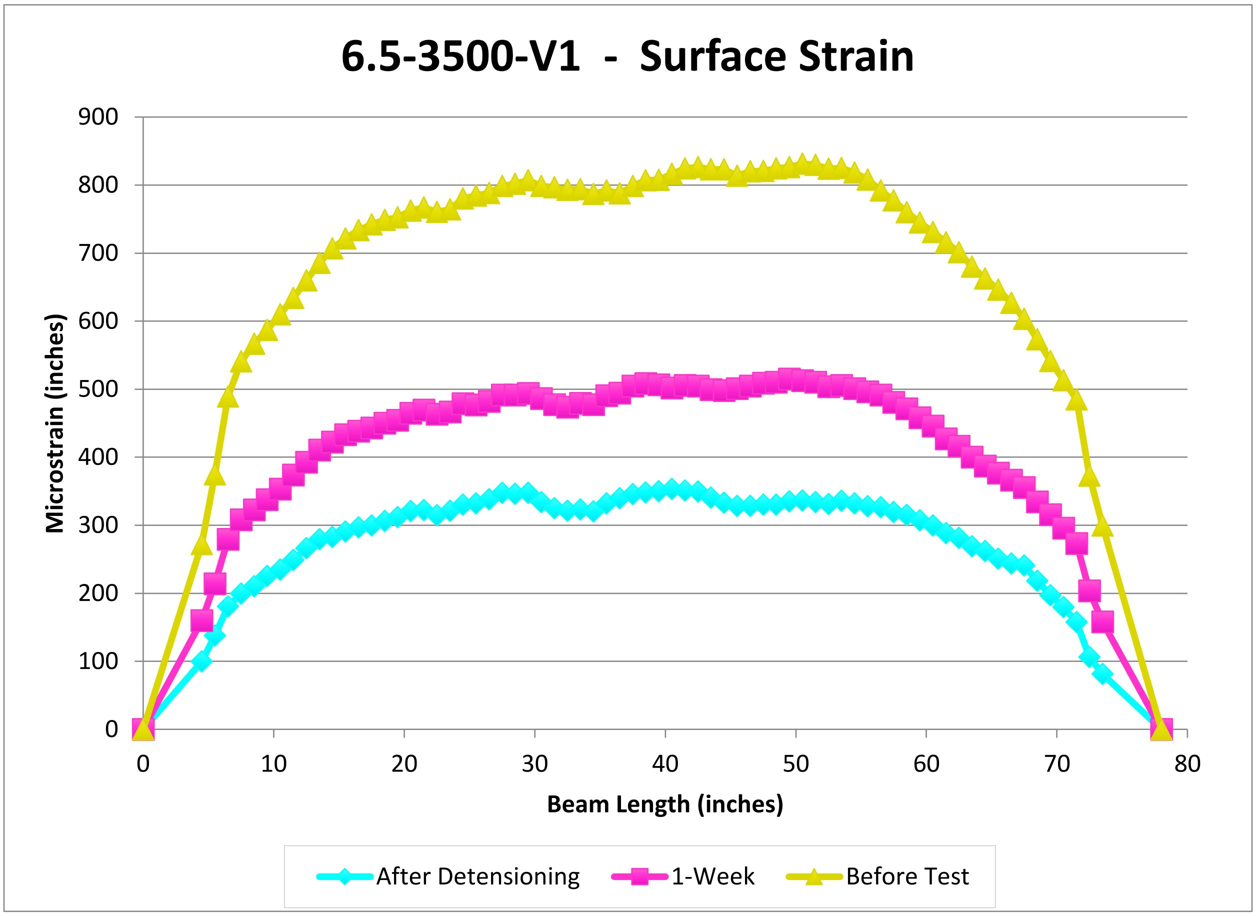

Figure C.8: Surface Strain Measurements for Beam 6.5-3500-V1.

Table C.8: Transfer Length Summary for 6.5-3500-V1.

Transfer Length				
Time of Measurement	**Live End (AMS)**	**Dead End (AMS)**	**Live End (ZL)**	**Dead End (ZL)**
After Detensioning	19.5	19.9	18.3	19.1
1-Week	19.3	20.3	17.5	20.9
Before Testing	17.3	20.2	14.6	17.0

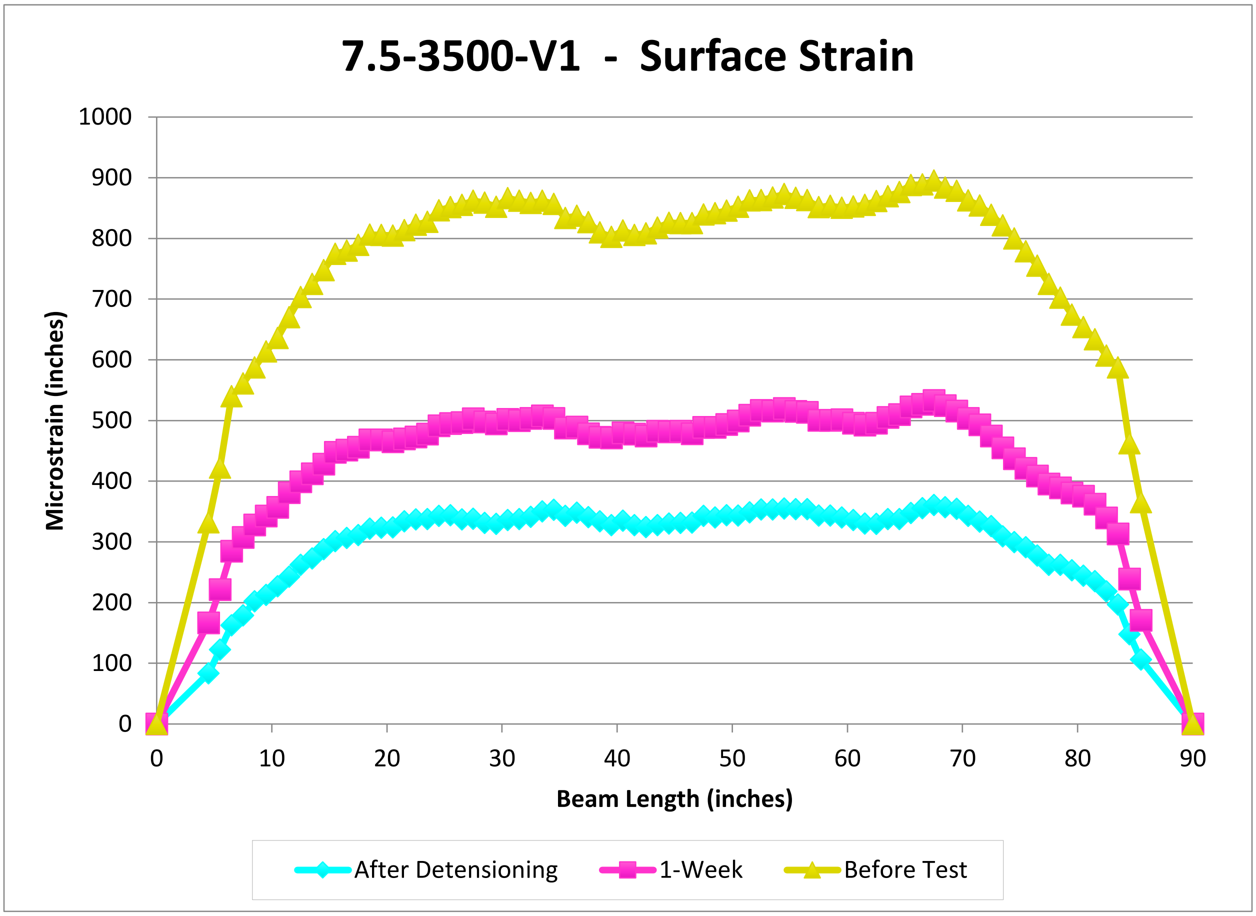

Figure C.9: Surface Strain Measurements for Beam 7.5-3500-V1.

Table C.9: Transfer Length Summary for 7.5-3500-V1.

Transfer Length				
Time of Measurement	**Live End (AMS)**	**Dead End (AMS)**	**Live End (ZL)**	**Dead End (ZL)**
After Detensioning	18.2	17.8	17.4	18.7
1-Week	17.9	17.9	17.5	18.8
Before Testing	17.5	16.2	14.4	13.3*

* Transfer Length calculated using the software shows a low value when compared to the plotted strain. Use of the 1-week transfer length is recommended.

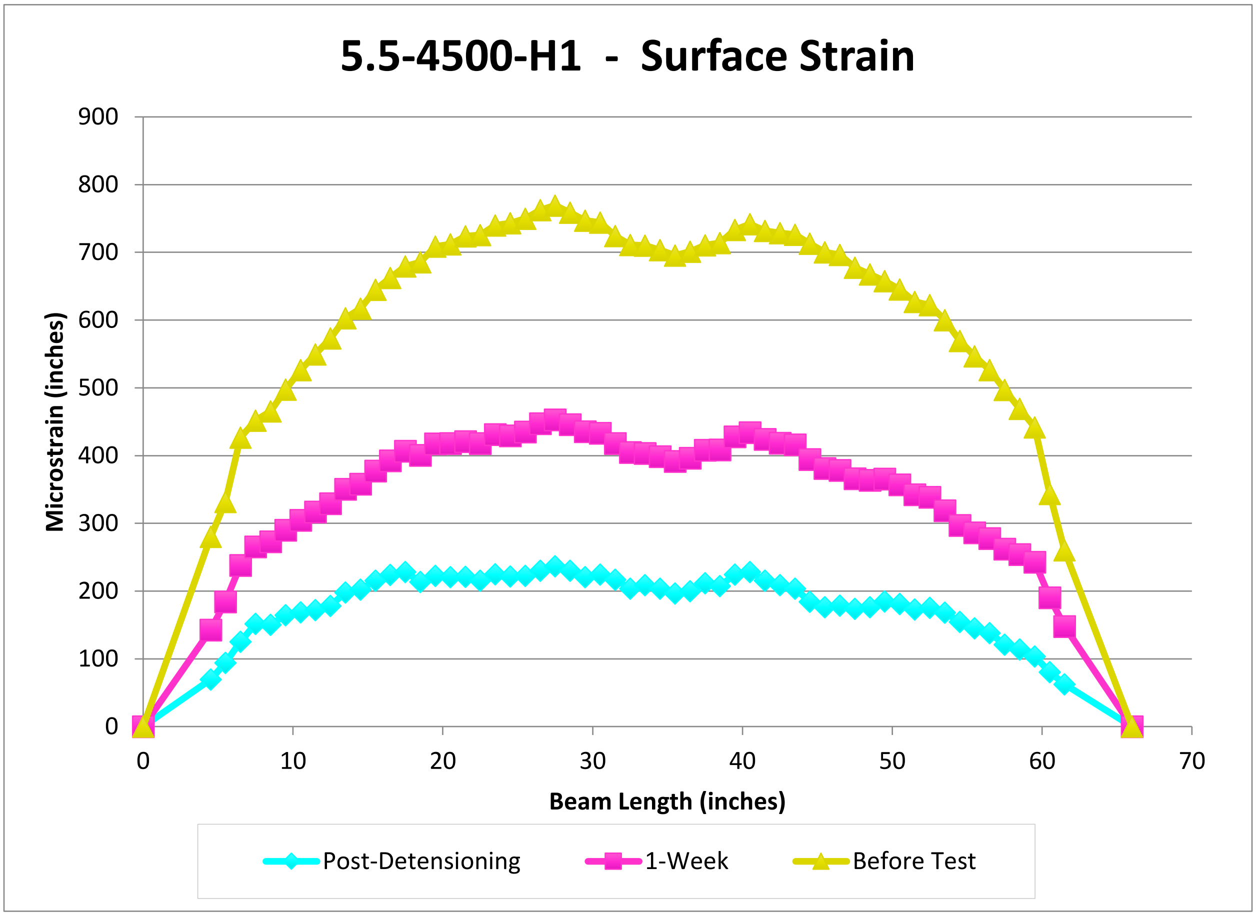

Figure C.10: Surface Strain Measurements for Beam 5.5-4500-H1.

Table C.10: Transfer Length Summary for 5.5-4500-H1.

Transfer Length				
Time of Measurement	**Live End (AMS)**	**Dead End (AMS)**	**Live End (ZL)**	**Dead End (ZL)**
After Detensioning	15.2	21.8	15.2	21.2
1-Week	18.9	21.0	19.0	21.0
Before Testing	19.2	18.1	17.9	15.4

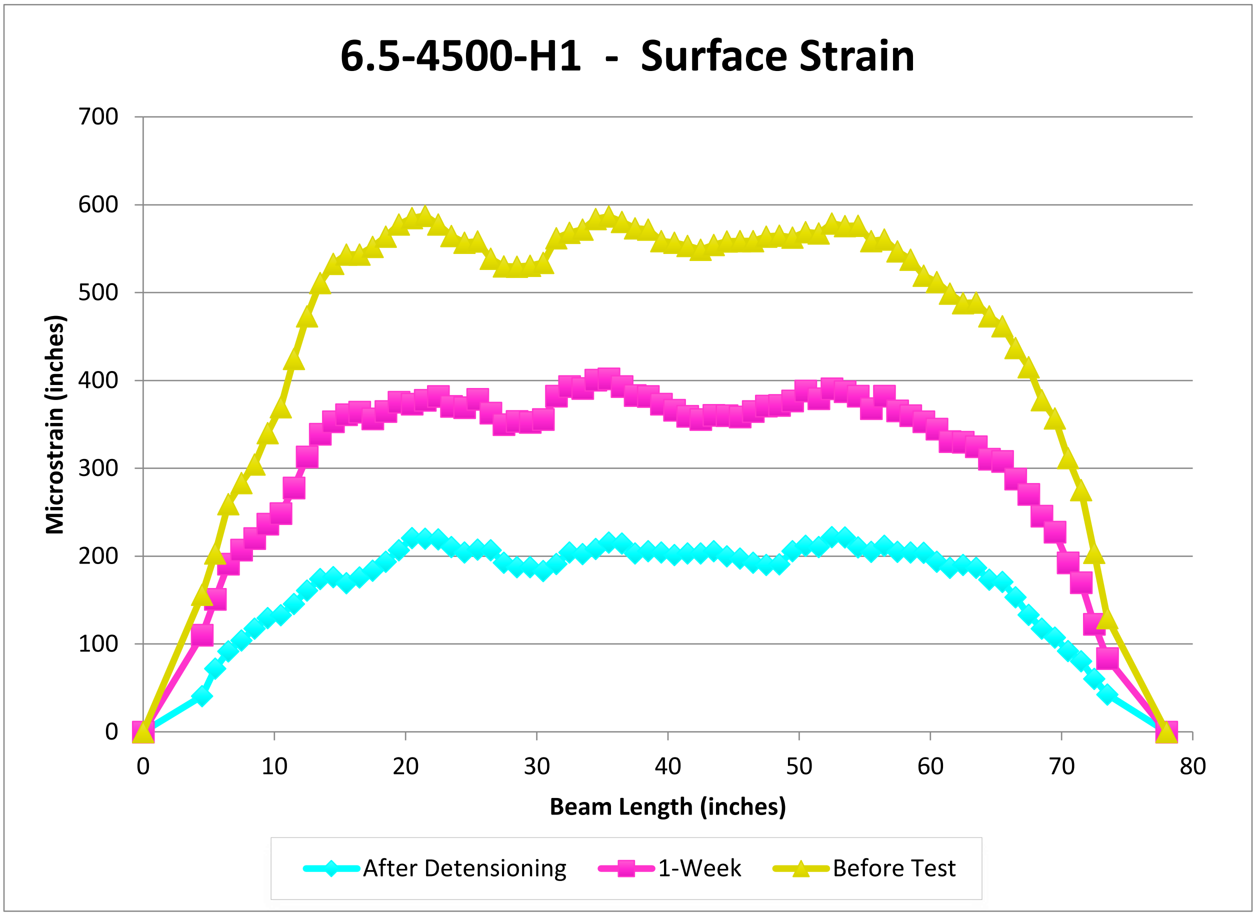

Figure C.11: Surface Strain Measurements for Beam 6.5-4500-H1.

Table C.11: Transfer Length Summary for 6.5-4500-H1.

Transfer Length				
Time of Measurement	**Live End (AMS)**	**Dead End (AMS)**	**Live End (ZL)**	**Dead End (ZL)**
After Detensioning	18.4	17.5	17.2	15.2
1-Week	15.0	18.1	16.1	15.5
Before Testing	14.8	18.9	15.6	15.8

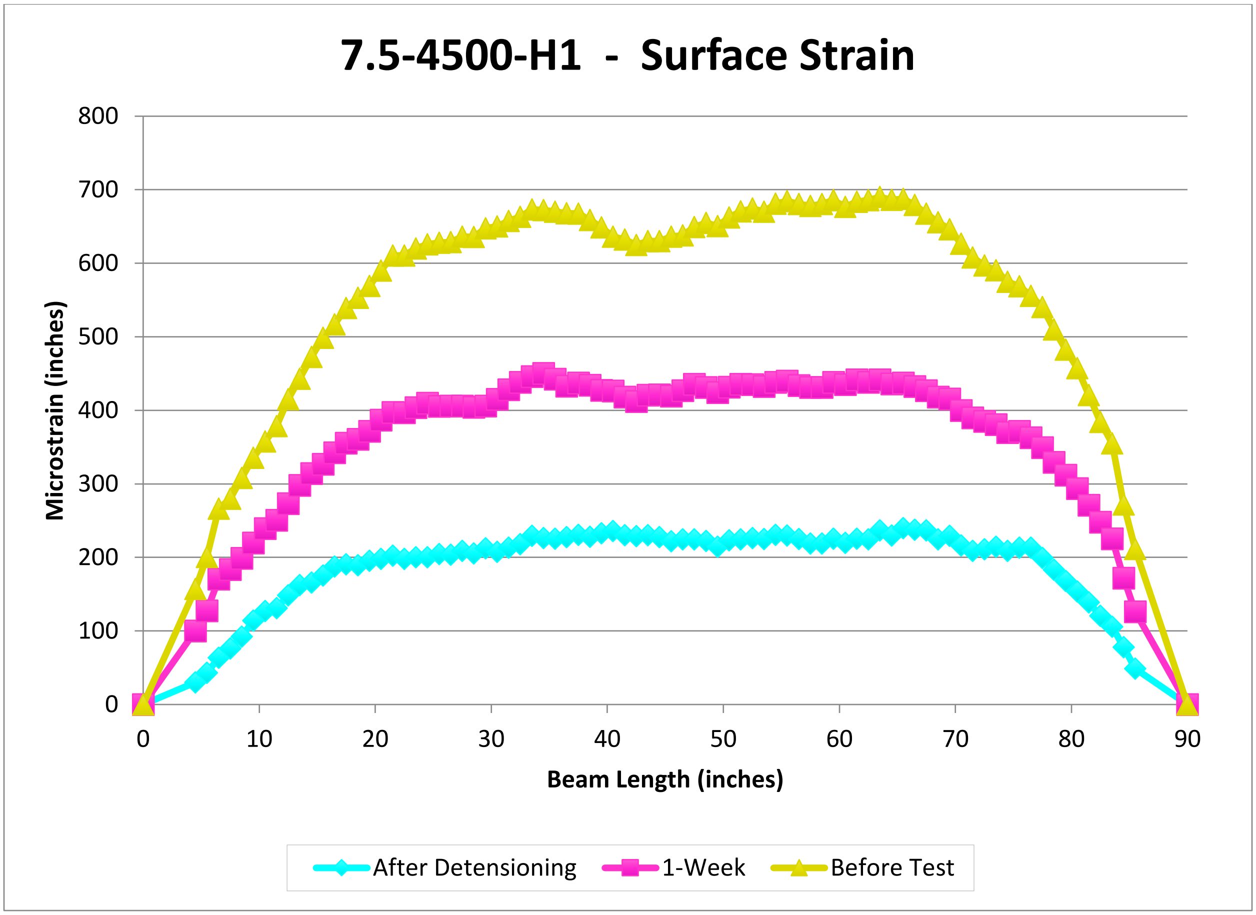

Figure C.12: Surface Strain Measurements for Beam 7.5-4500-H1.

Table C.12: Transfer Length Summary for 7.5-4500-H1.

Transfer Length				
Time of Measurement	**Live End (AMS)**	**Dead End (AMS)**	**Live End (ZL)**	**Dead End (ZL)**
After Detensioning	26.8	13.5	18.2	13.3
1-Week	23.1	20.1	21.5	18.4
Before Testing	22.7	19.8	22.2	18.7

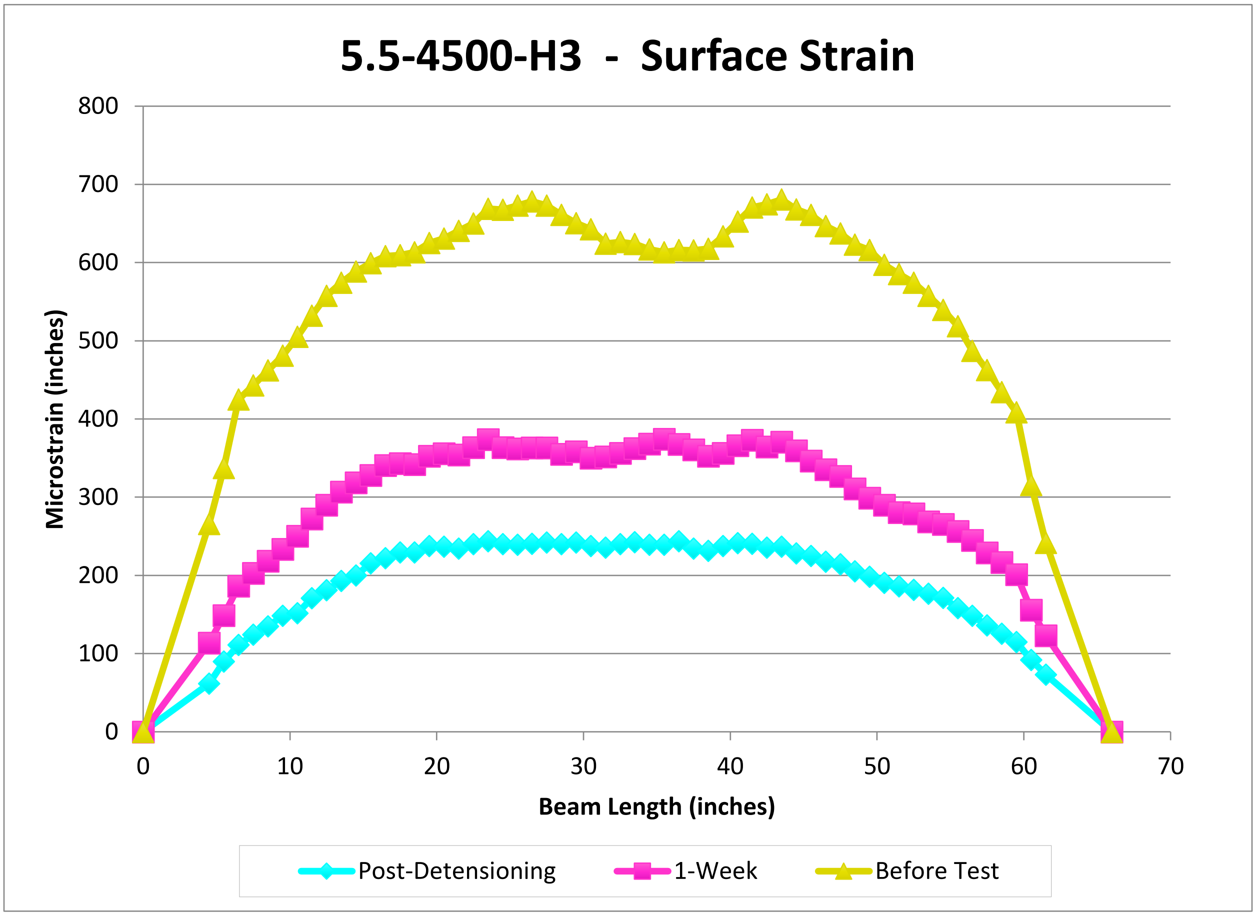

Figure C.13: Surface Strain Measurements for Beam 5.5-4500-H3.

Table C.13: Transfer Length Summary for 5.5-4500-H3.

Transfer Length				
Time of Measurement	**Live End (AMS)**	**Dead End (AMS)**	**Live End (ZL)**	**Dead End (ZL)**
After Detensioning	17.2	20.6	17.7	21.4
1-Week	16.4	20.6	16.5	22.6
Before Testing	18.5	15.9	14.8	14.6

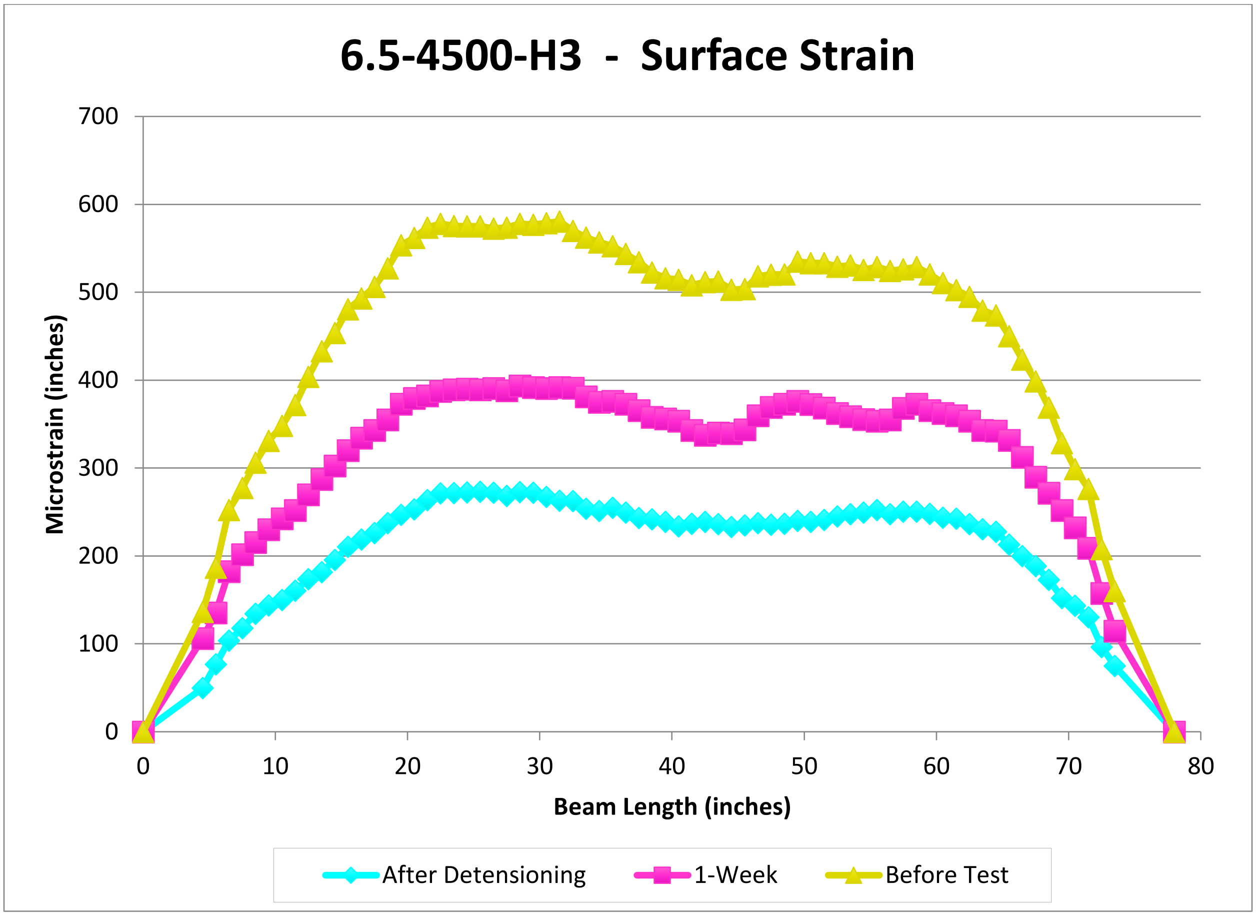

Figure C.14: Surface Strain Measurements for Beam 6.5-4500-H3.

Table C.14: Transfer Length Summary for 6.5-4500-H3.

Transfer Length				
Time of Measurement	**Live End (AMS)**	**Dead End (AMS)**	**Live End (ZL)**	**Dead End (ZL)**
After Detensioning	20.0	14.2	19.8	13.9
1-Week	19.1	13.3	19.7	12.8
Before Testing	18.9	15.4	18.8	14.8

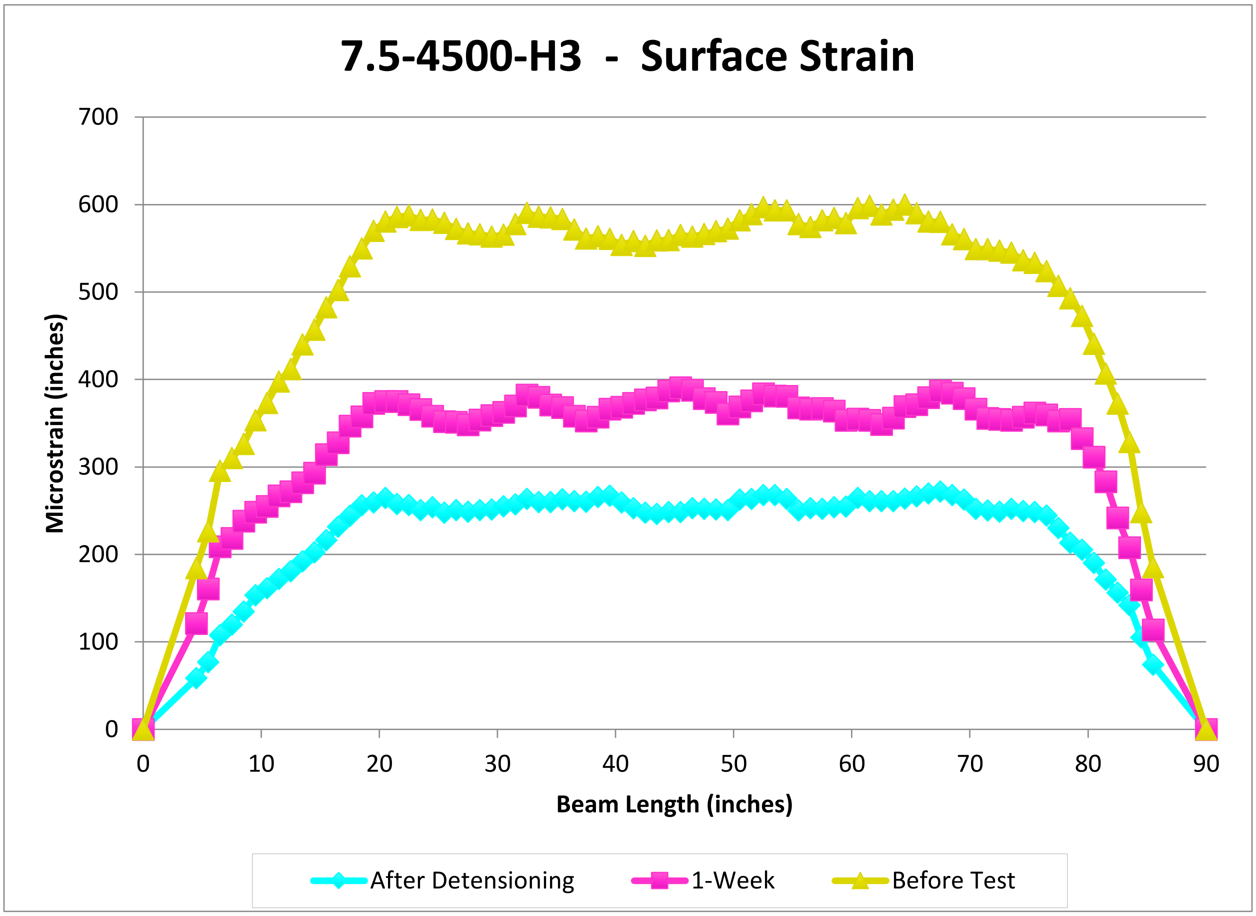

Figure C.14: Surface Strain Measurements for Beam 7.5-4500-H3.

Table C.14: Transfer Length Summary for 7.5-4500-H3.

Transfer Length				
Time of Measurement	**Live End (AMS)**	**Dead End (AMS)**	**Live End (ZL)**	**Dead End (ZL)**
After Detensioning	17.5	13.7	17.8	13.6
1-Week	17.6	11.3	19.1	10.9
Before Testing	18.2	16.9	19.4	13.7

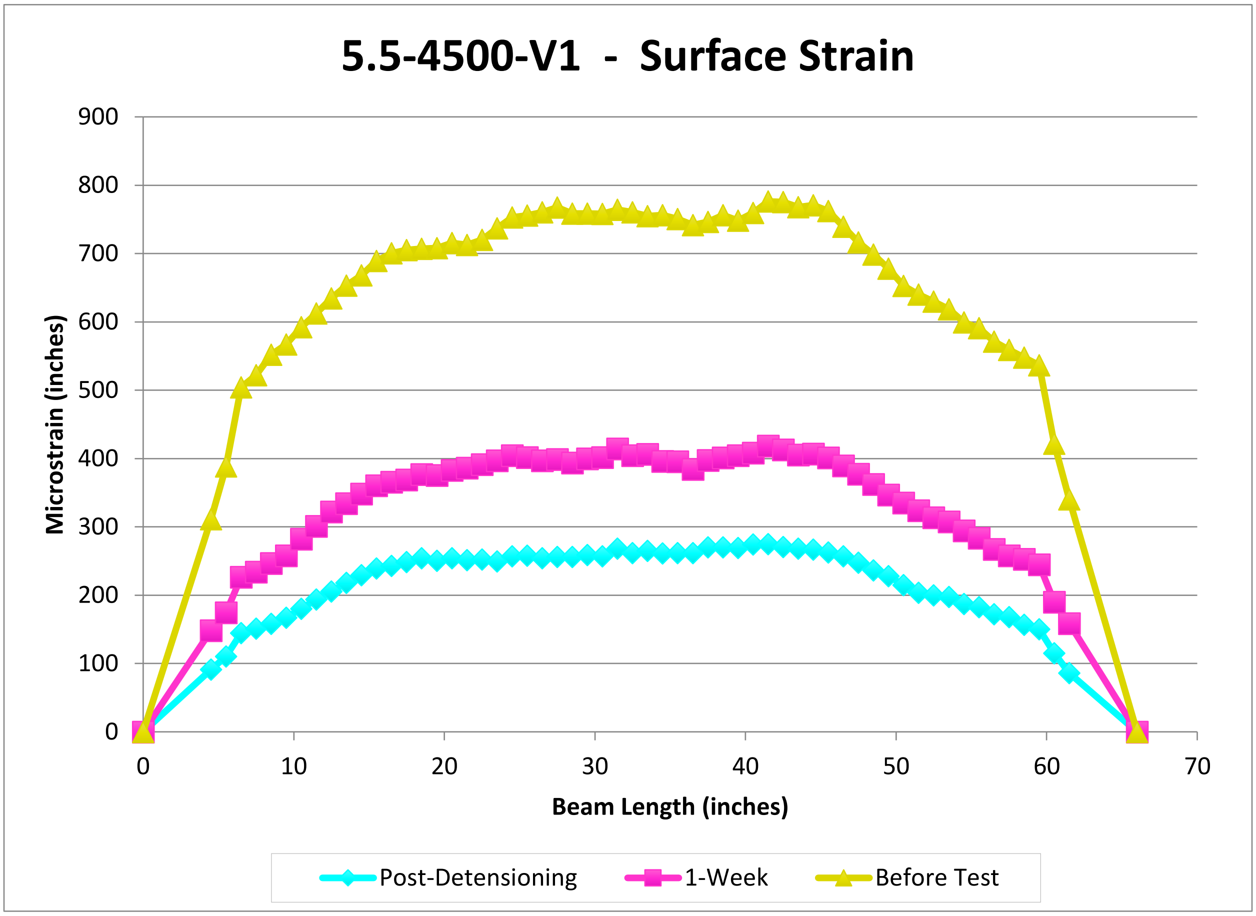

Figure C.15: Surface Strain Measurements for Beam 5.5-4500-V1.

Table C.15: Transfer Length Summary for 5.5-4500-V1.

Transfer Length				
Time of Measurement	**Live End (AMS)**	**Dead End (AMS)**	**Live End (ZL)**	**Dead End (ZL)**
After Detensioning	16.5	19.3	17.0	21.0
1-Week	18.4	19.0	17.0	20.5
Before Testing	16.4	18.0	13.4*	13.6*

* Transfer Length calculated using the software shows a low value when compared to the plotted strain. Use of the 1-week transfer length is recommended.

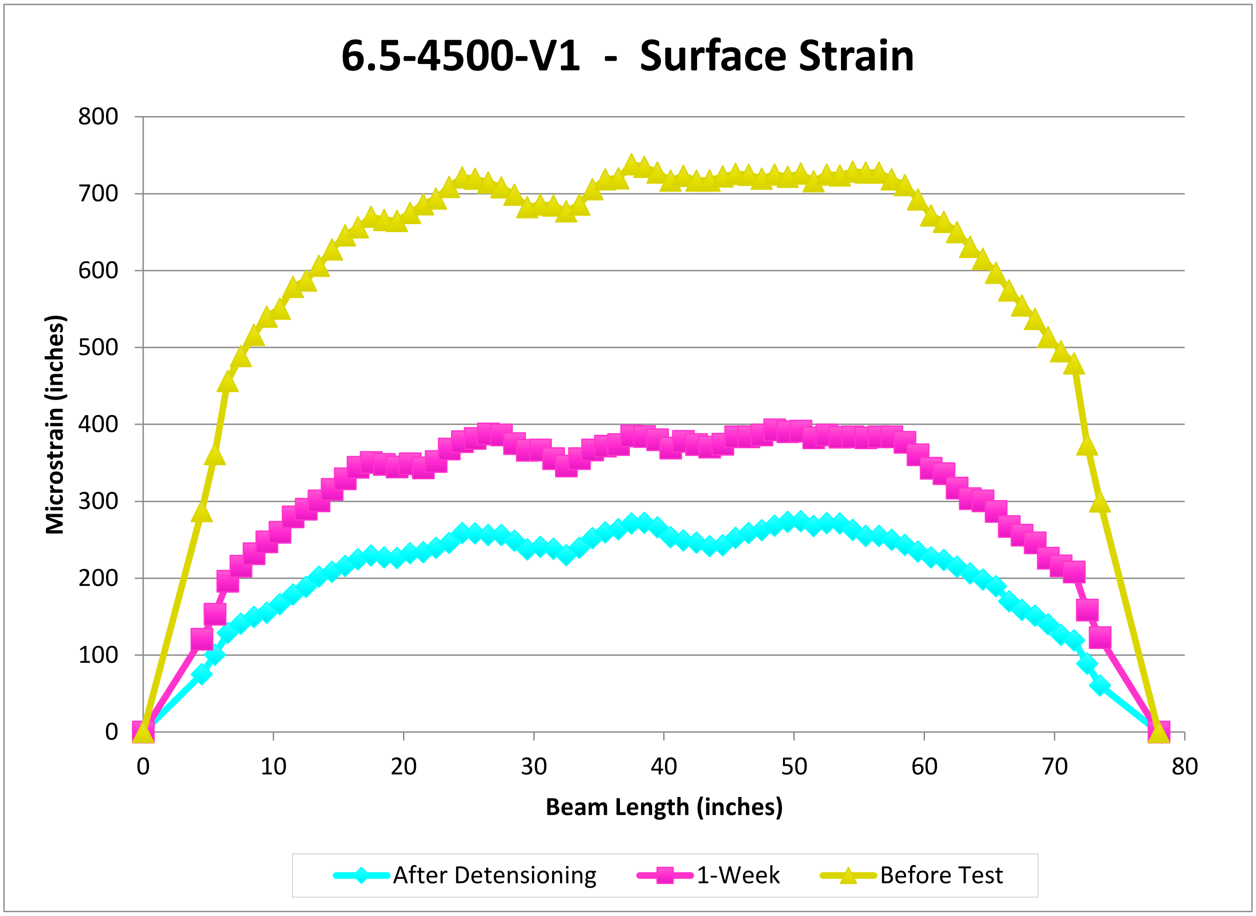

Figure C.16: Surface Strain Measurements for Beam 6.5-4500-V1.

Table C.16: Transfer Length Summary for 6.5-4500-V1.

Transfer Length				
Time of Measurement	**Live End (AMS)**	**Dead End (AMS)**	**Live End (ZL)**	**Dead End (ZL)**
After Detensioning	21.7	19.9	19.5	19.3
1-Week	17.0	18.7	18.0	20.1
Before Testing	16.8	18.0	14.2*	15.0*

* Transfer Length calculated using the software shows a low value when compared to the plotted strain. Use of the 1-week transfer length is recommended.

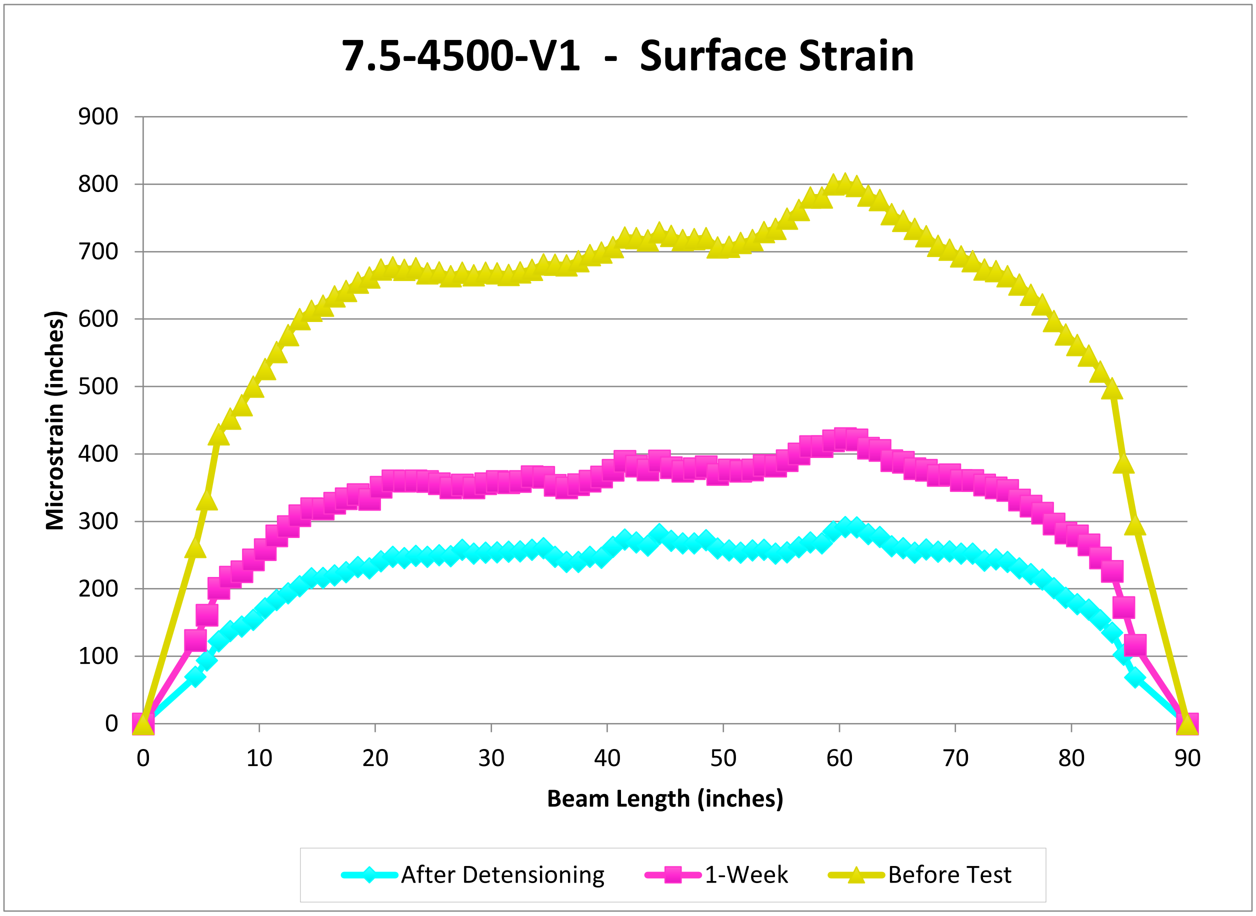

Figure C.17: Surface Strain Measurements for Beam 7.5-4500-V1.

Table C.17: Transfer Length Summary for 7.5-4500-V1.

Transfer Length				
Time of Measurement	**Live End (AMS)**	**Dead End (AMS)**	**Live End (ZL)**	**Dead End (ZL)**
After Detensioning	20.4	18.3	19.1	17.2
1-Week	20.0	20.5	18.3	19.0
Before Testing	17.8	20.1	15.4	14.3

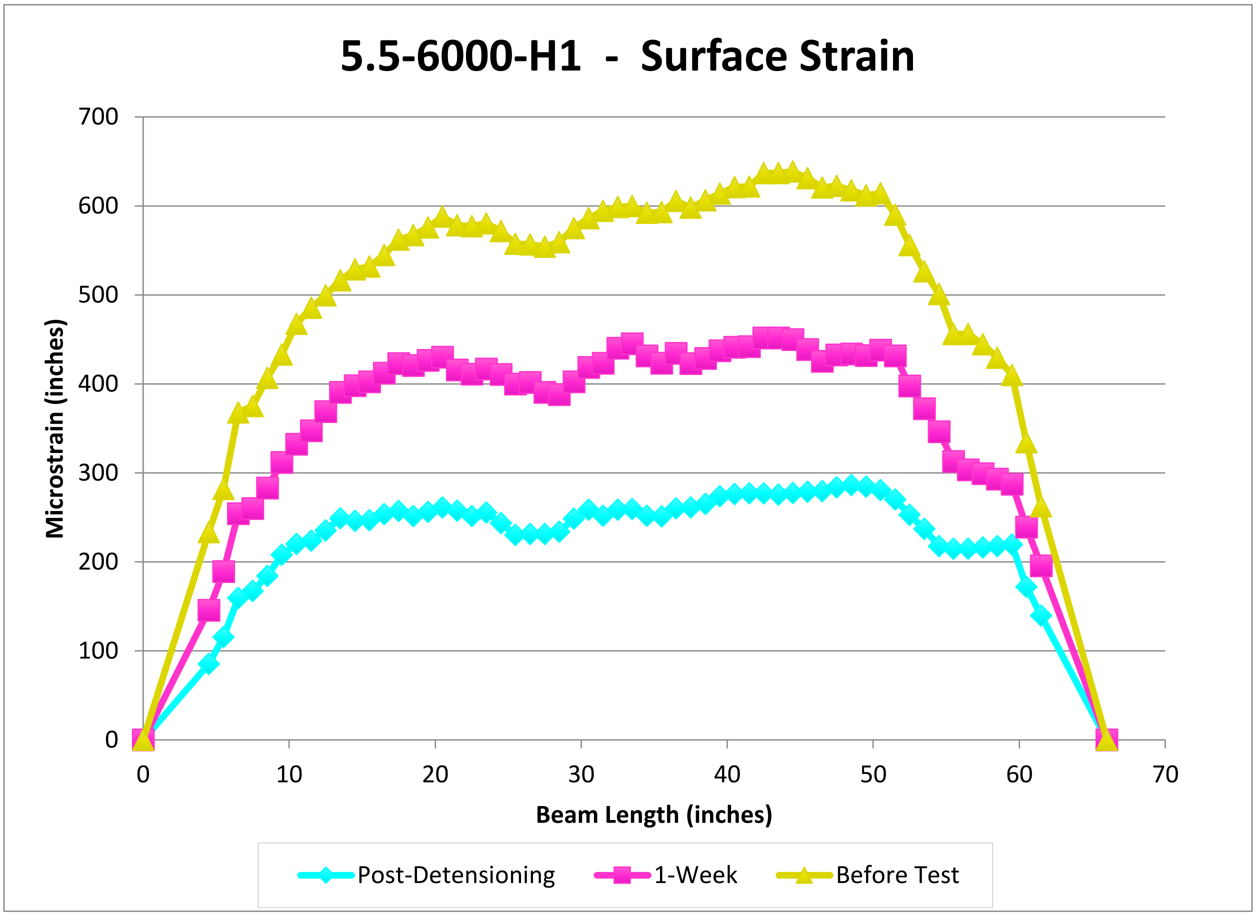

Figure C.18: Surface Strain Measurements for Beam 5.5-6000-H1.

Table C.18: Transfer Length Summary for 5.5-6000-H1.

Transfer Length				
Time of Measurement	**Live End (AMS)**	**Dead End (AMS)**	**Live End (ZL)**	**Dead End (ZL)**
After Detensioning	12.6	13.8	11.8	16.5
1-Week	13.7	14.1	14.7	16.8
Before Testing	16.3	14.4	15.3	14.8

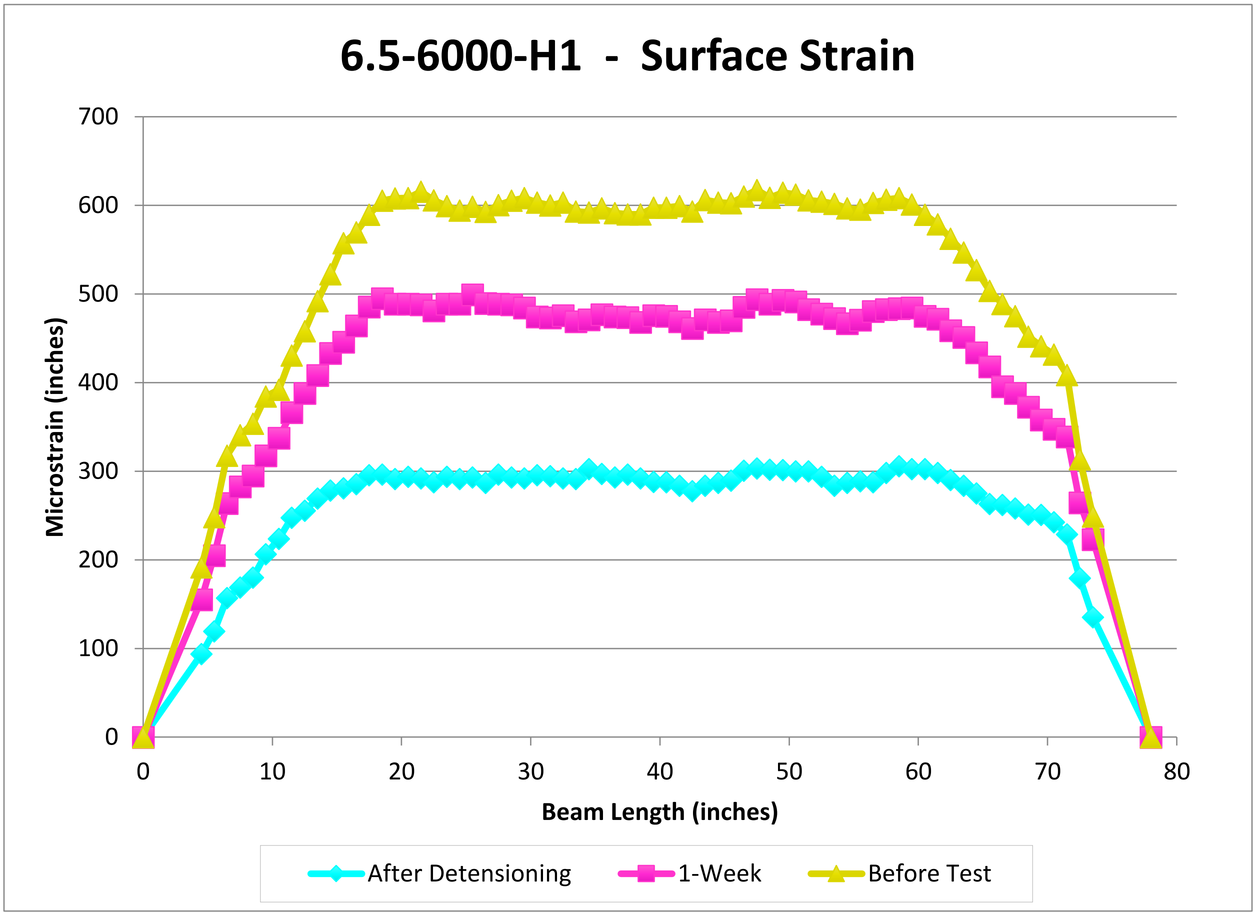

Figure C.19: Surface Strain Measurements for Beam 6.5-6000-H1.

Table C.19: Transfer Length Summary for 6.5-6000-H1.

Transfer Length				
Time of Measurement	**Live End (AMS)**	**Dead End (AMS)**	**Live End (ZL)**	**Dead End (ZL)**
After Detensioning	14.7	13.7	14.3	15.2
1-Week	16.2	14.9	16.4	15.1
Before Testing	16.6	16.1	17.2	15.2

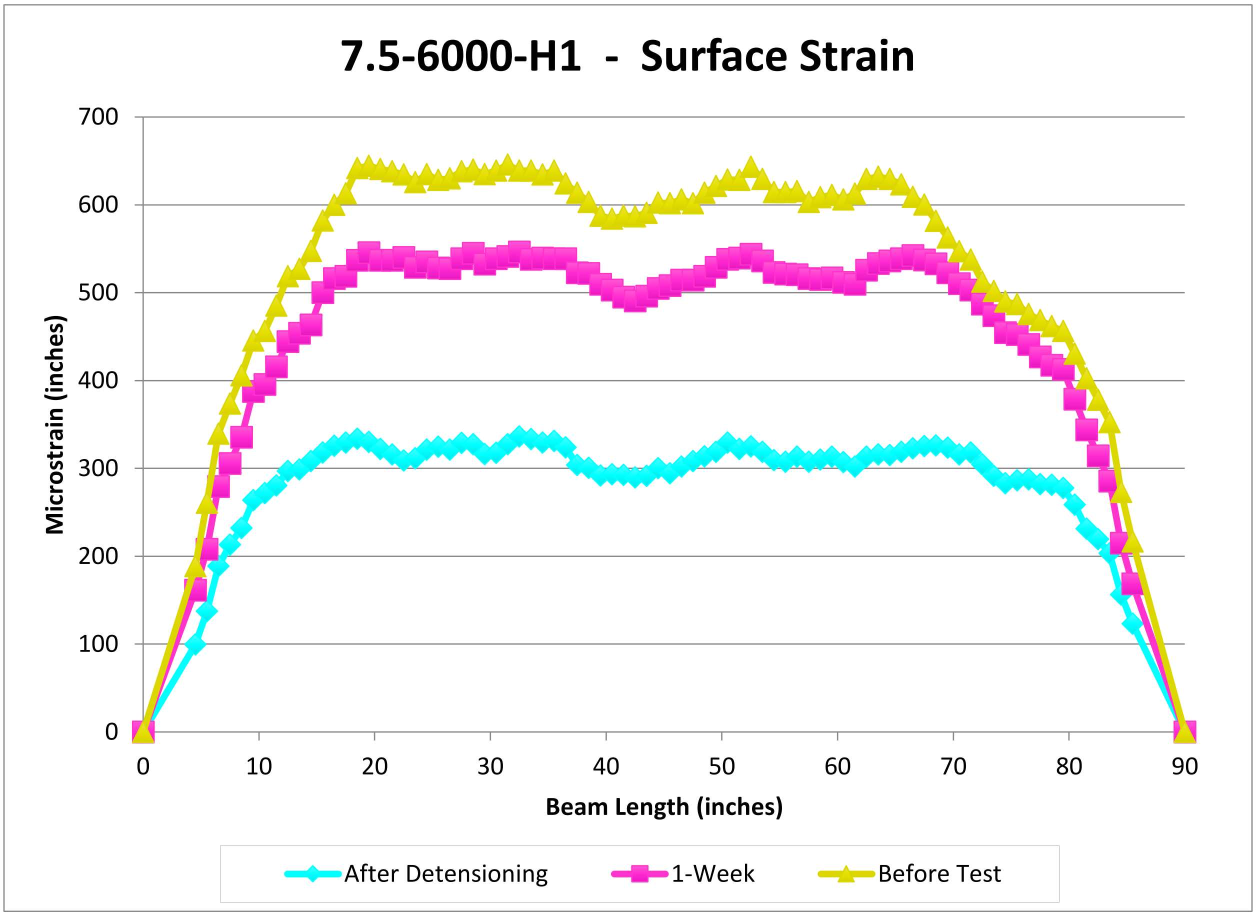

Figure C.20: Surface Strain Measurements for Beam 7.5-6000-H1.

Table C.20: Transfer Length Summary for 7.5-6000-H1.

Transfer Length				
Time of Measurement	**Live End (AMS)**	**Dead End (AMS)**	**Live End (ZL)**	**Dead End (ZL)**
After Detensioning	13.7	16.9	11.1	13.9
1-Week	15.6	18.1	15.2	17.6
Before Testing	16.0	21.7	16.0	21.0

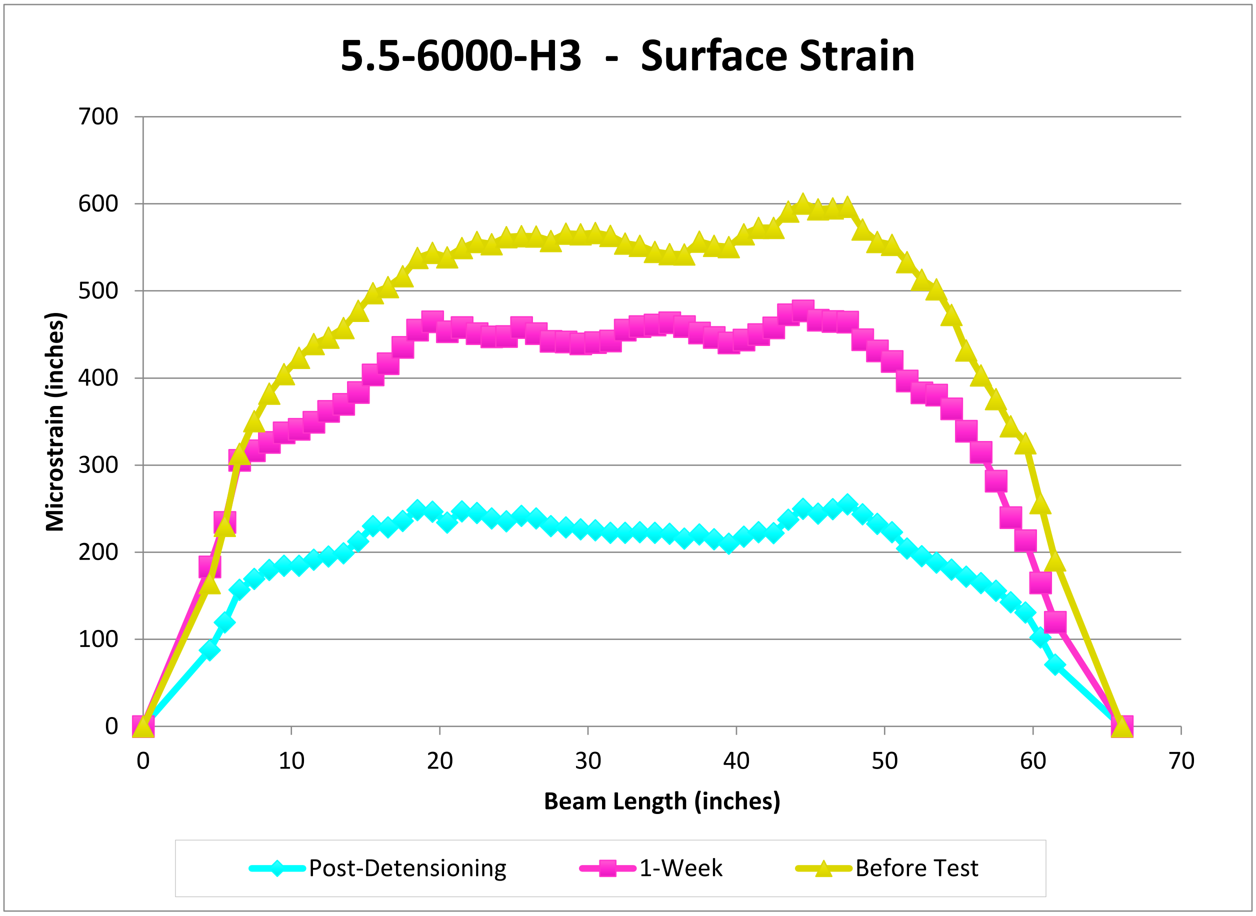

Figure C.21: Surface Strain Measurements for Beam 5.5-6000-H3.

Table C.21: Transfer Length Summary for 5.5-6000-H3.

Transfer Length				
Time of Measurement	**Live End (AMS)**	**Dead End (AMS)**	**Live End (ZL)**	**Dead End (ZL)**
After Detensioning	15.1	15.2	16.4	15.7
1-Week	17.1	16.6	18.2	15.3
Before Testing	17.9	14.8	17.4	14.9

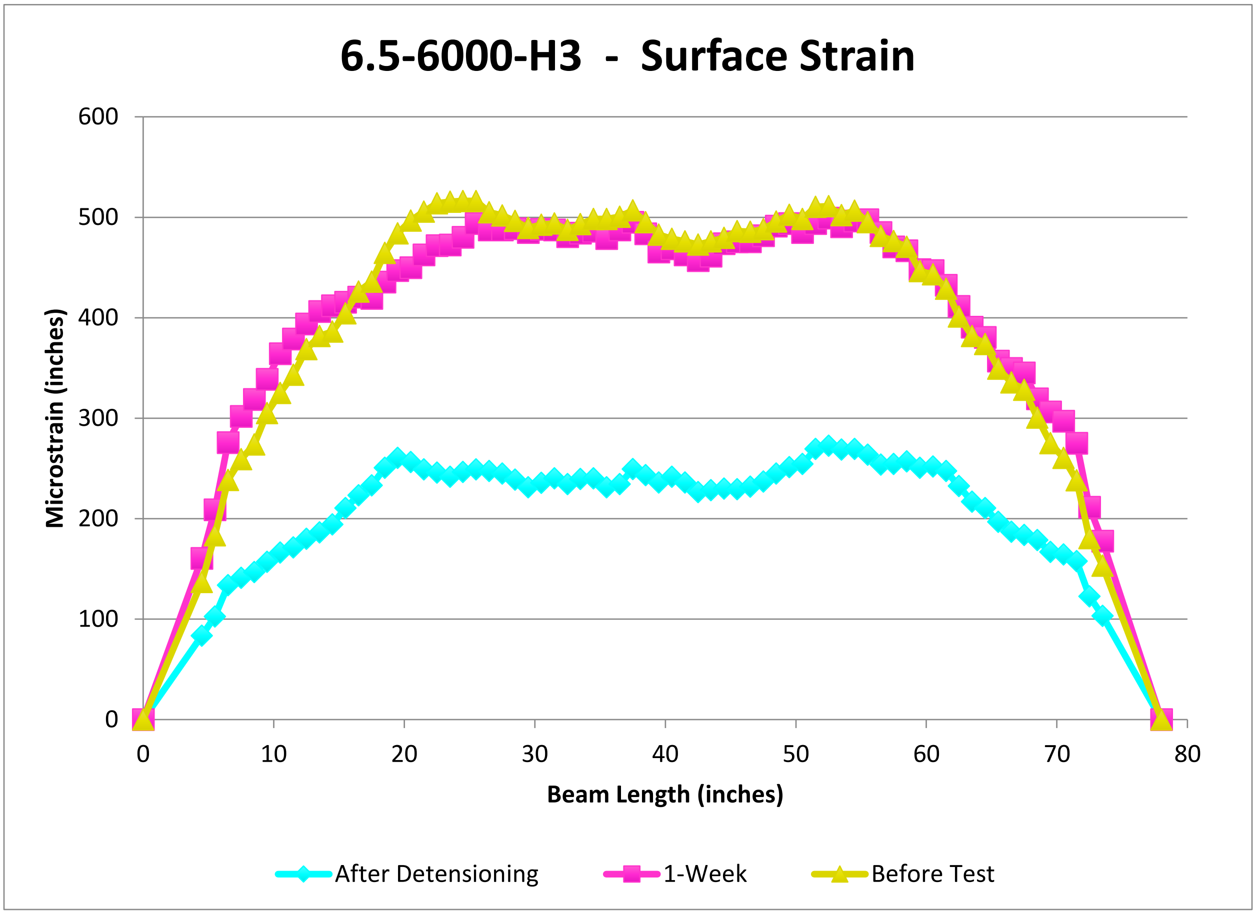

Figure C.22: Surface Strain Measurements for Beam 6.5-6000-H3.

Table C.22: Transfer Length Summary for 6.5-6000-H3.

Transfer Length				
Time of Measurement	**Live End (AMS)**	**Dead End (AMS)**	**Live End (ZL)**	**Dead End (ZL)**
After Detensioning	17.3	15.7	18.5	17.7
1-Week	20.8	19.0	20.8	19.9
Before Testing	19.1	19.3	19.9	19.9

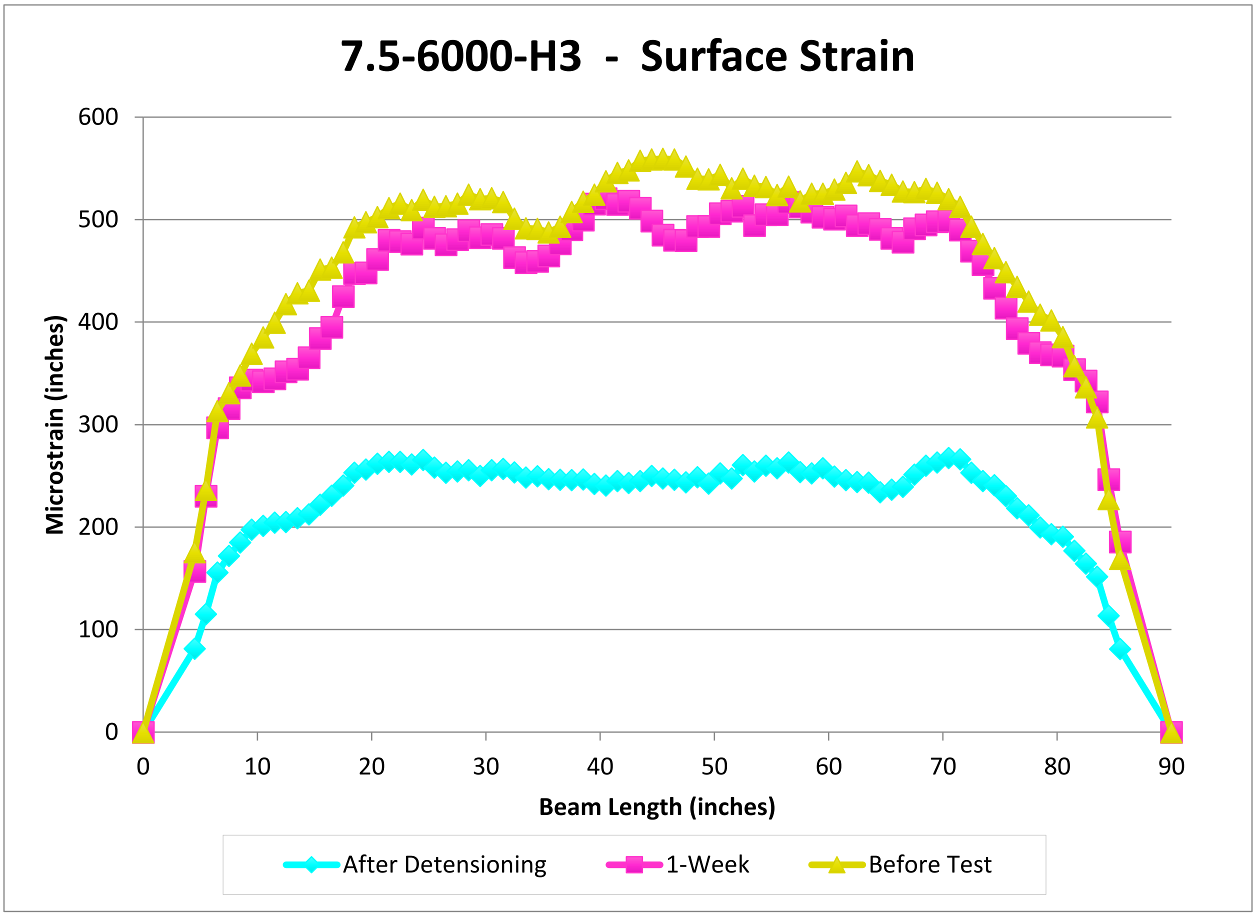

Figure C.23: Surface Strain Measurements for Beam 7.5-6000-H3.

Table C.23: Transfer Length Summary for 7.5-6000-H3.

Transfer Length				
Time of Measurement	**Live End (AMS)**	**Dead End (AMS)**	**Live End (ZL)**	**Dead End (ZL)**
After Detensioning	17.3	15.3	17.7	15.4
1-Week	20.6	17.7	22.6	18.8
Before Testing	18.4	18.2	19.3	18.6

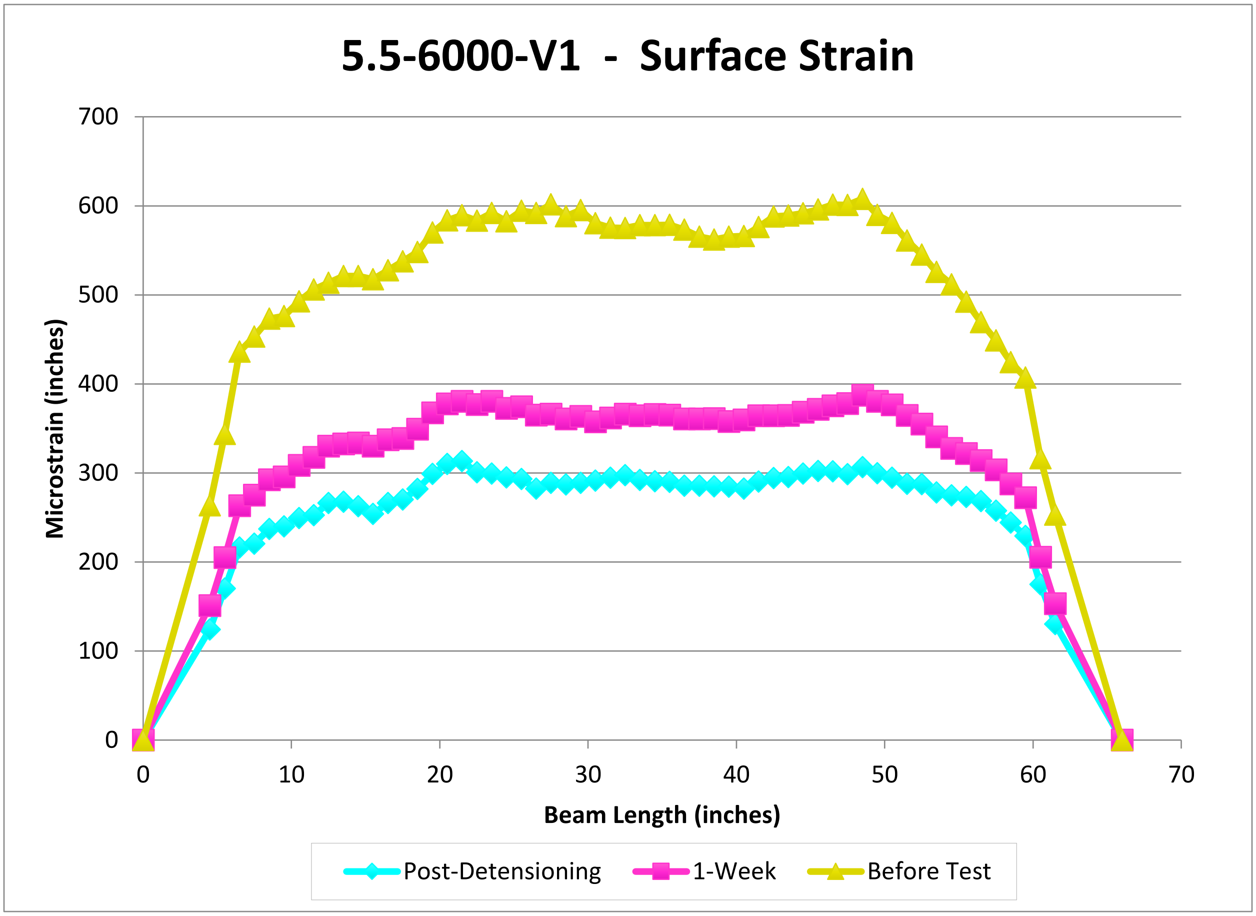

Figure C.24: Surface Strain Measurements for Beam 5.5-6000-V1.

Table C.24: Transfer Length Summary for 5.5-6000-V1.

Transfer Length				
Time of Measurement	**Live End (AMS)**	**Dead End (AMS)**	**Live End (ZL)**	**Dead End (ZL)**
After Detensioning	17.8	11.9	18.6	9.6
1-Week	17.8	13.0	17.7	12.0
Before Testing	18.1	13.9	11.1*	13.0

* Transfer Length calculated using the software shows a low value when compared to the plotted strain. Use of the 1-week transfer length is recommended.

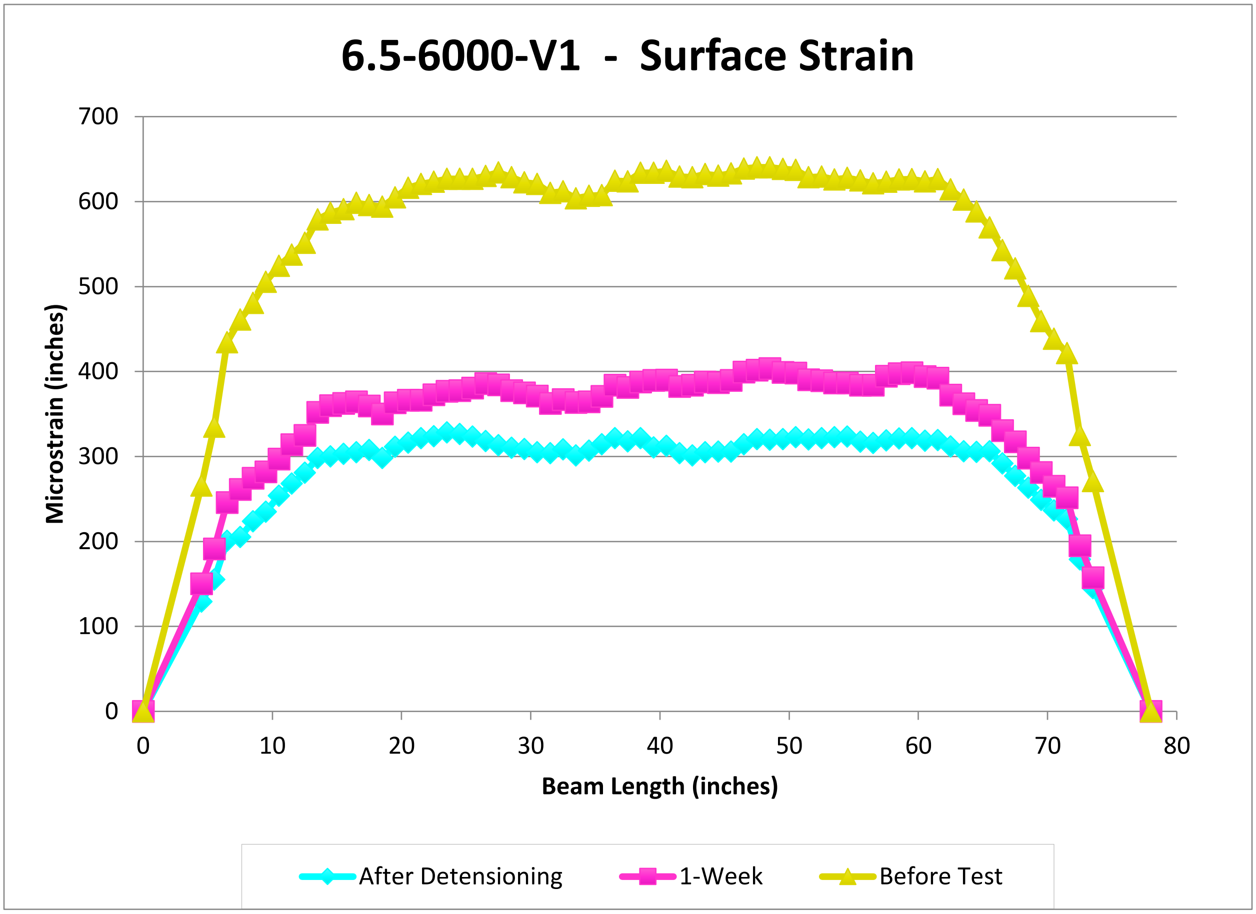

Figure C.25: Surface Strain Measurements for Beam 6.5-6000-H1.

Table C.25: Transfer Length Summary for 6.5-6000-H1.

Transfer Length				
Time of Measurement	**Live End (AMS)**	**Dead End (AMS)**	**Live End (ZL)**	**Dead End (ZL)**
After Detensioning	13.4	12.0	15.3	13.5
1-Week	13.6	15.4	15.8	15.3
Before Testing	14.0	14.2	12.5	13.6

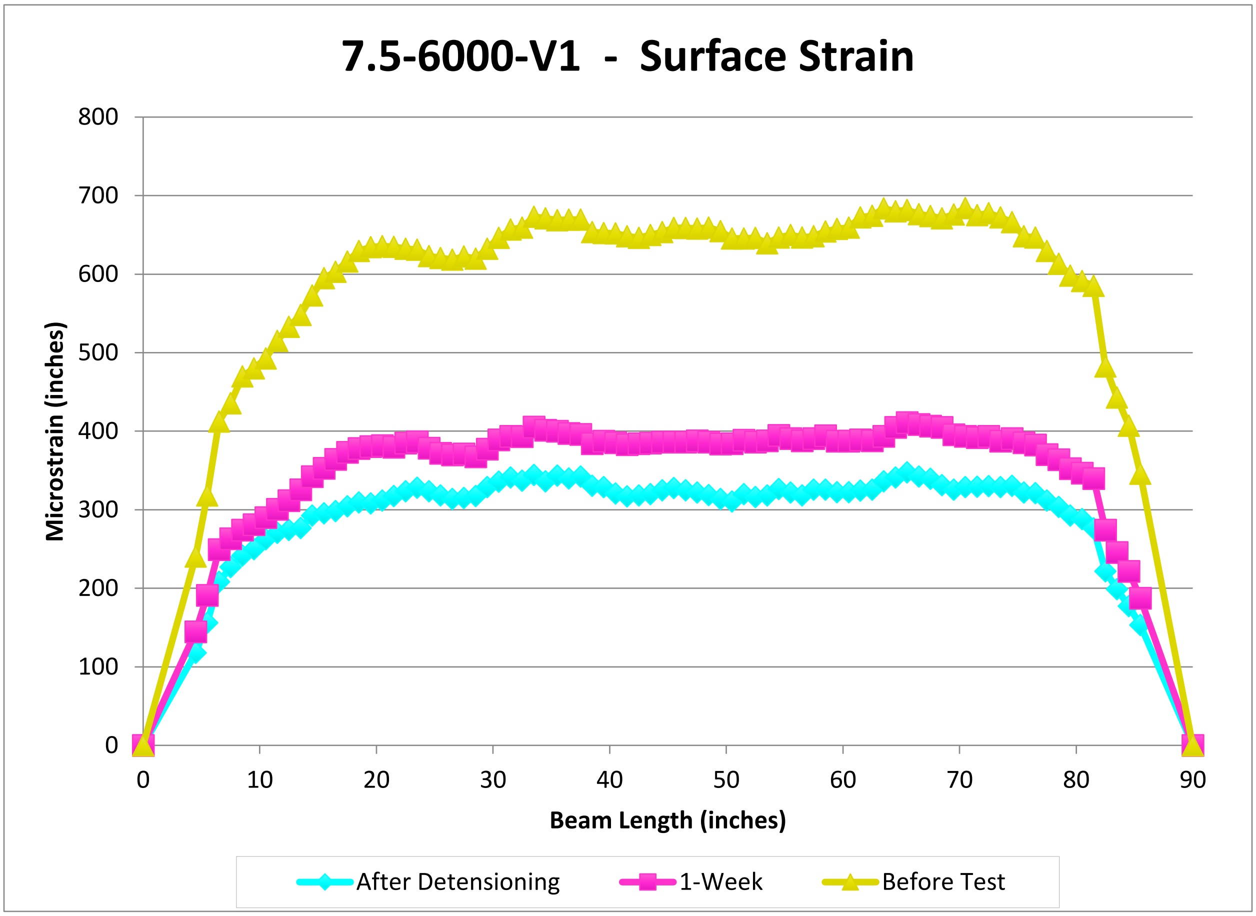

Figure C.26: Surface Strain Measurements for Beam 7.5-6000-V1.

Table C.26: Transfer Length Summary for 7.5-6000-V1.

Transfer Length				
Time of Measurement	**Live End (AMS)**	**Dead End (AMS)**	**Live End (ZL)**	**Dead End (ZL)**
After Detensioning	18.1	12.3	17.6	12.4
1-Week	16.7	12.7	17.9	11.6
Before Testing	17.1	12.5	15.8	7.6*

* Transfer Length calculated using the software shows a low value when compared to the plotted strain. Use of the 1-week transfer length is recommended.

Appendix D - Flexural Testing Results

Beam Identification:	5.5-3500-H1
Concrete Strength at Test:	9,000 psi
Embedment Length:	33”

Loading data for the flexural testing of this specimen was not recorded due to computer program error.

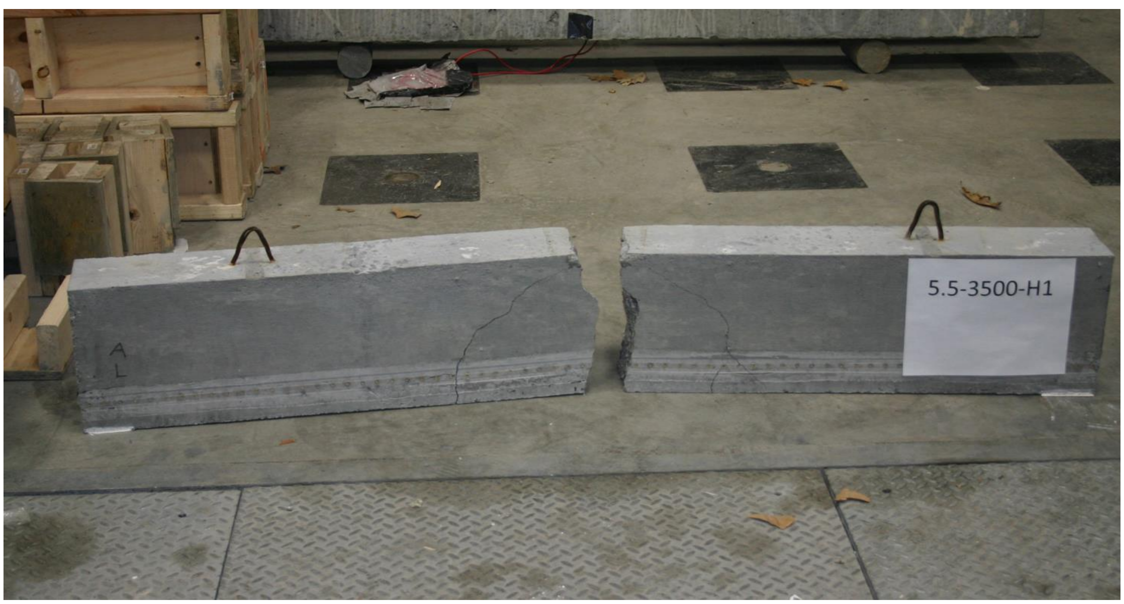

Figure D.1: Broken Beam Failing Through Strand Rupture.

Beam Identification:	6.5-3500-H1
Concrete Strength at Test:	9,000 psi
Embedment Length:	24”

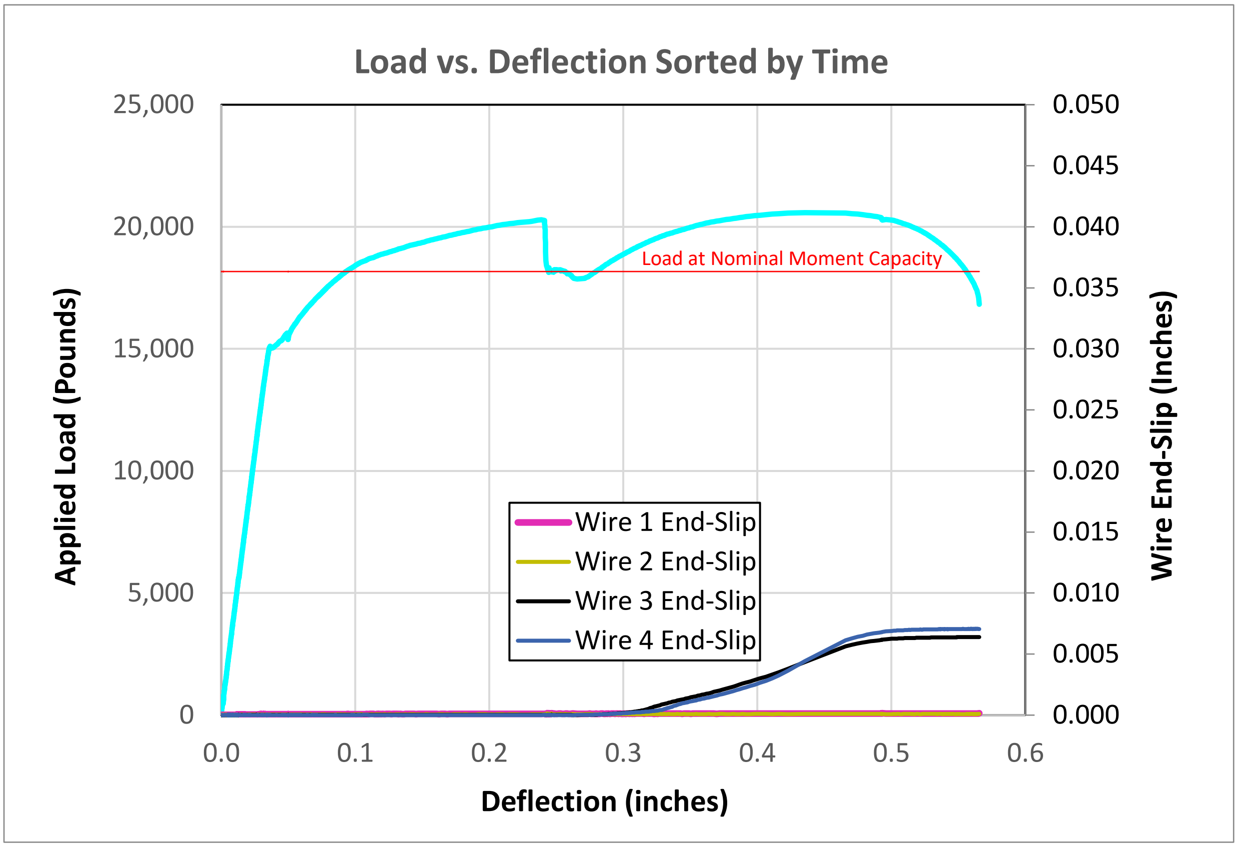

Figure D.2: Flexural Testing Results for Specimen 6.5-3500-H1.

Figure D.3: Broken Beam Failing Through Strand Rupture.

Beam Identification:	7.5-3500-H1
Concrete Strength at Test:	9,000 psi
Embedment Length:	21”

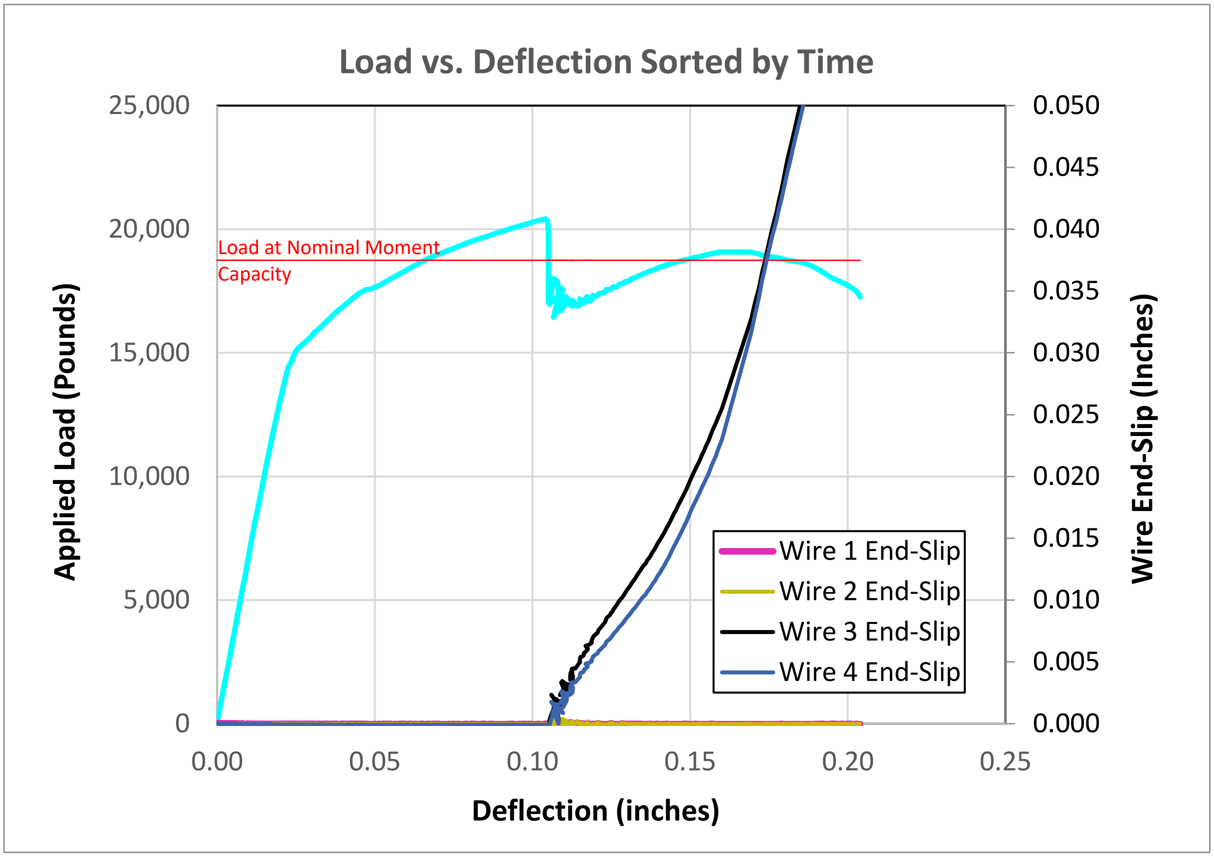

Figure D.4: Flexural Testing Results for Specimen 7.5-3500-H1.

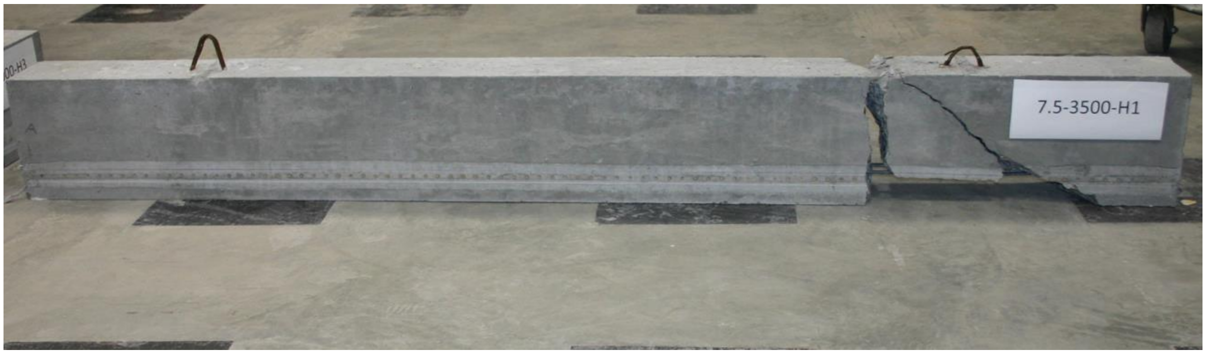

Figure D.5: Broken Beam Failing Through Loss of Bond.

Beam Identification:	5.5-3500-H3
Concrete Strength at Test:	7,000 psi
Embedment Length:	33"

Loading data for the flexural testing of this specimen was not recorded due to computer program error.

Figure D.6: Broken Beam Failing Through Strand Rupture.

Beam Identification:	6.5-3500-H3
Concrete Strength at Test:	7,000 psi
Embedment Length:	24”

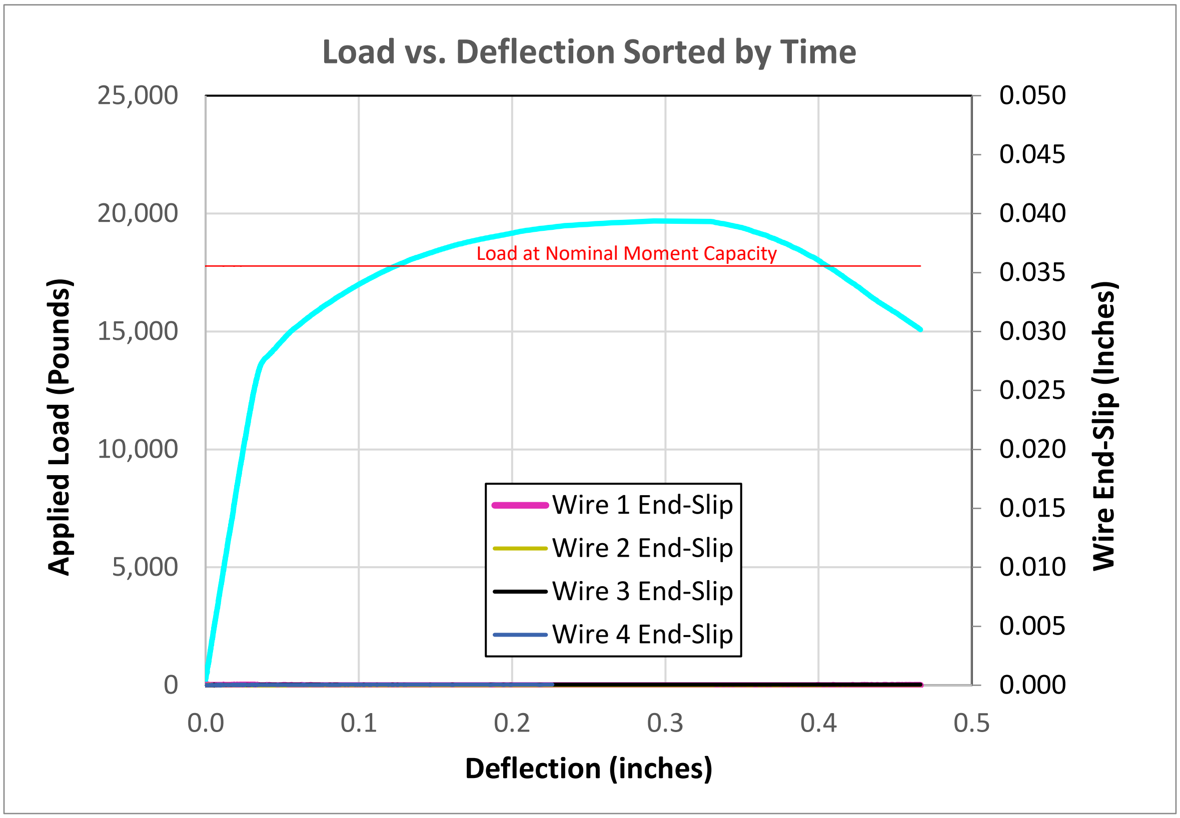

Figure D.7: Flexural Testing Results for Specimen 6.5-3500-H3.

Figure D.8: Broken Beam Failing Through Strand Rupture.

Beam Identification:	7.5-3500-H3
Concrete Strength at Test:	7,000 psi
Embedment Length:	21”

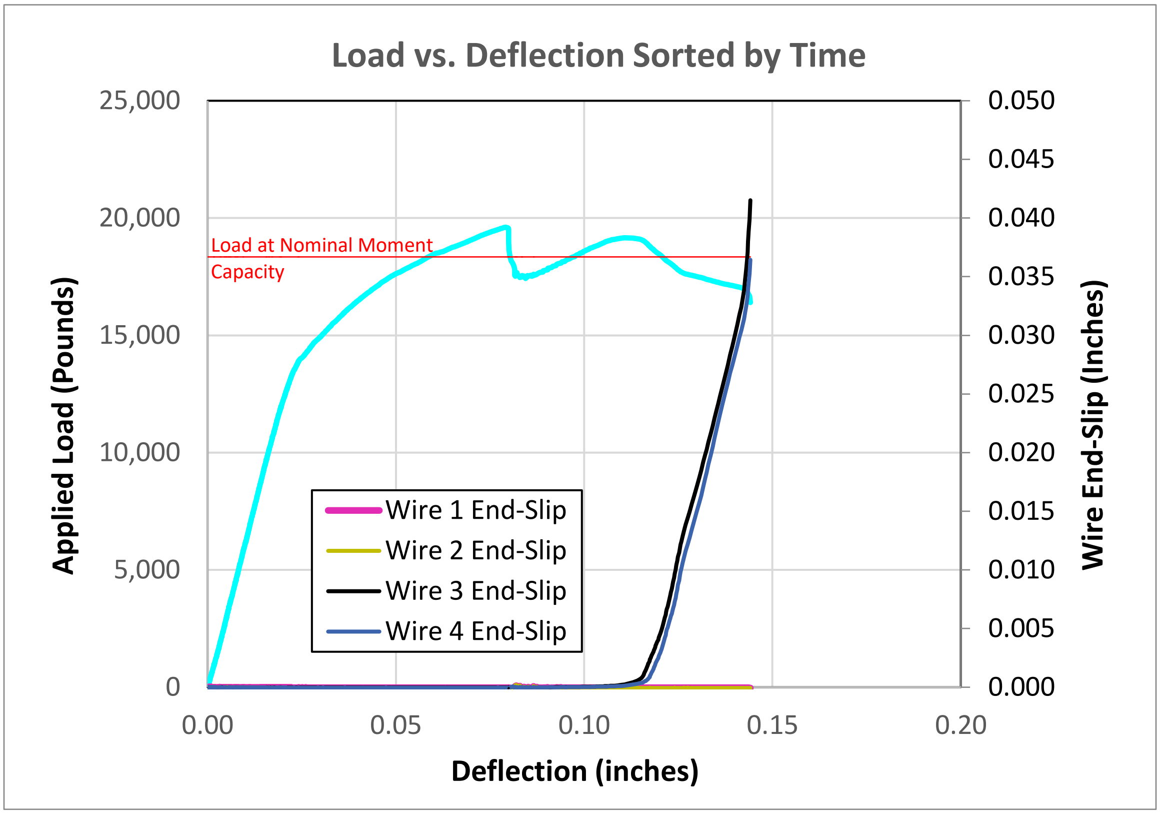

Figure D.9: Flexural Testing Results for Specimen 7.5-3500-H3.

Figure D.10: Broken Beam Failing Through Loss of Bond.

Beam Identification:	5.5-3500-V1
Concrete Strength at Test:	8,100 psi
Embedment Length:	33"

Loading data for the flexural testing of this specimen was not recorded due to computer program error.

Figure D.11: Broken Beam Failing Through Strand Rupture.

Beam Identification:	6.5-3500-V1
Concrete Strength at Test:	8,100 psi
Embedment Length:	24”

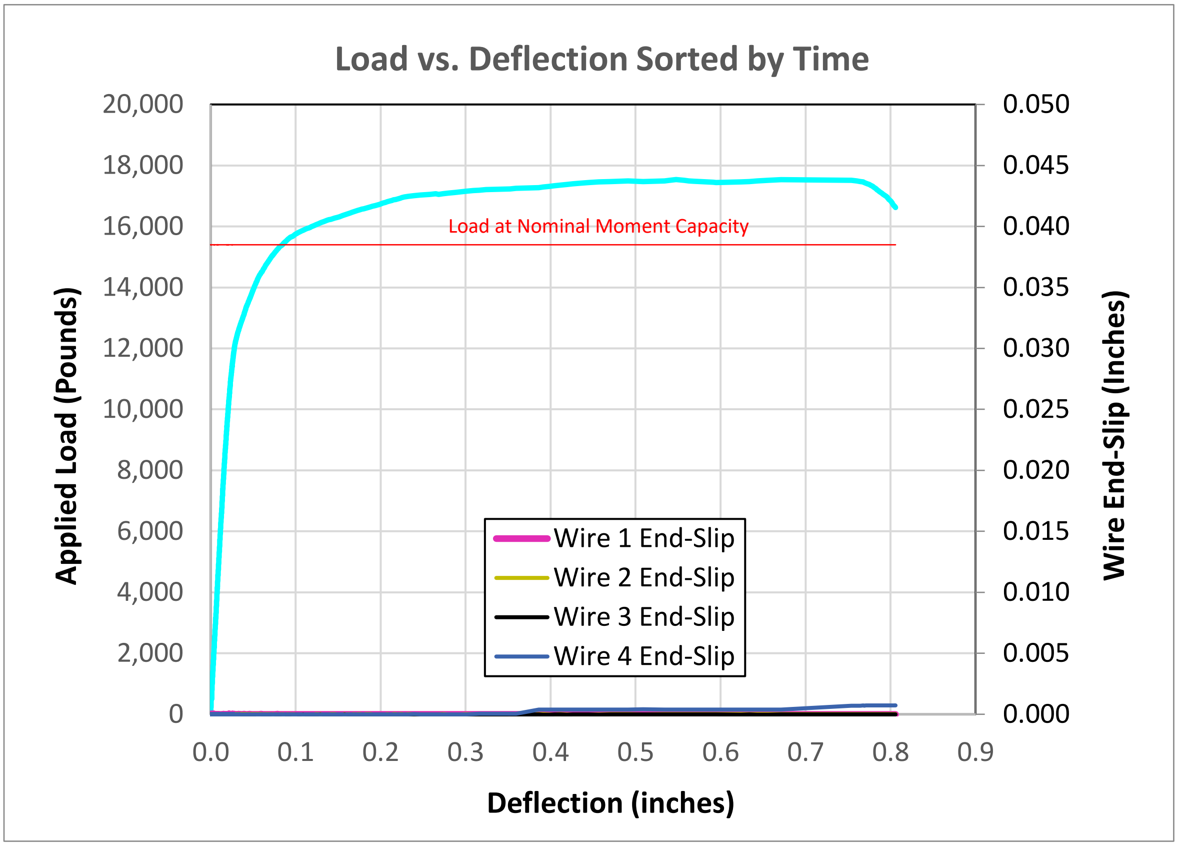

Figure D.12: Flexural Testing Results for Specimen 6.5-3500-V1.

Figure D.13: Broken Beam Failing Through Strand Rupture.

Beam Identification:	7.5-3500-V1
Concrete Strength at Test:	8,100 psi
Embedment Length:	21”

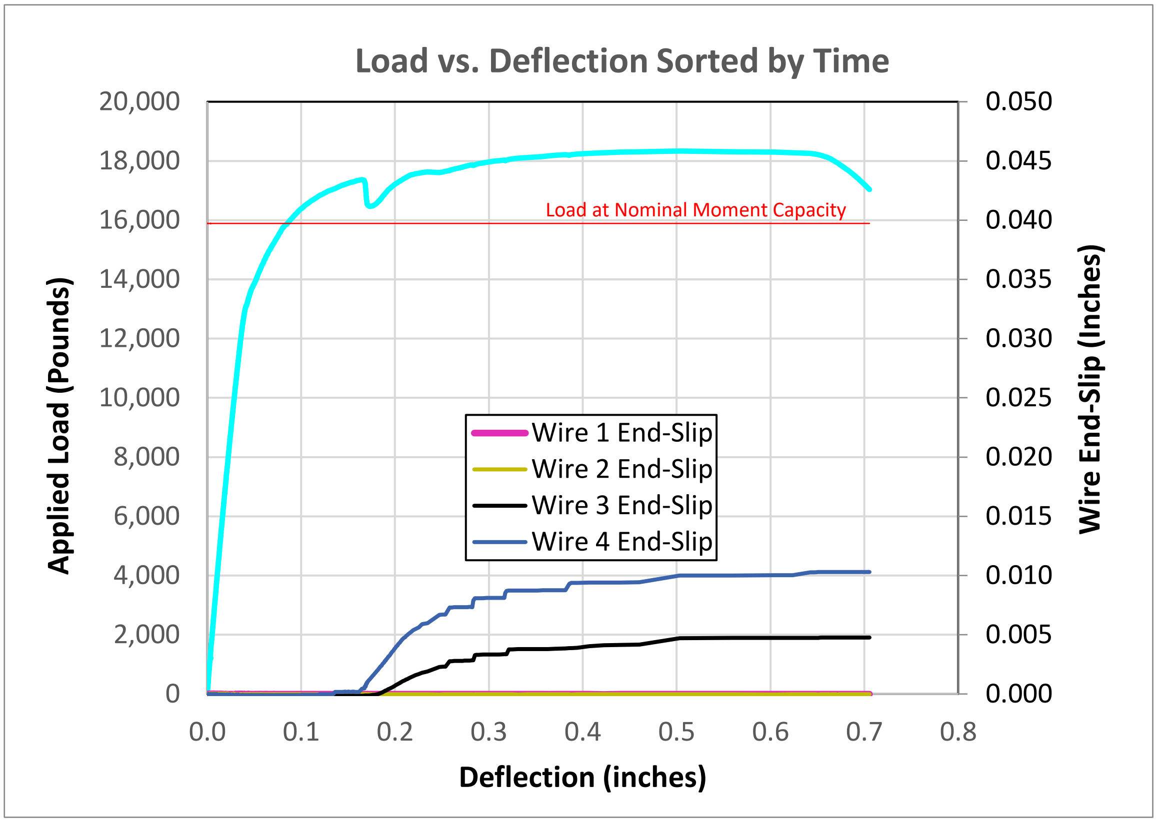

Figure D.14: Flexural Testing Results for Specimen 7.5-3500-V1.

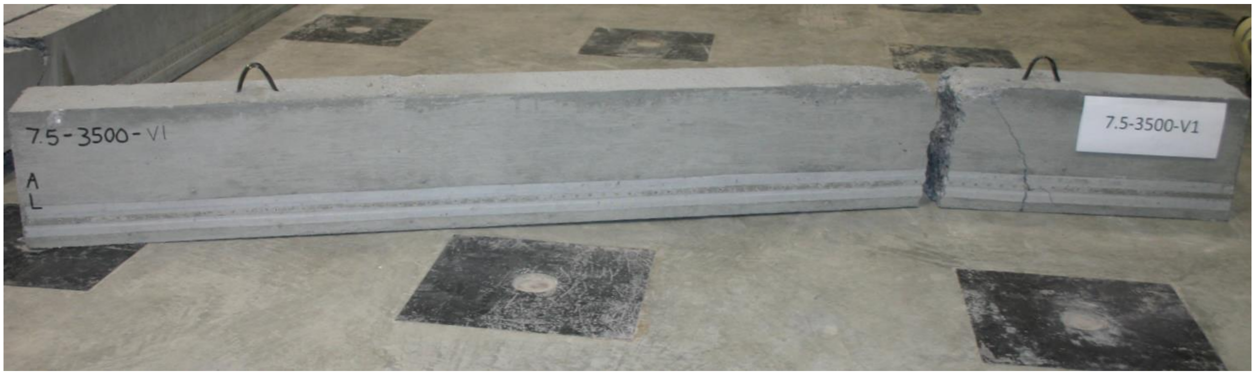

Figure D.15: Broken Beam Failing Through Strand Rupture.

Beam Identification:	5.5-4500-H1
Concrete Strength at Test:	9,000 psi
Embedment Length:	33”

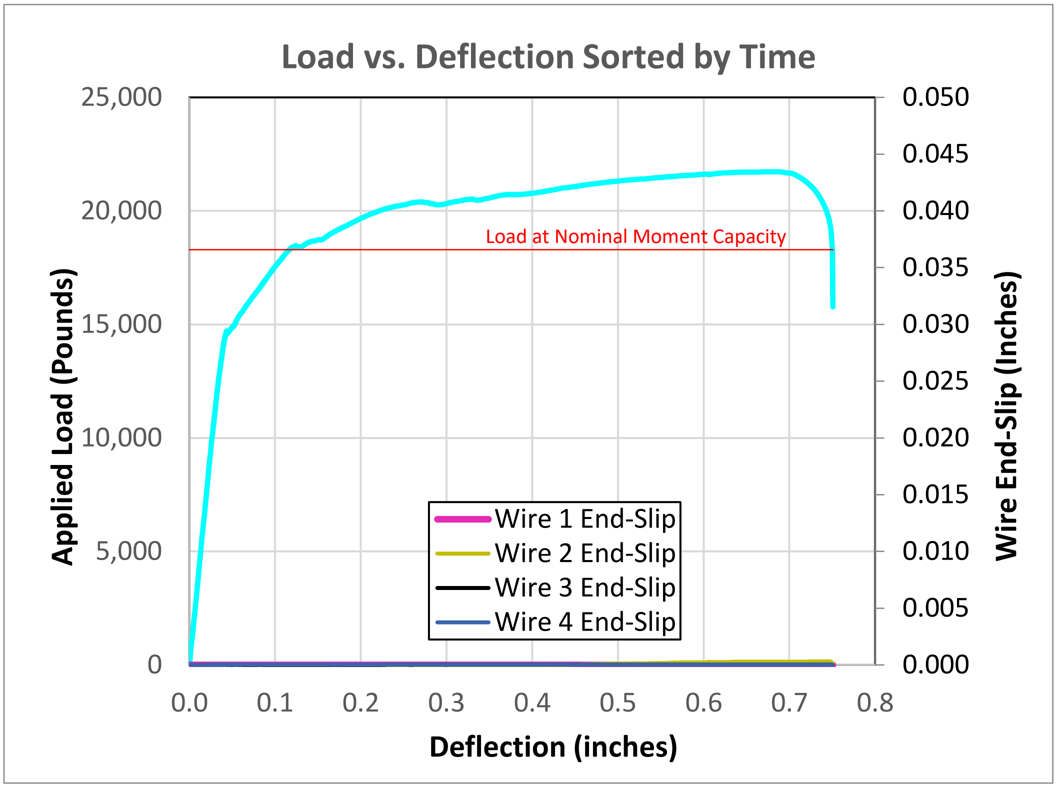

Figure D.16: Flexural Testing Results for Specimen 5.5-4500-H1.

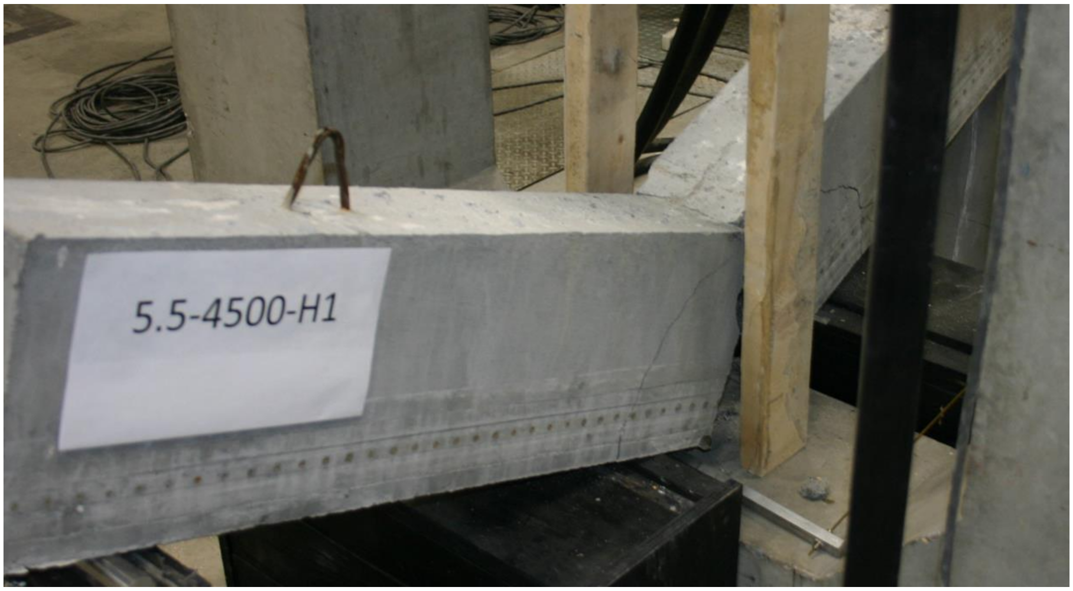

Figure D.17: Broken Beam Failing Through Strand Rupture.

Beam Identification:	6.5-4500-H1
Concrete Strength at Test:	9,000 psi
Embedment Length:	24”

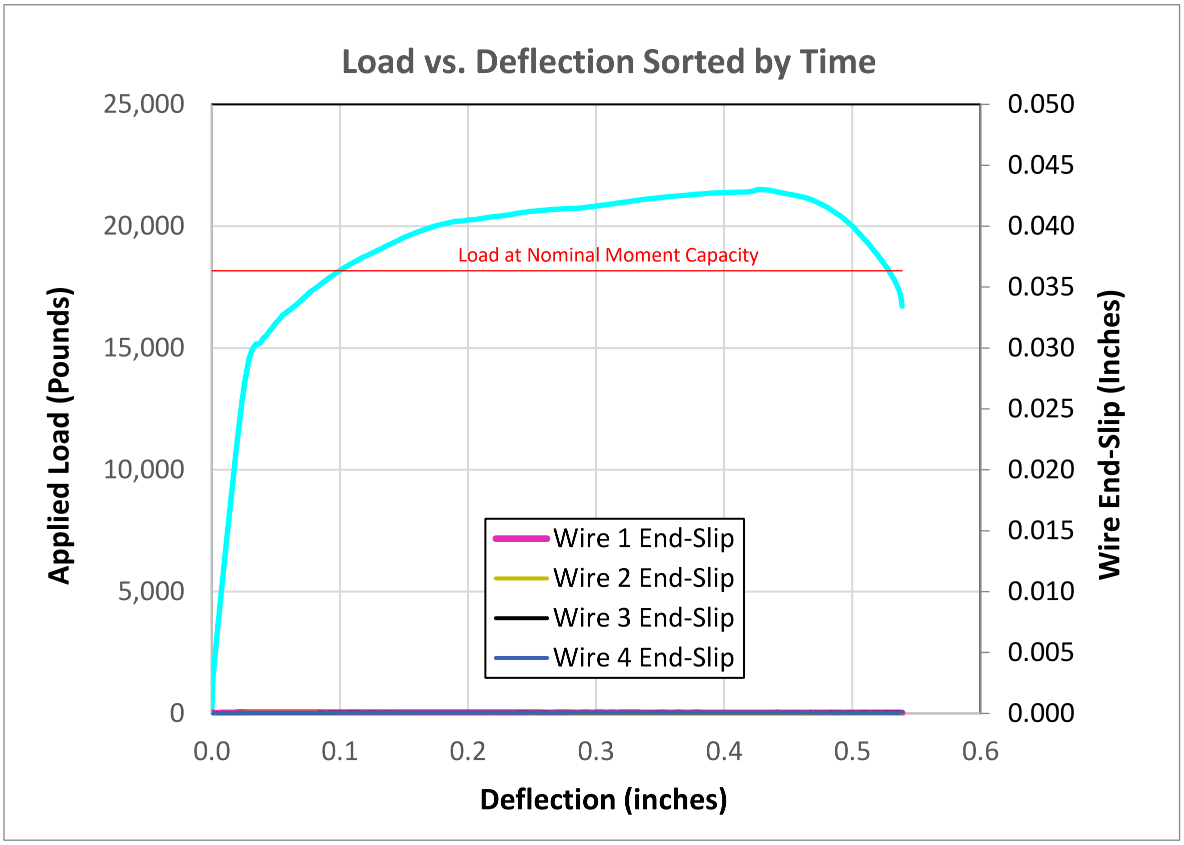

Figure D.18: Flexural Testing Results for Specimen 6.5-4500-H1.

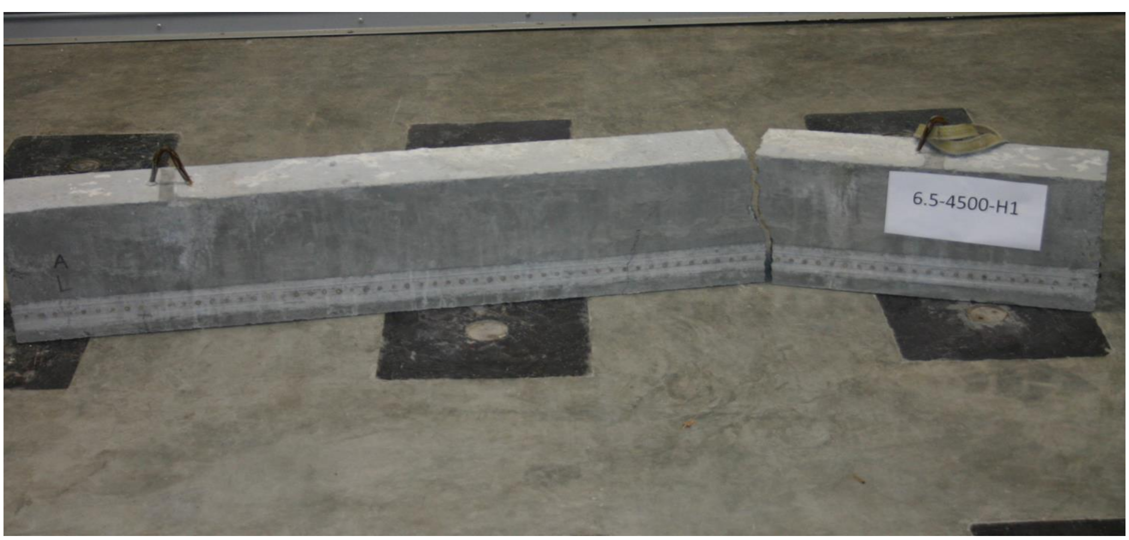

Figure D.19: Broken Beam Failing Through Strand Rupture.

Beam Identification:	7.5-4500-H1
Concrete Strength at Test:	9,000 psi
Embedment Length:	18”

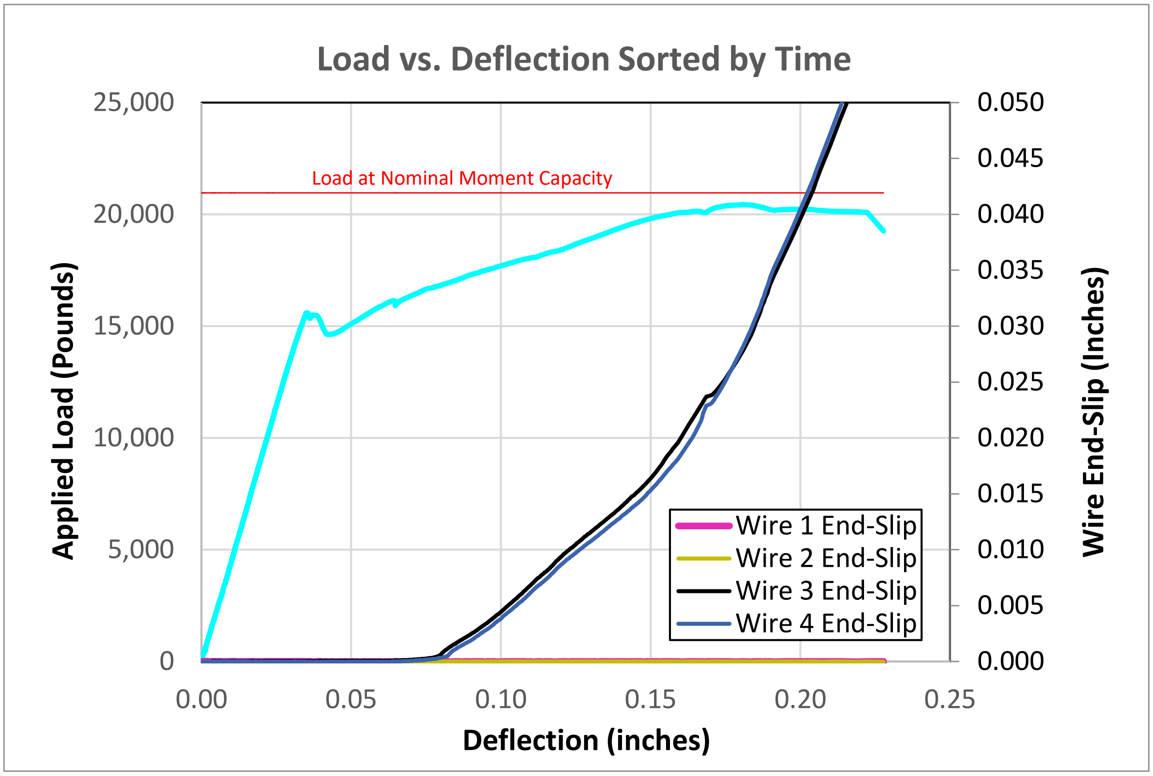

Figure D.20: Flexural Testing Results for Specimen 7.5-4500-H1.

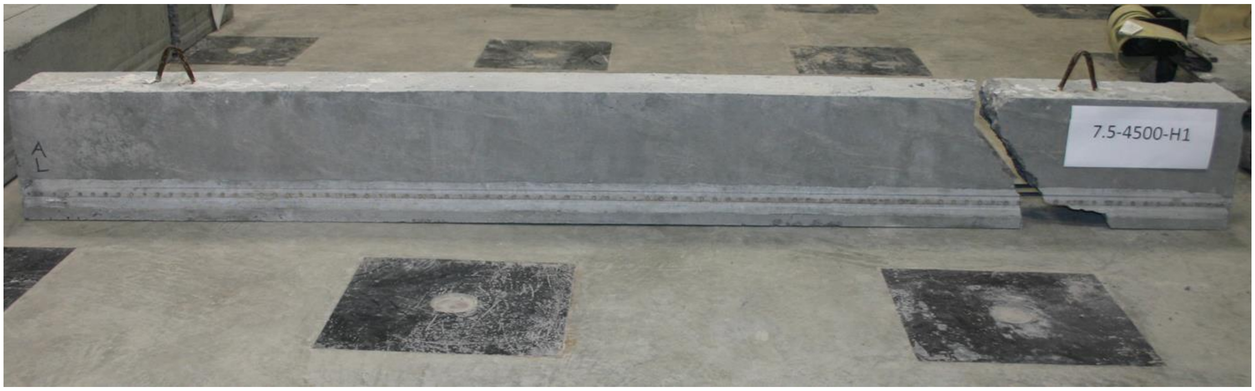

Figure D.21: Broken Beam Failing Through Loss of Bond.

Beam Identification:	5.5-4500-H3
Concrete Strength at Test:	7,000 psi
Embedment Length:	33”

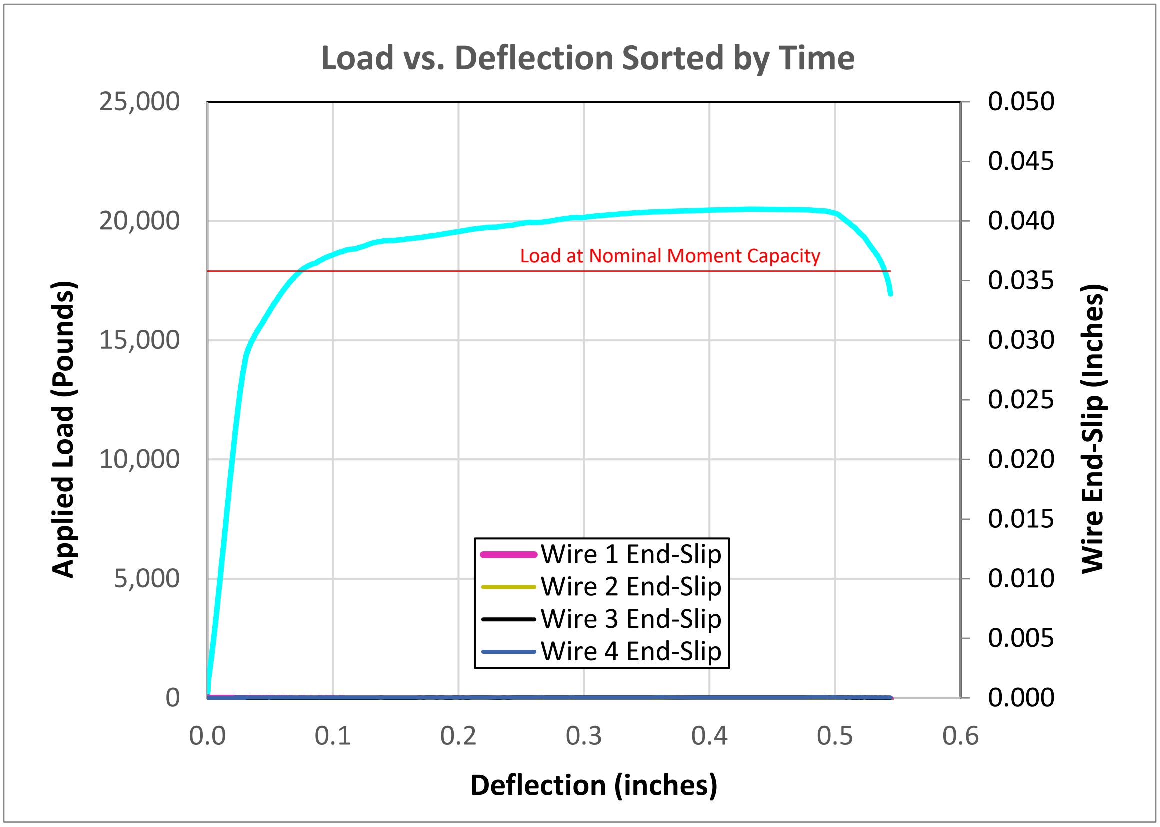

Figure D.22: Flexural Testing Results for Specimen 5.5-4500-H3.

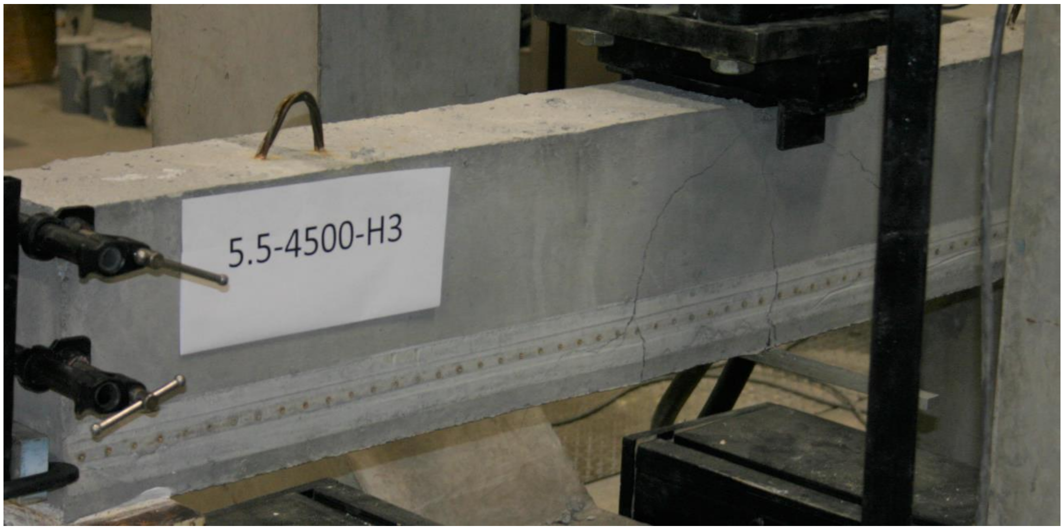

Figure D.23: Broken Beam Failing Through Strand Rupture.

Beam Identification:	6.5-4500-H3
Concrete Strength at Test:	7,000 psi
Embedment Length:	21”

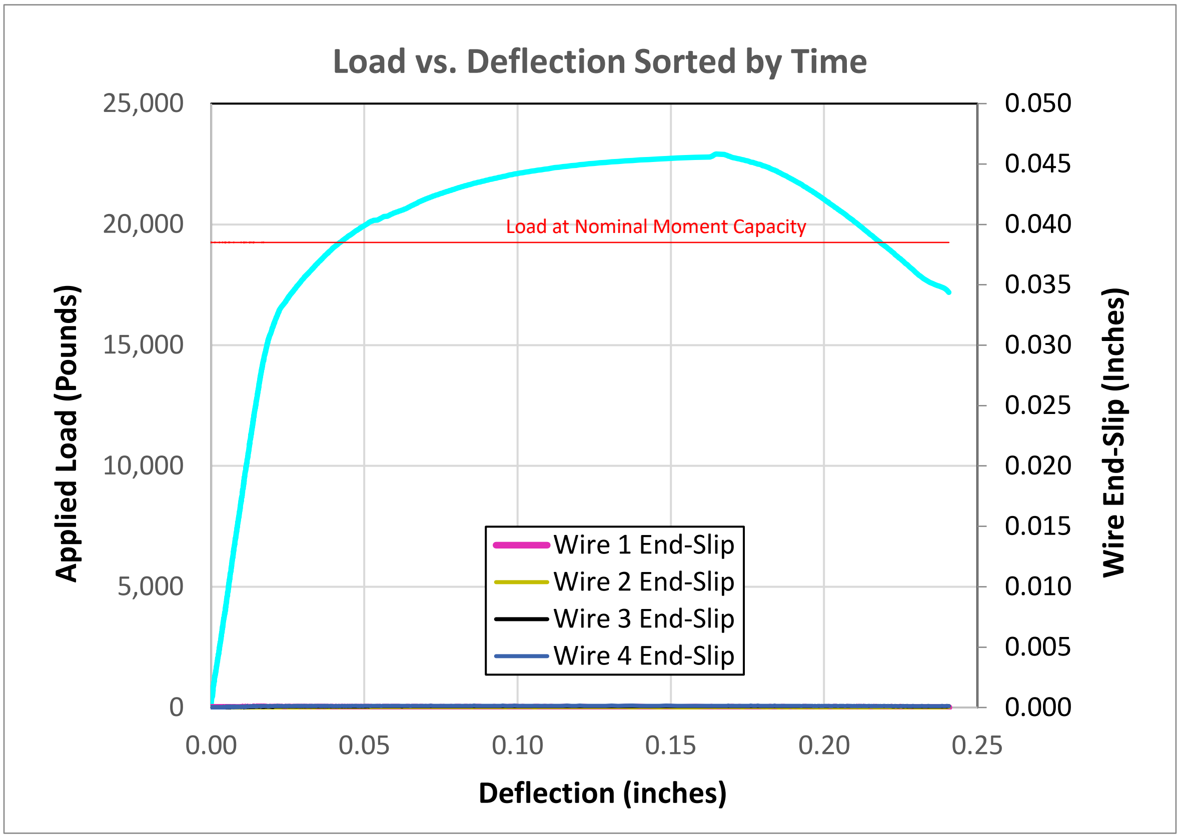

Figure D.24: Flexural Testing Results for Specimen 6.5-4500-H3.

Figure D.25: Broken Beam Failing Through Strand Rupture.

Beam Identification:	7.5-4500-H3
Concrete Strength at Test:	7,000 psi
Embedment Length:	18”

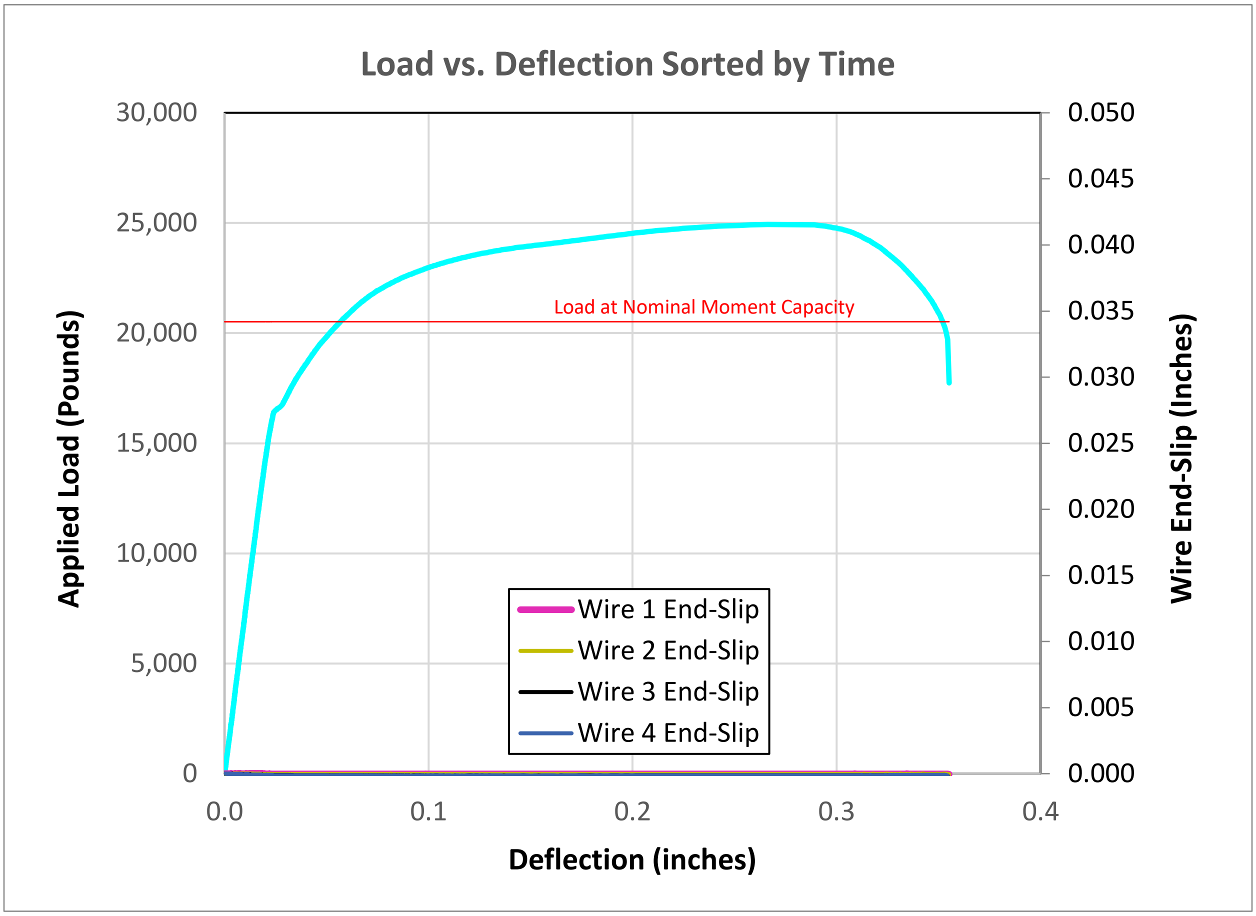

Figure D.26: Flexural Testing Results for Specimen 7.5-4500-H3.

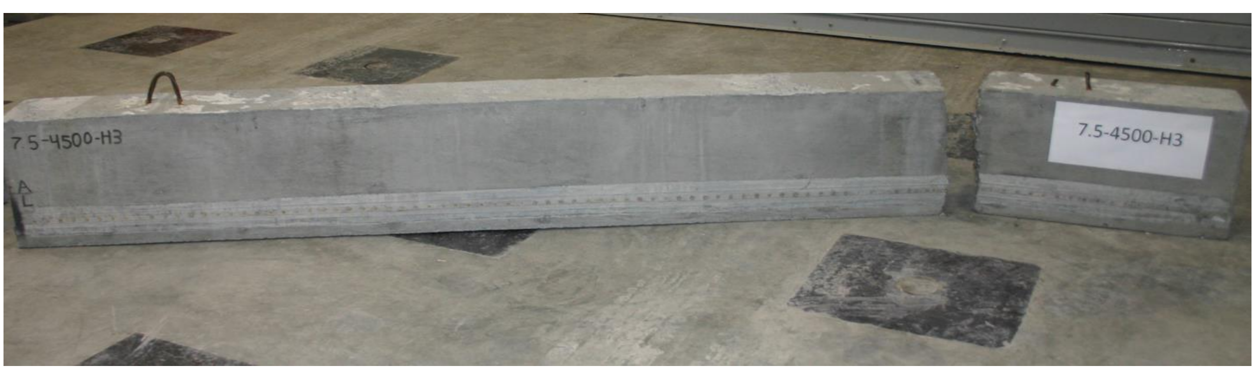

Figure D.27: Broken Beam Failing Through Strand Rupture.

Beam Identification:	5.5-4500-V1
Concrete Strength at Test:	8,100 psi
Embedment Length:	33”

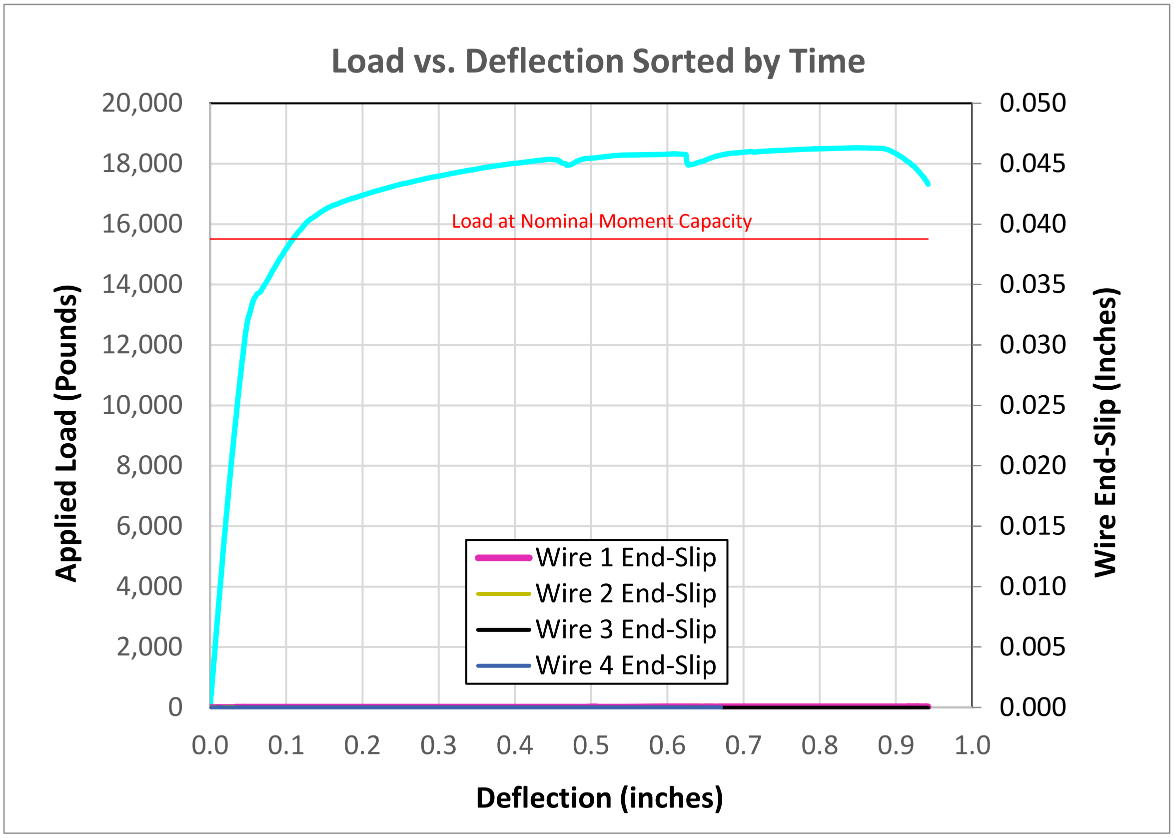

Figure D.28: Flexural Testing Results for Specimen 5.5-4500-V1.

Figure D.29: Broken Beam Failing Through Strand Rupture.

Beam Identification:	6.5-4500-V1
Concrete Strength at Test:	8,100 psi
Embedment Length:	21”

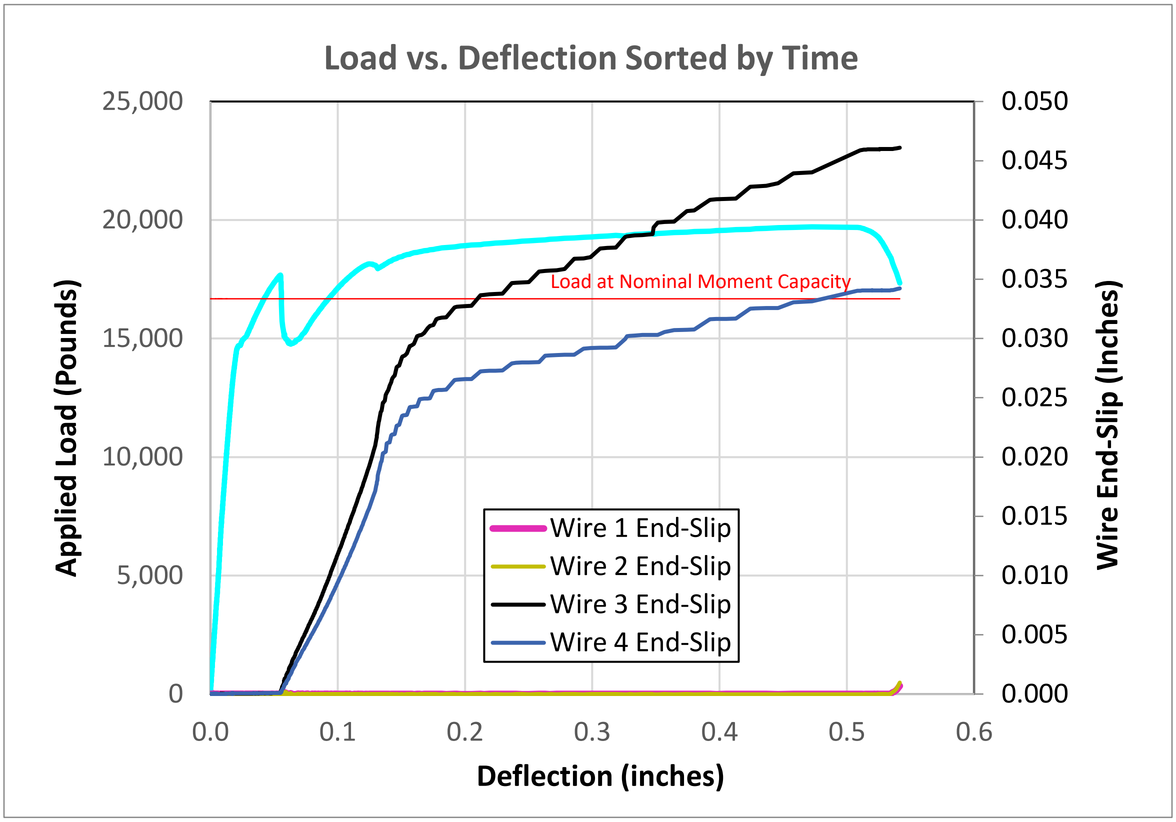

Figure D.30: Flexural Testing Results for Specimen 6.5-4500-V1.

Figure D.31: Broken Beam Failing Through Loss of Bond.

Beam Identification:	7.5-4500-V1
Concrete Strength at Test:	8,100 psi
Embedment Length:	18”

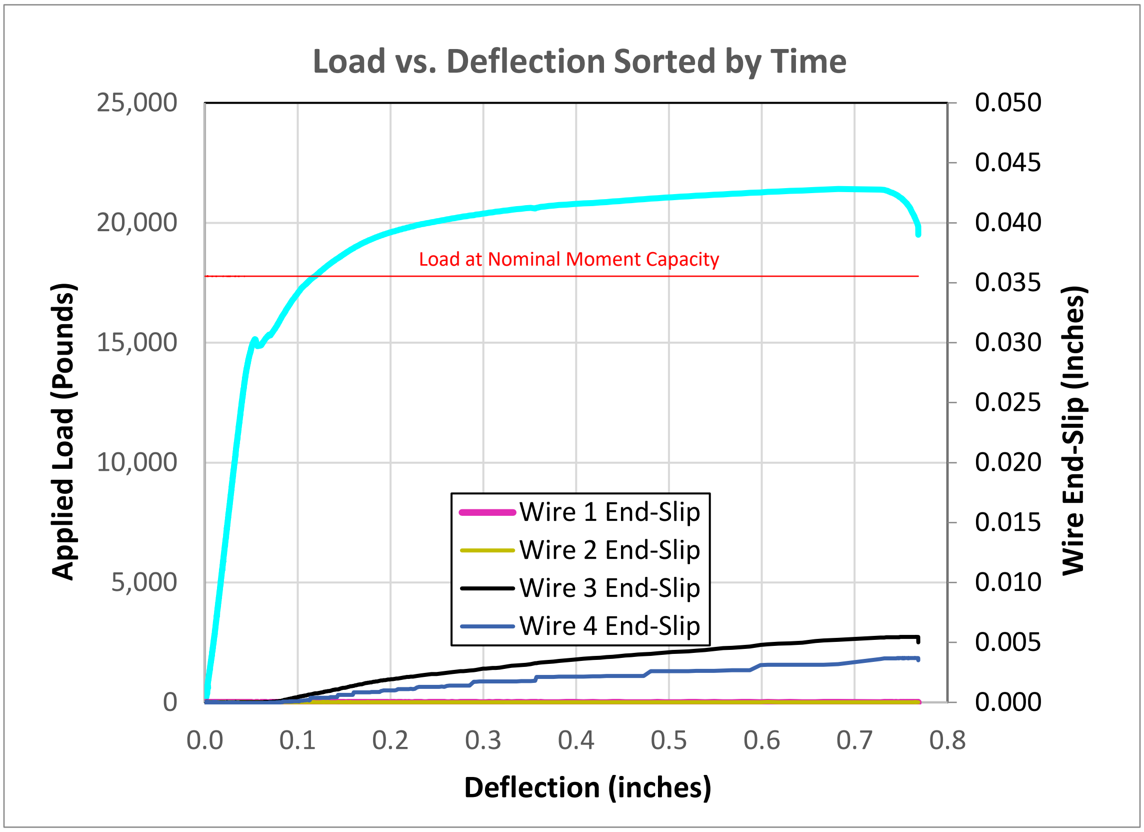

Figure D.32: Flexural Testing Results for Specimen 7.5-4500-V1.

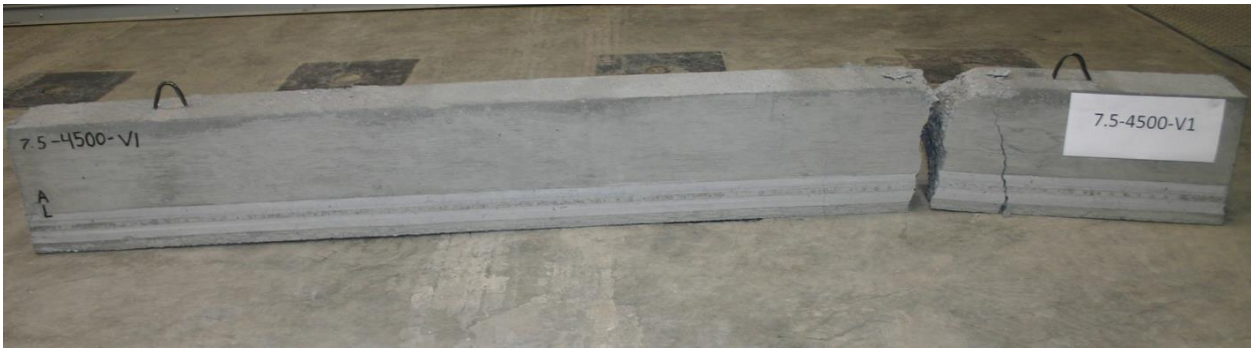

Figure D.33: Broken Beam Failing Through Strand Rupture.

Beam Identification:	5.5-6000-H1
Concrete Strength at Test:	9,000 psi
Embedment Length:	27”

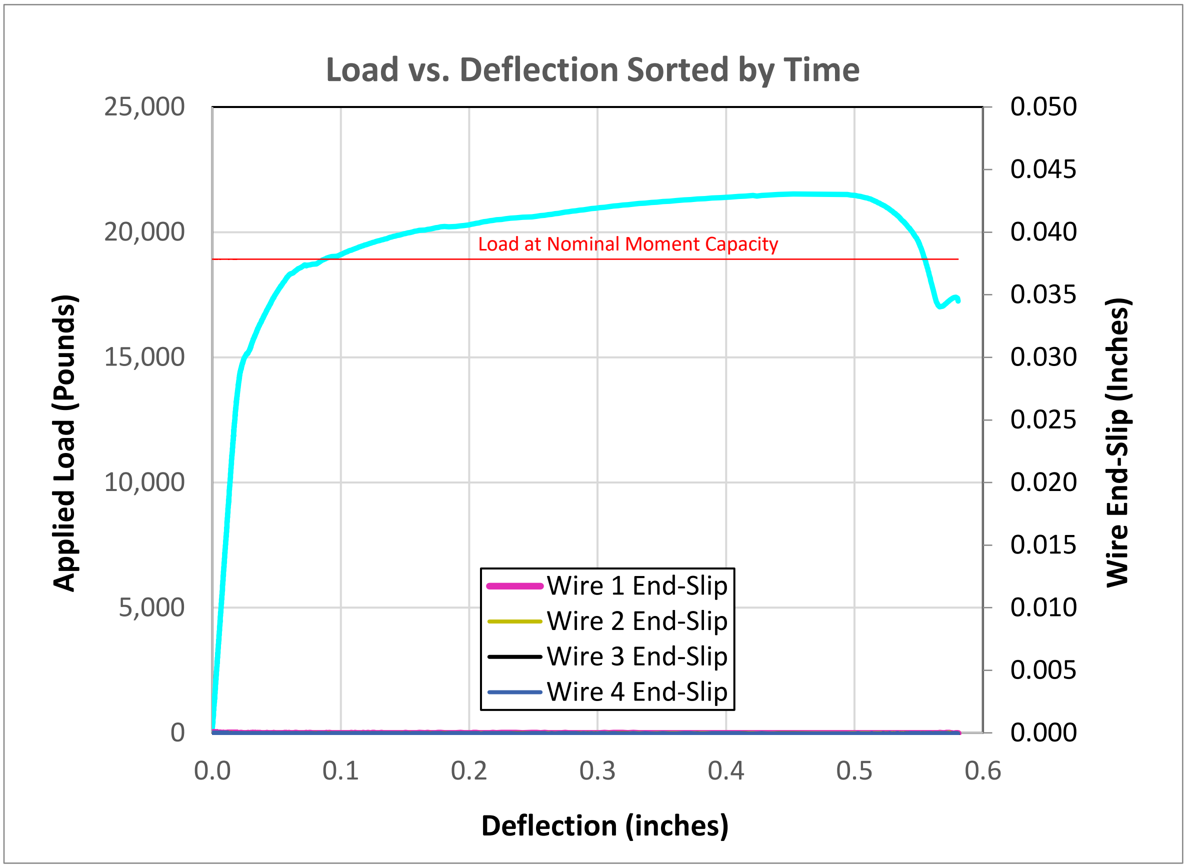

Figure D.34: Flexural Testing Results for Specimen 5.5-6000-H1.

Figure D.35: Broken Beam Failing Through Strand Rupture.

Beam Identification:	6.5-6000-H1
Concrete Strength at Test:	9,000 psi
Embedment Length:	21”

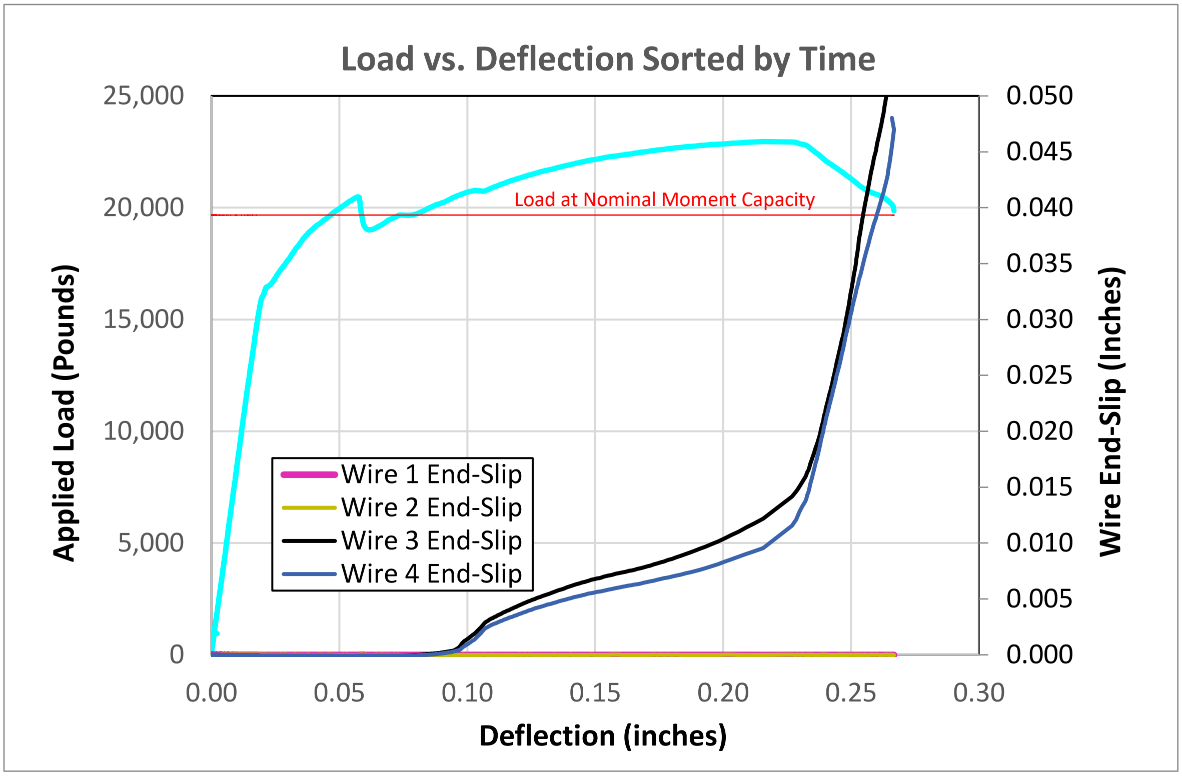

Figure D.36: Flexural Testing Results for Specimen 6.5-6000-H1.

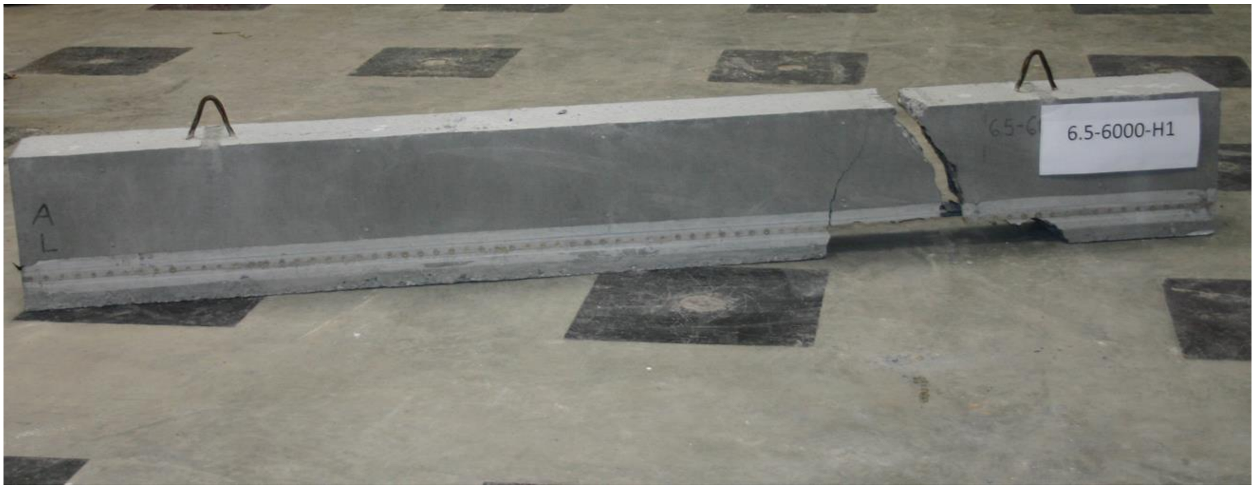

Figure D.37: Broken Beam Failing Through Loss of Bond.

Beam Identification:	7.5-6000-H1
Concrete Strength at Test:	9,000 psi
Embedment Length:	16”

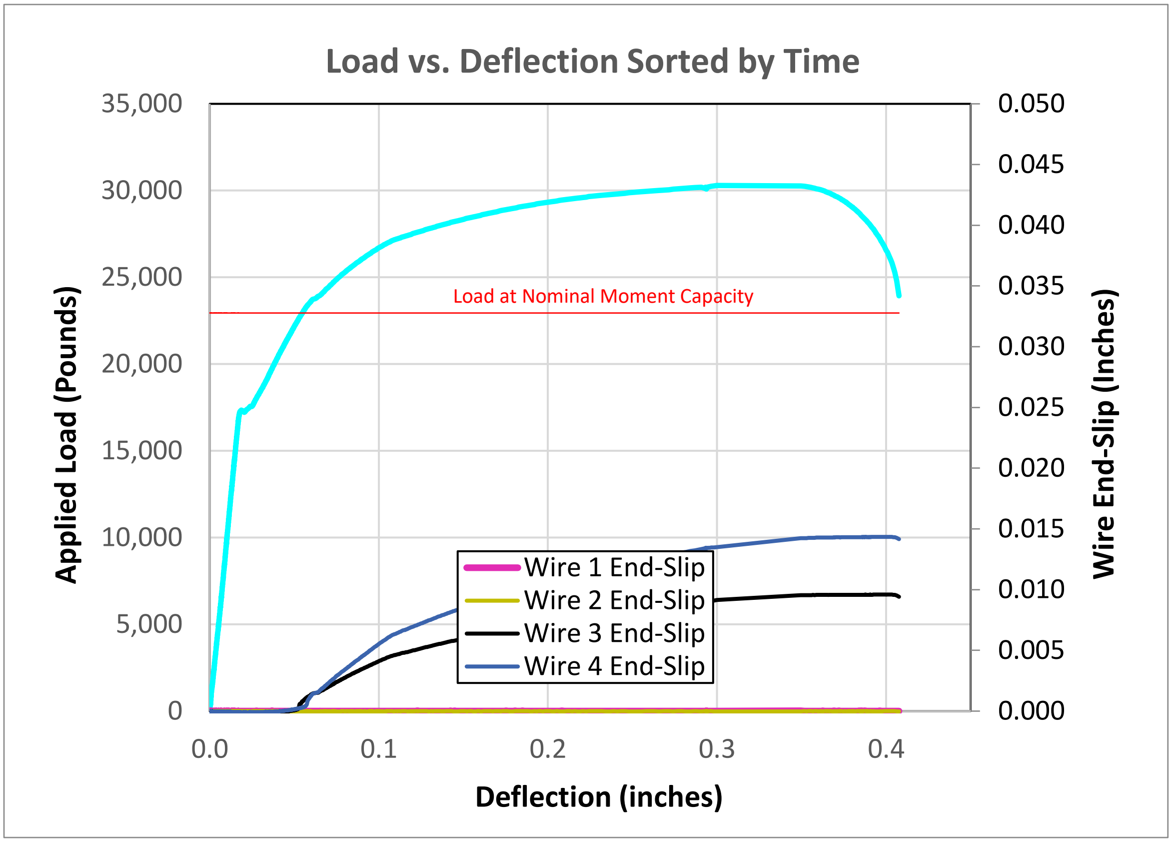

Figure D.38: Flexural Testing Results for Specimen 7.5-6000-H1.

Figure D.39: Broken Beam Failing Through Strand Rupture.

Beam Identification:	5.5-6000-H3
Concrete Strength at Test:	7,000 psi
Embedment Length:	27”

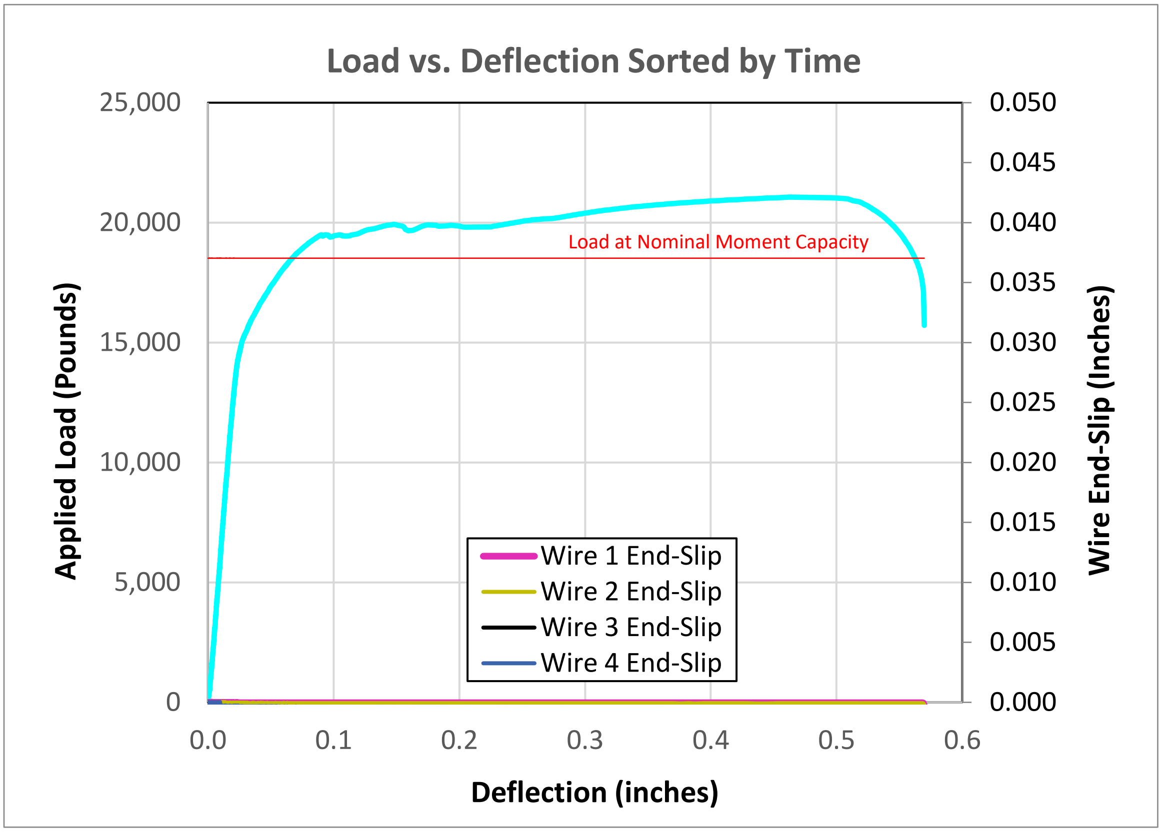

Figure D.40: Flexural Testing Results for Specimen 5.5-6000-H3.

Figure D.41: Broken Beam Failing Through Strand Rupture.

Beam Identification:	6.5-6000-H3
Concrete Strength at Test:	7,000 psi
Embedment Length:	21”

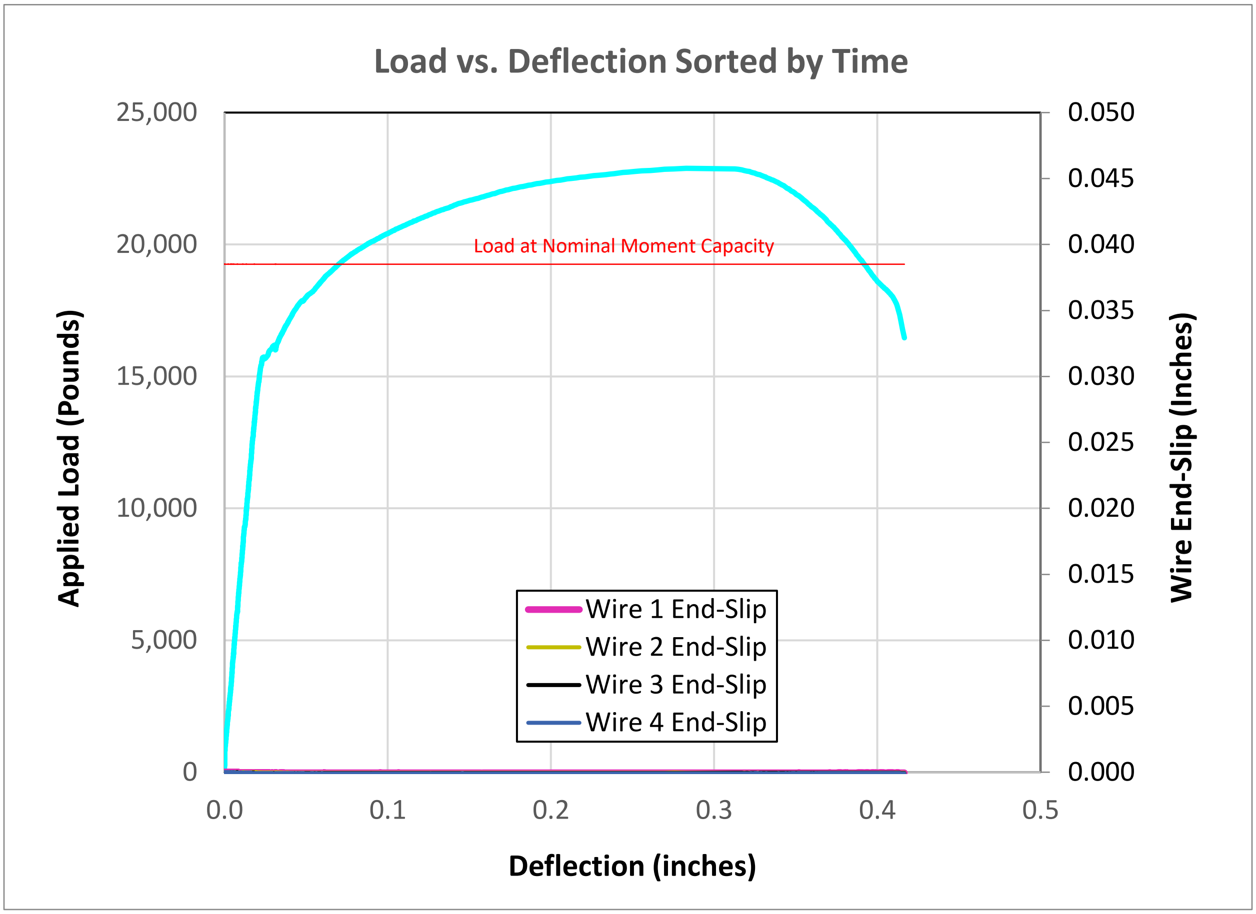

Figure D.42: Flexural Testing Results for Specimen 6.5-6000-H3.

Figure D.43: Broken Beam Failing Through Strand Rupture.

Beam Identification:	7.5-6000-H3
Concrete Strength at Test:	7,000 psi
Embedment Length:	16”

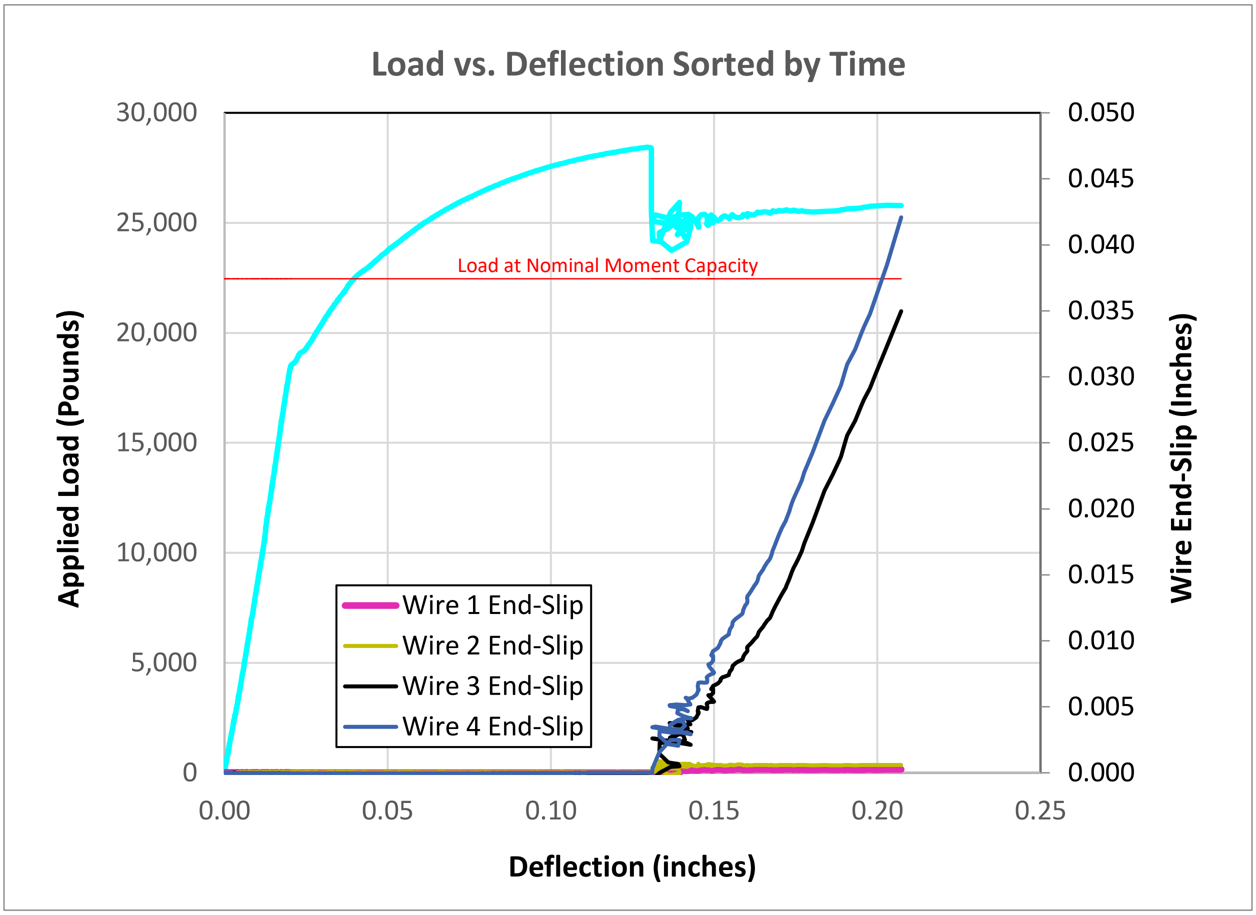

Figure D.44: Flexural Testing Results for Specimen 7.5-6000-H3.

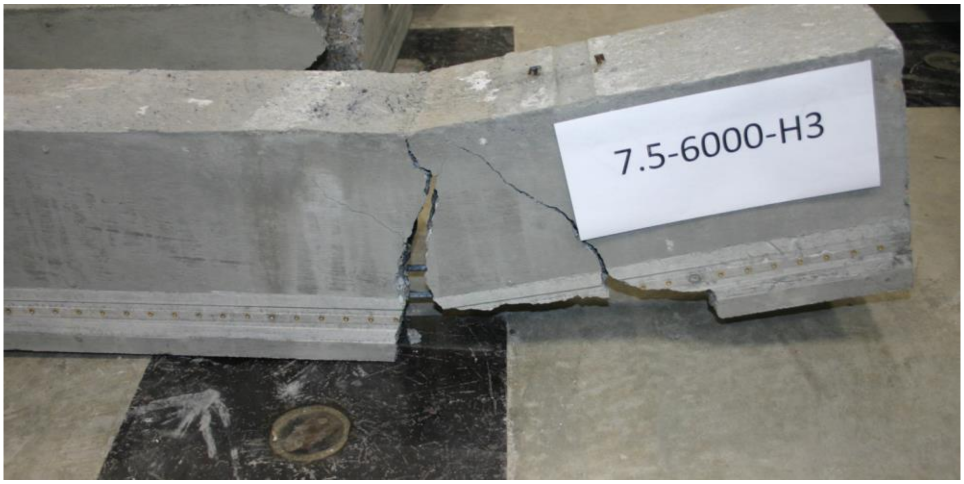

Figure D.45: Broken Beam Failing Through Loss of Bond.

Beam Identification:	5.5-6000-V1
Concrete Strength at Test:	8,100 psi
Embedment Length:	27”

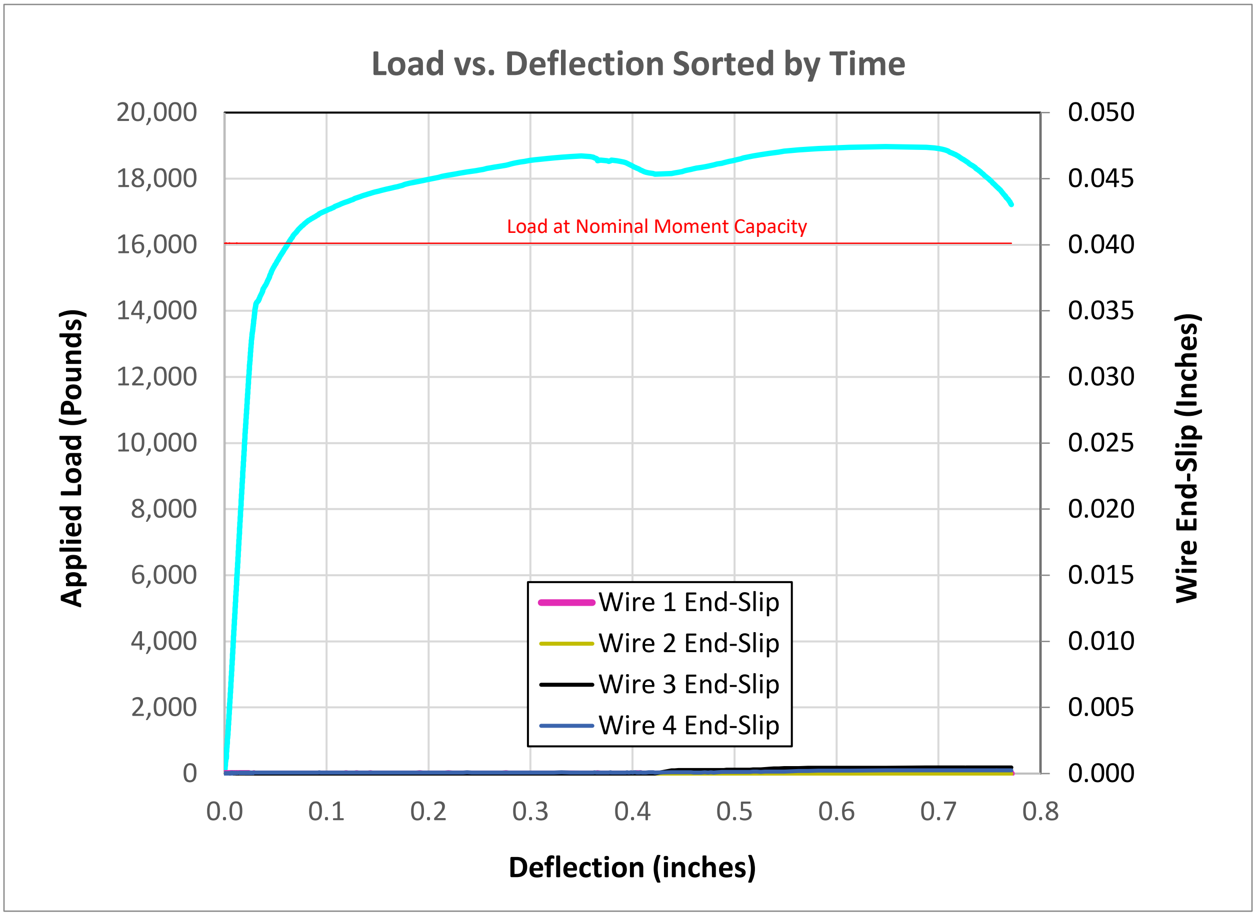

Figure D.46: Flexural Testing Results for Specimen 5.5-6000-V1.

Figure D.47: Broken Beam Failing Through Strand Rupture.

Beam Identification:	6.5-6000-V1
Concrete Strength at Test:	8,100 psi
Embedment Length:	21”

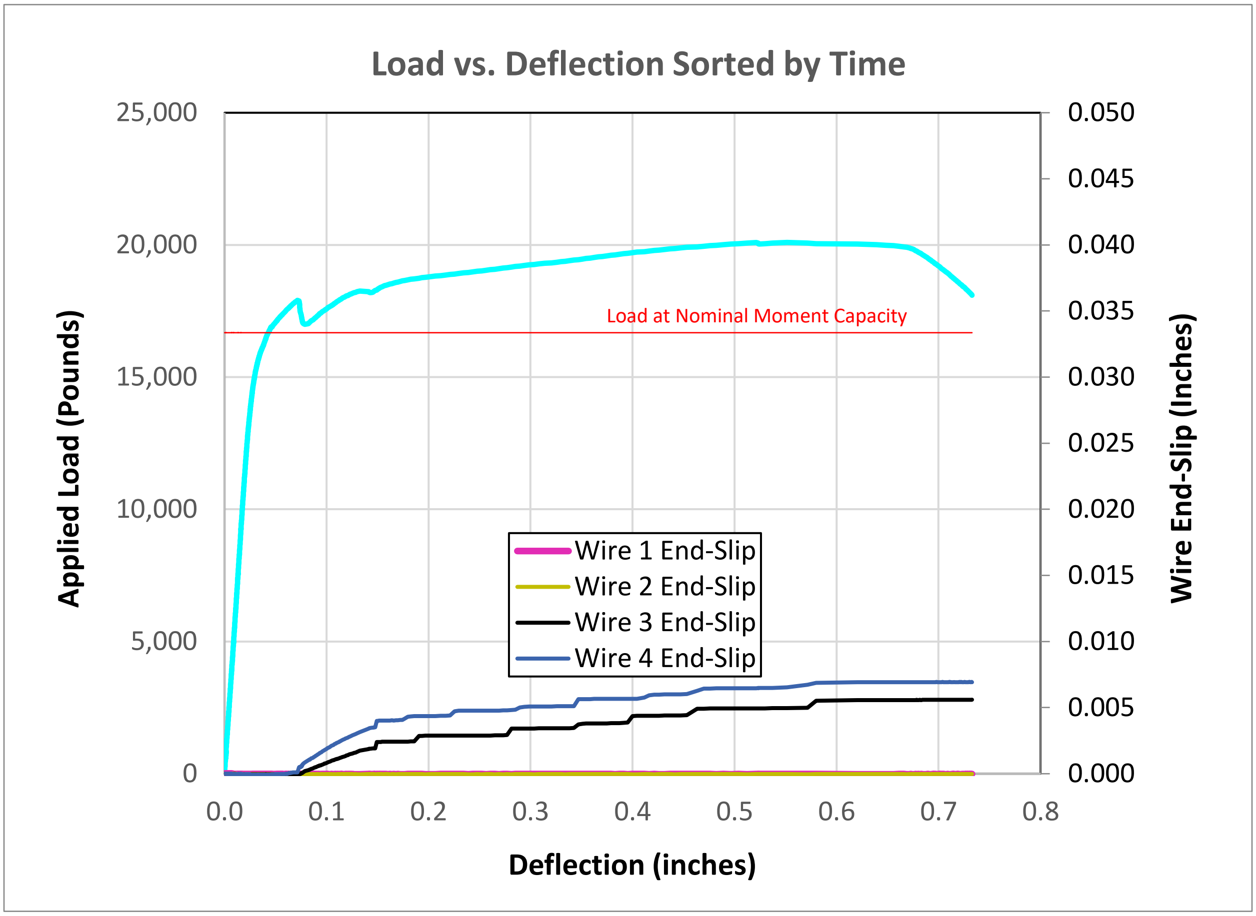

Figure D.48: Flexural Testing Results for Specimen 6.5-6000-V1.

Figure D.49: Broken Beam Failing Through Strand Rupture.

Beam Identification:	7.5-6000-V1
Concrete Strength at Test:	8,100 psi
Embedment Length:	16”

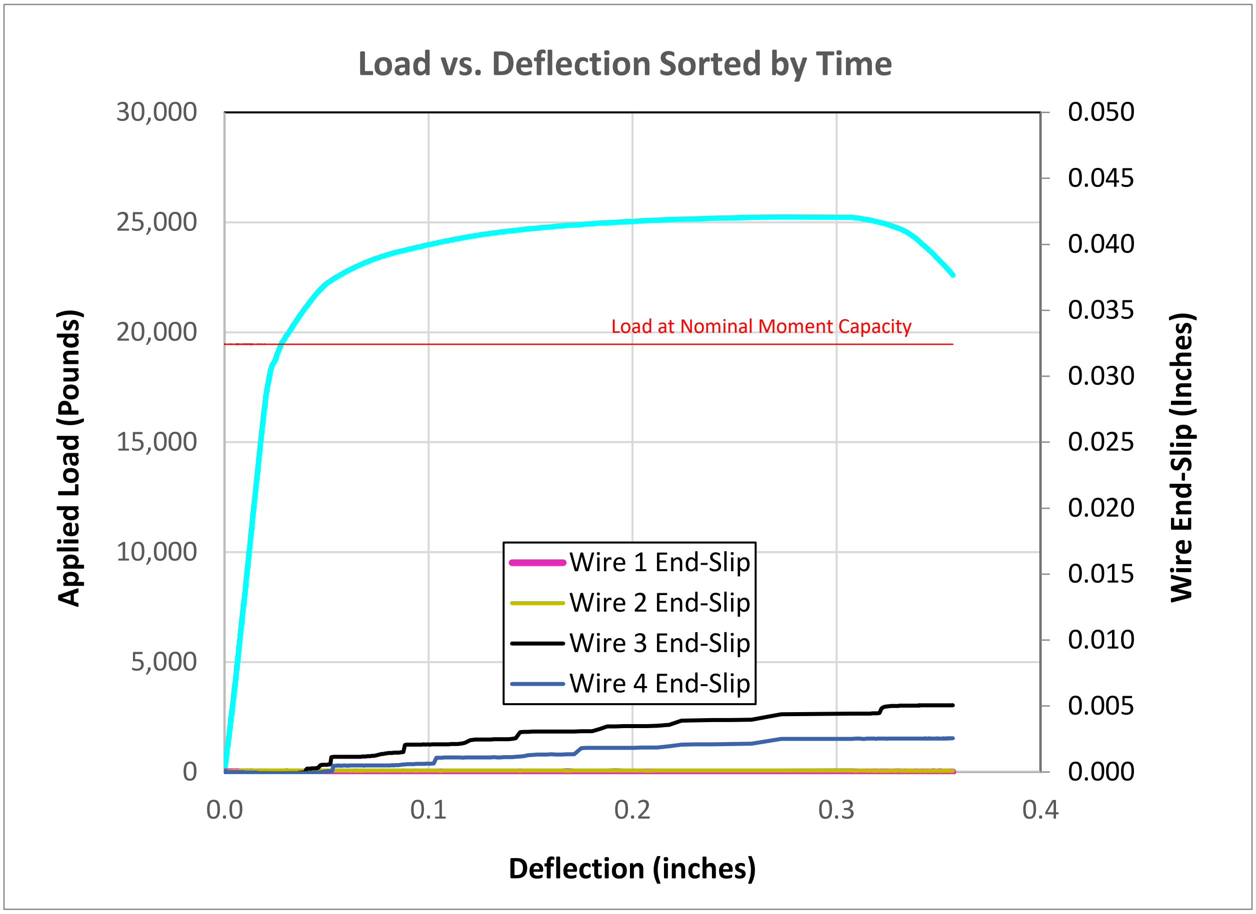

Figure D.50: Flexural Testing Results for Specimen 7.5-6000-V1.

Figure D.51: Broken Beam Failing Through Strand Rupture.